SUPERCHARGING OF FOUR STROKE ENGINES

THESIS

Submitted in partial fulfilment of the requirements for

The Degree of Master of Engineering

in

APPLIED THERMODYNAMICS (Steam & I. C. Engines)

By

Shyam Bahadur

MECHANICAL ENGINEERING DEPARTMENT

UNIVERSITY OF ROORKEE

ROORKEE

1962

and cost, further developments have come into light in the form of free piston engines and the gas turbine. Strictly speaking, the former have originated from the supercharging of two stroke engines and employ the engine cylinder merely as gas generator. In gas turbine also the engine cylinder has been replaced by the combustion chamber. The reciprocating engine, supercharged or unsupercharged, is a mechanically inefficient device because of the heavy weight of reciprocating parts and so the requirements of a large motoring power. Thus if the mechanical efficiency of the engine be 80 per cent, by doubling the power output of the engine with high supercharge without any appreciable additional increase in frictional losses, the mechanical efficiency may be raised to about 90 per cent. This will also result in the proportionate improvement of the overall efficiency. This implies that for the survival of the conventional internal combustion engine, the only remedy is to make it befittin for very high supercharge pressures and to dispense with several other inefficiencies.

It is solely with this directive that the preparation of this dissertation has been taken up. A critical review of the existing information on the supercharged four stroke engines has been made and compiled in the first four chapters. The development of the latest form of superchargers has been discussed taking into consideration the minute changes that have been envisaged over the existing ones for additional adaptability of the equipment for a particular application. The limitations if any, have also been indicated there and then. The fourth chapter

furnishes the performance curves for a few typical supercharged engines of all categories covering nearly all the ranges. The idea behind it has been to discuss the characteristics of the supercharged engines indicating the major points which have favoured the adaptability of that particular type of engine to a particular application. The main topic of controversy, at present, connected with the use of turbocharged engines in automotive applications has also been discussed at great length. The amendment in characteristics and the way in which it can be achieved has also been taken up. In the fifth chapter a procedure for the engine-turbocharger matching has been developed which has been illustrated by its application to an actual problem in the sixth chapter. Here the performance of the turbocharged engine has also been predicted on theoretical considerations and a comparison made with the performance of the engine in the naturally aspirated form and the experimental curves available for the supercharged version. The seventh chapter gives the concluding remarks with a few suggestions for further work.

It is hoped that the investigations taken up on the lines indicated will go a long way in strengthening the roots of the supercharged four stroke engine as a versatile power unit and will substantiate its co-existence along with other fast developing prime movers.

CHAPTER 1

ORIGIN AND DEVELOPMENT OF SUPERCHARGING

1.1 Historical- The initiation of internal combustion engine dates back to 1630 when the Dutch physicist Christian Huyghens (1-2) originated the first gunpowder engine in its primitive form. But the development was hampered due to the simplicity of the then popular steam engine, until in 1794 English engineer Robert Street developed the first gas engine working model employing flame combustion. Concentrated efforts were directed to improve upon this model by Lebon, Cecil, Barnett, Lenoir and Buron, till in 1862 Beau de Rochas gave birth to the first spark ignition engine. In 1876, Nikolaus August Otto, a German engineer, produced a satisfactory design of gas engine free from noise and roughness in operation.

Due to the high cost of fuel in Otto cycle engines, further experiments were carried out by Hock, Brayton, Siemens, Spiel and Priestman, but the credit for the development of first successful compression ignition engine goes jointly to the English engineer Norbert Ackroyd-Stuart (1890) and the German engineer scientist Dr. Rudolf Diesel (1892).

Supercharging was then applied to gas engines as early as 1895 (3), but due to the primitive stage of development of the engine itself, it could not exhibit its full potentialities. Some experiments were conducted here and there from time to time, but the progress was too slow. To start with, pressure-charging with mechanically driven chargers was tried, but the idea to partially conserve the heat of the exhaust which is unprecidable in a supercharged

engine, led Rateau of France to conceive of turbocharging in 1910. However, the first experiments utilizing exhaust gas turbines in combination with internal combustion engines were made in 1911 at the Sulzer Works, Winterthur, by Dr. A.J. Buchi, and the Buchi system was commercially introduced in 1920. The principles of the Buchi system have been applied in all the turbocharged engines produced so far.

The immense need of aircraft engines, with increased power for long range and high altitude flights, in the first World War (1914-18) resulted in the crucial development of supercharging. Consequently, supercharging could be applied to both American and French fighters. The work on supercharging was continued during the peace time (1918-38) as well. Thus the first turbocharged engine was produced by the Bristol Company in 1923. It was then applied in the Boeing model of American and several other aircrafts all over the World. The continued development resulted in high performance and reliability of supercharged engines so that several English and Italian passenger and cargo vessels employing Buchi turbocharging were commissioned in 1928 (4). During the last forty years the supercharged engines have also been extensively used in power stations, rail traction, earth moving machines, and several other installations.

Fig. 1.1 shows the progress made in the field of supercharging to date. It should be noted that the specific weight of the engine decreased upto 1940 and then started showing a slight increase. However, the rate of increase of b.h.p. is much in excess of the rate of increase of engine specific weight. This accounts for the successful work done.

1.2 Increasing the Power Output- It has already been pointed out

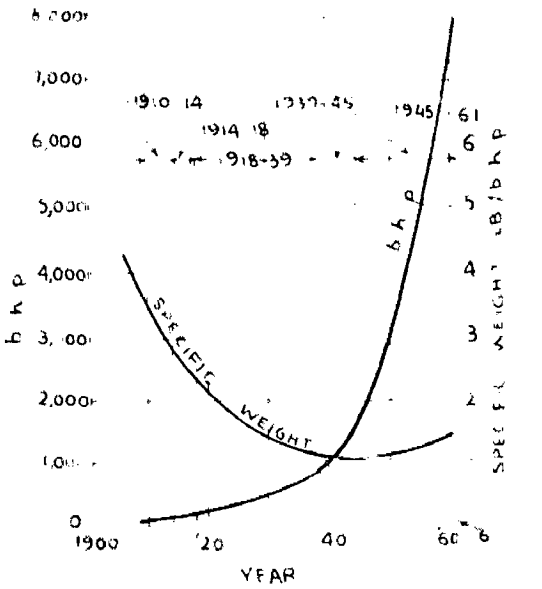

SUPERCHARGING DEVELOPMENT

FIG.

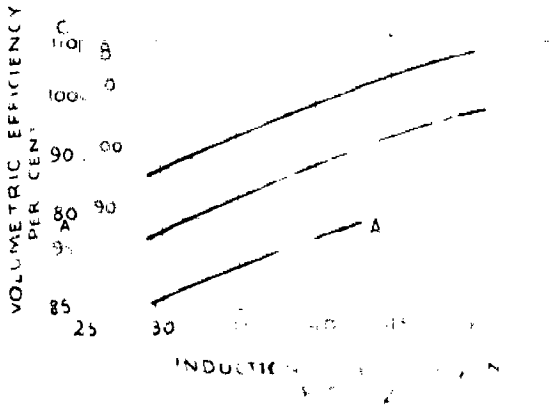

INDUCTION

A 4
B - 4 0
C - 3 5 COM RAT

F 5

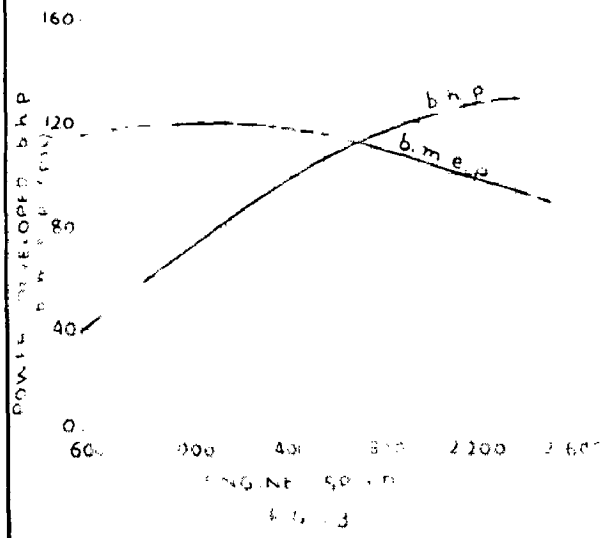

ENGINE

4 6 3

REF

INDICATOR DIAGRAM

C
2 3
8 F

that supercharging originated from the consideration of increased specific power output from the engine. In order to achieve this the following are the only alternative methods:

(1) Increasing the compression ratio,

(2) raising the rotational speed,

(3) increasing the air density at the intake air manifold.

(1) Increasing the Compression Ratio- Ricardo performed the tests on a variable compression petrol engine and gave the following results:

Compression ratio	4.0	5.0	6.0	7.0	8.0
Indicated mean effective pressure ($lb./in.^2$)	122	136	147	157	163

It may be seen that with the increase in compression ratio, the indicated mean effective pressure, which is a measure of the power of engine, increases at a reduced rate. The thermal efficiency of the engine also increases, but with the increase of compression ratio beyond 8, progressively smaller gain in thermal efficiency and i.m.e.p. is obtained. The thermal efficiency as well as the i.m.e.p. of a diesel engine will also increase with the compression ratio.

With the increase in compression ratio the volumetric efficiency will go down (5), Fig. 1.2, and the maximum cylinder pressure and the combustion temperature will increase. The latter will produce excessive mechanical and thermal loading on the engine thereby necessitating larger bearings, heavier reciprocating parts, and other stress bearing members, and so increased engine weight and bulk. Further in case of spark ignition engines, there will be

a danger of detonation. Hence this alternative is not used.

(2) Raising the Rotational Speed- The horsepower of an engine is proportional to the product of the brake meaneffective pressure (b.m.e.p.) and the engine speed. This implies that power output can be increased by increasing the engine speed, provided the b.m.e.p. is not lowered. However, the engine speed is limited by the considerations of piston and bearing rubbing velocities, engine balance, increased frictional losses, and loss of volumetric efficiency etc. Further, reduction in volumetric efficiency and period of combustion results in the loss of b.m.e.p. at very high engine speeds. Hence this method is also not practicable.

(3) Increasing the Air Density- The pressure of the atmospheric air may be raised in an external blower, so that its density increases, and a much larger quantity of air is entrapped in the cylinder during suction stroke. If adequate quantity of fuel be supplied, the potential power output in this case will be much higher. It, therefore, follows that by pressure-charging the engine cylinder (known as supercharging), the power output of an engine can be increased.

1.3 Supercharging- As already pointed out, supercharging results in entrapping of larger quantities of air in the engine cylinder which may give volumetric efficiencies even greater than 100%. This air will be capable of burning a larger quantity of fuel thereby producing more power. It is clear from Fig. 1.4, wherein with the increase in boost pressure, the area of indicator diagram increases.

Expressed mathematically, the heat of charge (H) per cycle in an engine cylinder is given by

$$H = \left(\frac{\pi}{4} D^2 . L \right) \eta_v . \frac{1}{v_a} . \frac{1}{A_f} . C$$

where D - the diameter of cylinder,

L- the length of stroke,

η_v - volumetric efficiency,

v_a - specific volume of air inducted,

A_f - Air-fuel ratio by weight,

and C - the calorific value of fuel.

For an engine of given proportions, employing a particular quality of fuel and specified air-fuel mixture, the above equation may be written as

$$H = \text{Constant} \times \left(\frac{\eta_v}{v_a}\right)$$

Thus the heat of charge or, in other words, the power output of an engine can be increased by raising the density of air at the induction manifold and by improving upon the volumetric efficiency. Both of these requirements are met by supercharging.

Supercharging may thus be defined as the process of introducing air into the engine cylinder at a pressure higher than atmospheric, so as to burn greater quantity of liquid fuel. Sometimes it is also known as boosting because of its boosting effect on the power output.

1.4 Objects of Supercharging- Supercharging has been applied to various four stroke engines with the following objectives:

(1) To reduce the weight of the engine per horsepower developed as in aircraft and racing car engines.

(2) To reduce the bulk of the engine to enable it to be fitted into a limited space as in locomotive and marine practice.

(3) To overcome the effect of altitude on engine output as in aircraft engines and stationary engines installed at high altitudes.

(4) To augment the power of an existing engine as is often

demanded in case of pipe line pumping stations.

(5) To obtain high torque at low speed as in earth moving machinery.

CHAPTER 2

SUPERCHARGING APPLIED TO ENGINES

2.1 Introduction- It has been mentioned that supercharging increases the charge density in order to produce a boost in power output. This results in an increase in the pressure and temperature of the charge at the engine intake and consequently a general increase in the pressure and temperature throughout the cycle. Thus the engine suffers some change in its behaviour as regards to the fundamental factors like the tendency to incipient knock or detonation, rate of heat flow, and the mixture conditions etc. that govern it successful operation. It is intended to study here the effect of supercharging upon these factors so as to examine the suitability of the process when applied to an actual engine cycle.

2.2 Effect of Supercharging on the Maximum Pressure and Temperature: Fig. 2.1 shows the P-V diagram for a supercharged engine cycle. Here 6-7 represents the atmospheric pressure line, 7 corresponds to the ambient conditions, and 1 refers to the intake conditions of the high pressure charge. Whatever may be the nature of the compression process, the pressure and temperature at the end of compression (P_2, T_2), and hence at the end of combustion (P_3, T_3), will definitely be higher than for a naturally aspirated engine. But the difference in the rise of pressure and temperature during combustion is not large because whereas pressure charging increases the quantity of fuel burnt, the quantity of the charge also increases proportionately. This is of paramount advantage, as it safeguards against rapid deterioration and ensures the reliability and life of the engine.

The results of J.G. Cameron (6) based upon analytical inver-

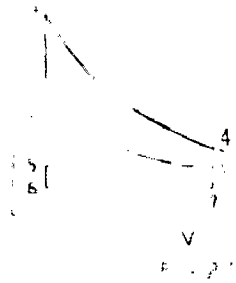

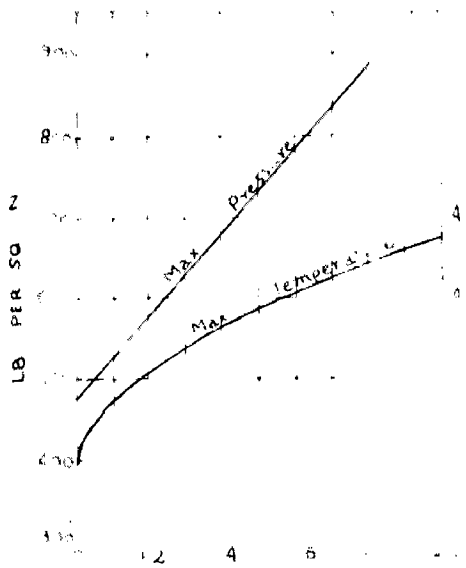

SUPERCHARGE PRESS
(OTTO CYCLE)
FIG 2

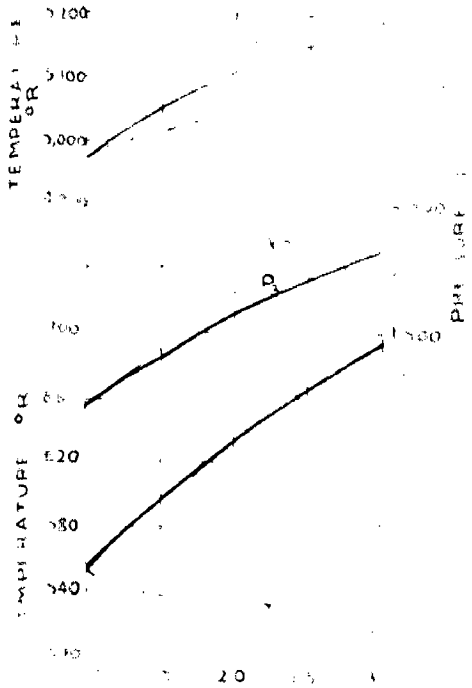

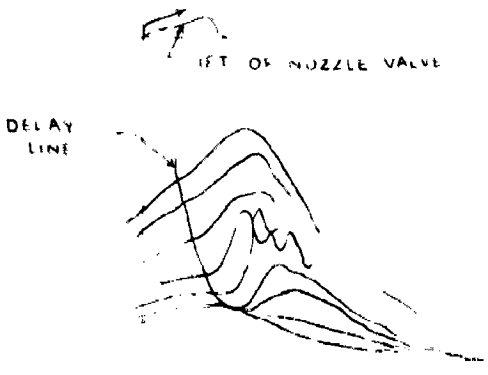

REF 8

tigations utilizing known practical combustion data are shown in Fig. 2.2. It should be observed that with the increase of supercharge pressure, the maximum temperature and the maximum pressure go on increasing.

The effect of supercharge pressures upon T_1, T_3, and P_3 for adiabatic and isothermal compression are shown (7) in Fig. 2.3. Both P_3 and T_3 are found to increase with the degree of supercharge, the values of T_3 being lower and for P_3 being higher for isothermal compression.

Both the diagrams discussed above relate to an Otto engine cycle, wherein the maximum pressure is nearly 900 psi. The behaviour of the maximum pressure and temperature for a constant pressure cycle will also be similar, except with the difference that the maximum pressure may go up to about 1200 psia, whereas the maximum temperature will be comparatively lower.

2.3 Effect of Supercharging on Delay Period. Boerlage and Broeze (8) of the Bataafsche Petroleum Co. Laboratory, Delft, Holland, were the first to point out vividly the effect of inlet pressure on the delay period. They took a number of "90° offset" indicator diagrams (Fig. 2.4) with an ordinary piston type of oil indicator. The air supply to the engine was throttled step by step to get the lower values of intake pressures after every adjustment. With the decrease in injection pressure, the delay period as well as the maximum pressure were found to increase.

A test on a single cylinder 5 x 7 in. experimental engine also showed that the delay period was reduced from 17 to 13° when the intake pressure was increased from 2/3 atmos. to 1.3 atmos.

The investigation on delay period were also made by Prof. Bird at Cambridge University who plotted his results in a three-

dimensional diagram (Fig.2.5). The charge density being directly proportional to its pressure (P) and inversely proportional to its temperature (T) has been plotted along the X-axis in terms of $\frac{P}{T}$. The intake air temperature in degrees Fabs. is plotted along the Y-axis, and the delay period in seconds along the Z-axis. The diagram shows that the ignition lag decreases with the increase in charge density, intake air temperature, or both.

The delay period is also affected by the compression ratio. Fig. 2.3 obtained by tests on the C.F.R. engine (Cooperative Fuel Research) shows the effect of compression ratio on delay period for two different grades of fuel. Obviously the delay period decreases with the compression ratio.

2.4 Effect of Supercharging on Detonation in S.I. engines- Detonation depends upon a number of factors, comprising both the design factors and the factors of operation. These are the shape of the cylinder, the situation of the spark plug, the temperature of the induction charge, the ignition advance, and the type of fuel used.

With the degree of supercharge, the temperature of the charge increases resulting in greater tendency to detonation due to the inefficiency of the supercharger. Fuels having a high anti-knock value, because of the presence of a large percentage of aromatic hydrocarbons, are more severely affected by high temperatures than those rich in napthelenes or tetra-ethyl lead. Thus supercharging will tend to promote detonation to a larger extent in a fuel rich in aromatics than the equivalent lead doped fuel.

It has also been observed that when the normal proportion of residual gases in an engine is reduced by effective scavenging, the engine becomes more prone to detonation. This is so because the smaller ratio of the residual gases to the fresh charge results

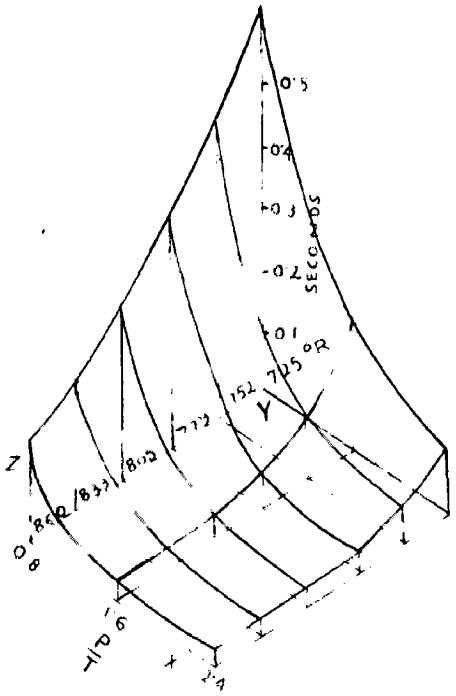

EFFECT OF CHARGE DENSITY AT INTAKE TEMPERATURE ON IGNITION LAG

FIG. 2·5

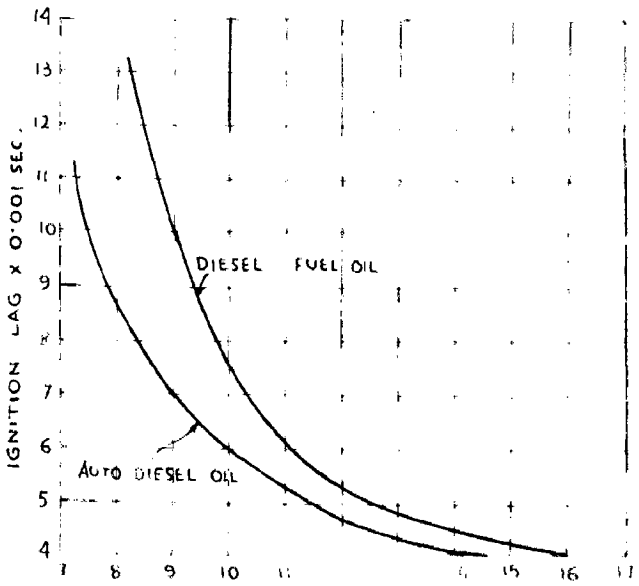

EFFECT OF COMPRESSION RATIO ON IGNITION

REF 8

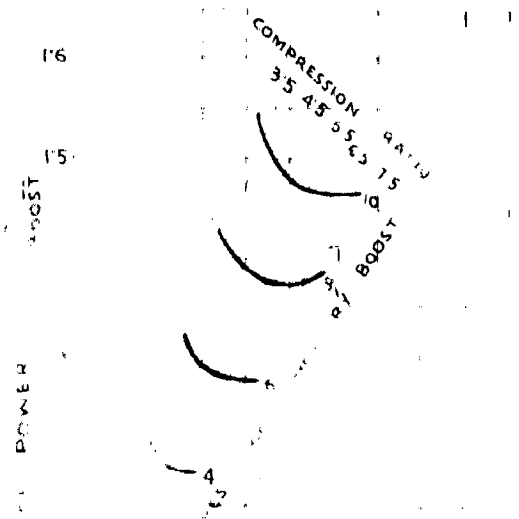

BOOST

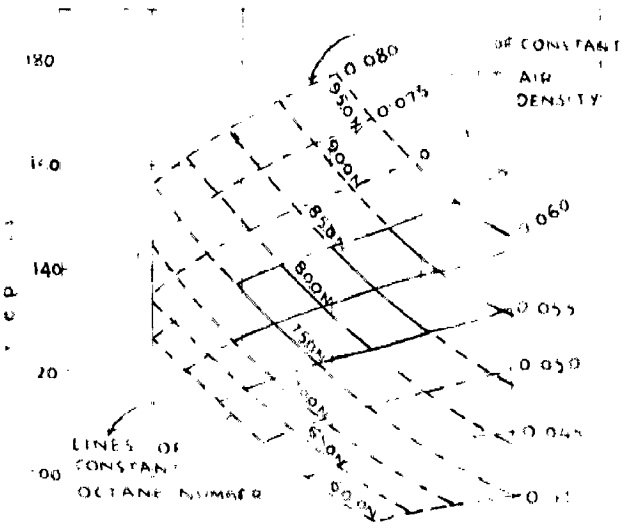

COMPRESSION RATIO

FIG. 2·8.

in higher cycle temperatures.

It may thus seem advisable in a supercharged spark ignition engine to sometimes reduce the compression ratio in order to obtain lower cycle tempratures, and thus reduce the danger of detonation.

The reduction of delay period by supercharging in a compression ignition engine results in a reduction of the rate of pressure rise during the second stage of compression. Further, increase in density reduces the voatility of the fuel, and hence the tendency to knock is mitigated. Thus the engine runs smoother.

2.6 Effect of supercharging on Heat Flow- The amount of heat developed in the engine cylinder is proportional to the weight of the charge inducted. The heat to be rejected to the surroundings will, therefore, also be in the same proportion. But in spark ignition engines supercharging results in increased tendency to detonation and, therefore, the compression ratio is slightly lowered from its value in the normally aspirated case, this resulting in a lowering of the thermal efficiency. Thus the proportion of waste heat is comparatively large in supercharged engines. It has further been experimentally observed that in a supercharged engine the transferrence of heat takes place in a reduced proportion to the charge weight.

The rate of heat flow with increased intake pressures was investigated by Ricardo on a single cylinder sleeve valve 4½ x 5½ in. spark ignition engine running at 1,500 r.p.m. at a compression ratio of 4.3. The results (9) obtained are shown in table 2.1 below.

TABLE 2.1

Intake air pressure (atm.)	Mean air temperature °C	Relative charge density	Heat to cooling water in h.p.			B.H.P. observed	B.H.P. corrected	H.B.P. (observed)
			To cylinder head	To cylinder barrel	Total (H)			
1.00	19.75	1.000	3.29	10.71	14.00	15.3	15.3	0.915
1.52	23.50	1.485	4.93	15.25	20.00	28.8	27.6	0.700
2.02	27.00	1.975	6.55	19.50	26.05	41.5	39.1	0.630
2.50	27.00	2.410	8.00	23.00	31.90	53.3	49.5	0.600

It may be observed from the first and last columns that the ratio of the heat flow to the observed B.H.P. goes on decreasing with increased intake pressures.

The above engine was charged by an externally driven supercharger, and a part of the B.H.P. observed was due to the pneumatic work of the compressed air on the engine piston during the induction stroke. Therefore, the values shown in table 2.1 have slight deviation from the actual ones. These may, however, be modified by taking into account the positve work on the piston due to the pumping of air into the engine cylinder and also the compression of the residual gases from the atmospheric pressure to the sup rcharge pressure. The values will alter but the nature of variation will still be the same.

O.L. Gehey and V.C. Rollin (6) also performed tests on the N.A.C.A. variable compression engine and found that upto supercharge pressures of 50 percent atmospheric value, the heat losses to the cooling water are linearly proportional to the degree of supercharge. The graphs based on the above observations are shown in Fig. 2.7, from which the following inferences can be drawn.

(i) With increased boost pressures, the power output increases.

(ii) For an increase in the degree of supercharge, the percentage increase in power is greater than the percentage increase in losses to the cooling water.

(iii) With the decrease in compression ratio, the ratio of heat loss to the cooling water, with boost and no boost, decreases.

In a compression ignition engine, with increased supercharging the operation of the engine becomes smoother and better controlled, so that there is no necessity of lowering the compression ratio. Consequently, the thermal efficiency and the proportion of waste heat remains unchanged resulting in simpler cooling problem.

2.6 Effect of Supercharging on Fuel-air Ratio.- Hucklow (9) performed a series of tests on a supercharged single cylinder unit fitted with a Rolls Royce and a Napier cylinder running at 1,600 r.p.m. on compression ratios varying from 4 to 7. The fuel used was benzol. For each variation in the induction pressure, the air-fuel ratio was measured for the two extremes i.e., towards the weak end as well as the rich end. The results as obtained by him are given in table 2.2.

It is clear from the data obtained that the mixture-range gets narrowed down by supercharging regardless of the constant or variable ignition advance. With a fixed ignition advance, the range is shifted largely towards the weak end, because on the weak end the variation is too slow whereas on the

rich end the shifting towards the weak end is too brisk. But with successive adjustments in the ignition advance, the variation on either side is fairly equal, so that the symmetrical arrangement is retained. It should further be noted that with increased compression ratio the mixture range on the weak end is increased, whereas on the rich end it remains more or less unaffected.

TABLE 2.2

Compression ratio	Induction pressure (atm.)	Ignition advance degrees	Permissible air-fuel ratio	
			Weakest	Richest
4	0.00	43.5°	13.1	8.8
	1.24	43.5°	14.0	10.7
	1.47	43.5°	14.3	11.8
	1.70	43.5°	14.8	13.2.
	2.00	43.5°	15.7	14.3
5	1.00	43.5°	14.0	8.8
	1.25	43.5°	15.3	10.3
	1.51	43.5°	15.8	12.8
6	0.99	43.5°	15.4	9.2
	1.17	45.0°	15.7	9.6
	1.35	40.0°	15.4	10.7
	1.50	35.0°	14.7	9.7
	1.70	28.0°	13.5	9.9
7	0.99	40.0°	16.2	9.3
	1.20	35.0°	15.2	9.5

To give a mental picture of the reduction in mixture-range, it may roughly be stated that whereas a supercharged engine (compression ratio 7) with an intake pressure of 2 atm. will operate on an effective range of 10:1 to 15:1, a naturally aspirated engine (same compression ratio) may work satisfactorily on mixtures ranging from 18: 1 to 8.5:1

2.7 Supercharging Applied to Spark Ignition Engines- With respect to the spark ignition engines, the following difficulties encountered with supercharging need consideration:

(a) With increased density of air and its consequential increase in temperature, the tendency to pre-ignition and detonation is enhanced. This necessitates the use of high octane fuels and the lowering in compression ratio as shown (10) in Fig. 2.8 and still restricts the degree of supercharge that can possibly be provided. However, pre-ignition and detonation can also be suppressed to some extent by using a mixture 50 to 60 per cent rich above the chemically correct value. The mechanism involved in the latter case is that by the evaporation of the excess fuel, the intake temperature is lowered. But this is applicable only to fuels having a high latent heat e.g. alcohol-group fuels, and not hydrocarbon fuels. The advantage of this property of the alcoholic fuels is made use of in racing car engines.

(b) With the increased degree of supercharging, the delay period is reduced, whereas the spread of inflammation is accelerated. This increases the turbulence and thus makes the engine more sensitive to air-fuel mixture.

(c) The heat loss from the engine is not increased in pro-

portion to the degree of supercharging. This results in the piston, the exhaust valves and the sparking plugs getting overheated. Due to the higher temperature level, the engine becomes more liable to detonation, as a result of which the compression ratio may have to be lowered. This will reduce the thermal efficiency and so the waste-heat proportion will be increased. Hence the engine will be put to a still more severe problem of heat dissipation.

Thus the engine design should be such that this additional heat may be disposed of easily. In practice the measures adopted are the provision of light high heat-resistant alloys for piston with improved cooling arrangement, sodium cooling of the valves, adequate flow of air around the spark plugs and special finning or water cooling around the hotter parts of the cylinder.

Sometimes, intercooling system in the form of heat exchanger, water or water and methanol injection have also been employed in case of highly supercharged engines such as military aero-engines. Although this results in a reduction in the tendency to detonate, the complications involved are quite large.

Due to all these difficulties, the normal supercharging that is provided in spark ignition engines is to increase the power rating by 20 percent. However, with additional intercooling system, the power rating may be increased even up to 40 to 50 per cent, the maximum permissible pressure being about 900 psi.

It may be noted that supercharging improves the scavenging of the exhaust gases. The mechanical efficiency of the engine is also improved because of the considerable increase in power compared to the slight increase in frictional losses.

2.8 Supercharging Applied to Compression Ignition Engines. The problems involved when supercharging is applied to a C.I. engine are given below:

(a) The danger of knocking is reduced with increased air density, so that the operation of the engine is smoother, better controlled and noiseless.

(b) Due to the suppression of volatility of the fuel, the tendency to knock is reduced, so that the use of fuels with a wider range of cetane numbers is rendered possible.

(c) The increased intake air temperature though reducing the volumetric efficiency of the engine, also assists in combustion unlike its tendency to cause detonation in a S.I. engine.

(d) The combustion in a C.I. engine taking place practically at constant pressure, the maximum pressure developed is not much affected by the variation in the pressure of the intake air. So high pressure supercharging of C.I. engines is possible, thus giving higher power ratings and higher mechanical efficiency, inspite of the higher frictional losses due to heavier reciprocating parts.

To safeguard against the excessive scuffing of the piston rings and liner wear, overloading of the bearings, and the leakage past the cylinder due to the sprinting of the cylinder

head bolts, some design limitations have been imposed. Accordingly the permissible maximum pressure prescribed is 1200 psia corresponding to a supercharge pressure of 2 atmospheres and compression ratio of 15:1. The increase in power rating obtained will be about 40 to 50 per cent.

2.9 Supercharged Spark Ignition Engine versus Supercharged Compression Ignition Engine- From a comparative study of the conditions in the two representative types of engines, it may be inferred that supercharging should normally be applied to a S.I. engine to compensate the deficiency of power arising from the rarefaction of air at high attitude as in aircrafts. With suitable arrangement for intercooling and rich fuel-air mixture it may also be employed for the increase of power rating as in military aircrafts and racing cars. This will reduce the weight and bulk of the engine for a given output at the cost of reduction in fuel economy.

On the other hand, supercharging should be applied to compression ignition engines for the enhancement of power rating under two obvious categories:

(i) Moderate supercharging applied to an engine designed to run under normally aspirated conditions. The compression ratio need not be altered in this case.

(ii) High supercharging applied to an engine designed specifically for the purpose, keeping within limits the permissible maximum pressure. Here a comparatively lower value of compression ratio will be adopted.

Normally the result of supercharging in the above cases is an appreciable improvement in fuel economy and the reduction of weight and bulk of the engine.

It should be remembered that a compression ignition engine, naturally aspirated or supercharged, is always heavier than a spark ignition engine of the same type for the same size and bulk. But the fuel and operating costs are lower. So a spark ignition engine still dominates where the haulage load has to be kept down to a minimum regardless of the cost, as in aircraft and racing car engines. In driving the pumps on natural gas pipe lines and on sewage works, normally supercharged engines, with spark ignition or pilot injection, are used due to the availability of gas in such installations. In all other cases compression ignition engines are most frequently used.

CHAPTER 3

METHODS OF SUPERCHARGING

3.1 Introduction- In a supercharged engine, the charge is admitted to the engine cylinder at a pressure above atmospheric. Hence the compression of the air charge external to the engine is required. Several methods of supercharging have so far been tried and tested and more important of these are enumerated below:

(1) electric motor driven supercharger

(2) engine driven supercharger

(3) Underpiston supercharging

(4) induction ramming

(5) Kadenacy system

(6) exhaust gas turbocharging.

The first method requires a separate power source. Alternatively, if the engine is generating power, some of it will have to be supplied to the supercharger at the expense of the net power available.

The second method where the compressor or blower is driven by the engine itself is one of the most widely used methods. The blowers normally used are either of the centrifugal type or of positive displacement type, most common of these being the Roots, Vane, B.I.C.E.R.A. , Ricardo wobble-plate, Hamilton whitfield, and Lysholm blowers. Reciprocating compressors are used only with slow speed engines, these being costlier, bulkier and less dependable than the rotary blowers. Here a percentage of the engine power is absorbed in driving the

blowers, part of this being offset by the work that the compressed air does upon the piston during the induction stroke.

Under-piston supercharging has been used only in large marine engines of the cross-head type. Obviously there will be two compression strokes in each working cycle of the engine, and, therefore, the volumetric efficiency need not be high. This arrangement was first developed by the Werkspoor Company of Amsterdam and the Anglo Saxon Petroleum Company.

For achieving the ram effect, the ramming pipe arrangement is simple and effective, but the pipe should be tuned so as to induce resonant harmonic air oscillations, the kinetic energy of which will provide the ramming effect. The net increase of power output possible by this method is only 20 to 25 per cent, with the decided disadvantage that the inlet becomes noisy and is often difficult to accomodate conveniently on the engine.

The Kadenacy system utilizes the energy of the exhaust such that the sudden outrush of the exhaust gases produces an instantaneous depression in the engine cylinder, thereby inducing the excess of the fresh charge to be sucked in. However, due to small increase in power output, the system has been confined to two stroke cycle engines only.

The arrangement of pressure charging by exhaust gas driven compressors, popularly known as <u>turbocharging</u>, is most commonly used. Here the pulsating exhaust of the engine drives a turbine, the latter being coupled to either a centrifugal or axial flow compressor.

Out of all the methods, only the second and sixth have survived in connection with the supercharging of internal combustion engines. These will be discussed in detail in the succee-

ding articles under the following two headings:

A. Pressure charging by mechanically driven compressors,

B. Exhaust gas turbocharging.

SECTION A

PRESSURE CHARGING BY MECHANICALLY DRIVEN COMPRESSORS

3.2 Scope of Mechanically Driven Blowers- The blower is meant to furnish the engine with adequate amount of air at a hig charge density under all operating conditions without using up a disproportionate amount of power. It may either be driven mechanically i.e., directly from the engine, or by an exhaust gas turbine in which case it is known as turbocharger. The latter being small r in size and possessing an improved fuel economy is unassailable for the supercharging of large diesel engines of c capacity greater than 10 litres. The working efficiency of these turboblowers in high only over a relatively narrow speed range and that too on the upper side. But where high torque at low speeds is required, as in automobile or earth moving machinery, the gain in fuel economy of a turbo-blower becomes problematical, and the mechanically driven compressor proves to be a real asset. The mission of a constant power engine is also fulfilled only by this class of blowers where the requirement is a high degree of supercharge at low speeds and little supercharge at full speeds.

The economical limit of mechanical supercharging is nearly 30 per cent which gives a b.m.e.p. of slightly more than 100 psi. Above this limit, the power absorbed by the blower is excessive, and the law of diminishing returns holds good. In mechanically supercharged commercial engines, the supercharge pressure is nearly 5 to 7 psi. However, from the performance standpoint, the important characteristics of a blower are its volumetric

efficiency, adiabatic efficiency, and the rise in air temperature across it.

3.3. Volumetric Efficiency- It is a measure of the success of the blower in charging the cylinder with air, and is defined as the ratio of the actual volume of free air inhaled (at S.T.P.) to the swept volume of the piston. Thus the higher the volumetric efficiency, the lower will be the size of the blower required to deliver the required amount of air. The other desirable characteristic is that the volumetric efficiency curve should be flat, so that the delivery is not much affected by the speed and back pressure variations. This will enable the engine to receive fairly the same amount of air per cycle.

3.4 Adiabatic Efficiency- It is defined as the ratio of the work required for adiabatic compression of air to the actual work input to the compressor. The adiabatic efficiency of a compressor is of paramount importance in a mechanically driven supercharger, this affecting both the power consumed by the blower and the temperature rise of air during compression. In practice the usual variation of adiabatic efficiency is between 50 to 80 per cent. The overall mechanical efficiency of the blower is expressed by the adiabatic efficiency itself.

From the point of view of power requirement and temperature rise, the supercharging process should approach isothermal conditions. The advantage obtained is clearly shown in Fig. 3.1.

Isothermal compression may be achieved either by spraying cold water or water and methanol during compression, or by employing multistage compression with intercooling. Cooling has the effect of increasing the charge density which actually is equivalent to increasing the charger efficiency. Upto about 60

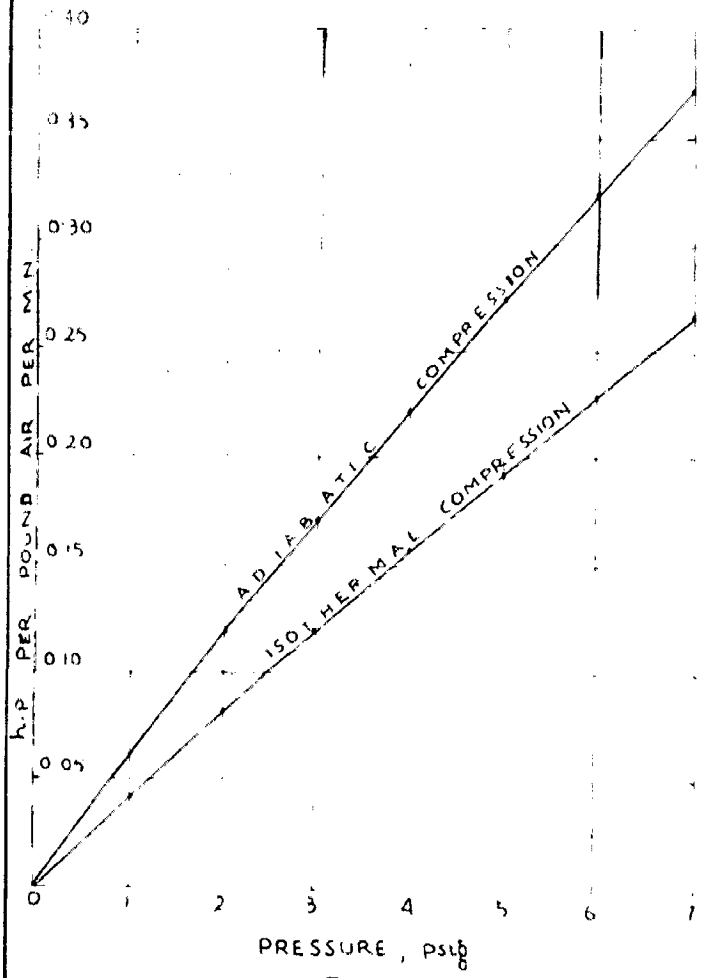

FIG. 3·1.

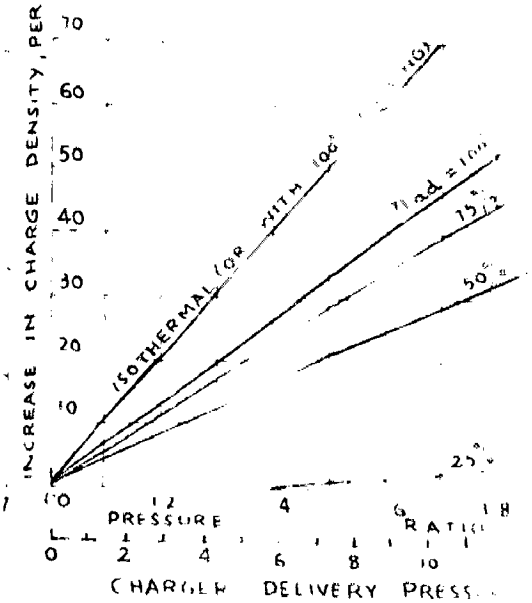

FIG. 3·2.

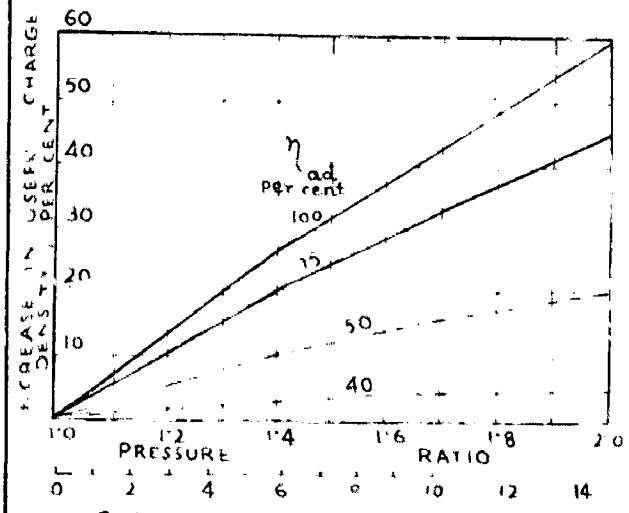

FIG. 3·3.

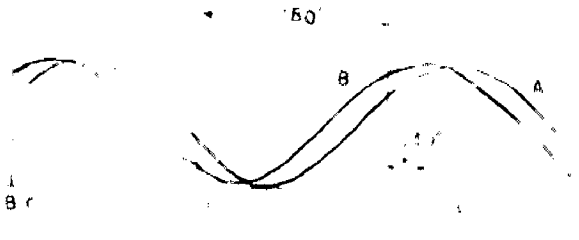

FIG. 3·4.

REFERENCES

per cent, cooling of the air by 10 per cent increases the charger efficiency by 5 per cent. Over 60 per cent cooling gives a more than proportionate improvement. Hence an effort should be made to achieve the maximum possible cooling in practice. But this requires additional equipment and hence becomes more complex. In some applications like road vehicles, intercooling is seldom practicable.

3.5 Charge Density- It should be understood clearly that the function of supercharging is to increase the charge density which depends upon the charge pressure and temperature. This has been illustrated (11) in Fig. 3.2 where it may be observed that for the same pressure ratio the isothermal compression gives the maximum charge density which reduces for adiabatic compression with decreasing adiabatic efficiencies.

It should also be marked that a blower with an efficiency of less than 25 per cent is of no use from the point of view of supercharging. But with further improvement in efficiency there is a rapid increase in charge density, in so much as the 50 per cent line corresponds more or less to that of Roots blower.

In practice, the power required to drive the supercharger is also taken from the engine which actually is obtained by the consumption of a part of the oxygen supplied to it. Thus while estimating for the surplus charge available to give out a power of the engine, suitable deduction for the increased blower input should also be made. This has been done for a typical engine giving 0.43 I.H.P. per cu. ft. per min. of free air supplied, and after deducting the fraction of the total charge that has to be burnt to drive the blower for various efficiencies, the increase in useful charge density for various pressure ratios has been shown (11) in Fig. 3.3. By comparing the figures 3.2 and 3.3 it may be

inferred that for high adiabatic efficiencies, nearly the whole of the additional charge is available for the increase of power output, while at low efficiencies a considerable proportion of it is required to drive the charger. Also an engine-driven charger must have an efficiency of about 40 per cent to give any increase in engine output against the requirement of 25 percent for an externally driven charger.

3.6 Recoverable Blower Work- In practice a part of the work input to the blower is recoverable due to the pneumatic operation of the engine as an air motor during the admission of the high pressure charge. There is no expansion excepting that caused due to the pressure difference occurring on account of the piston displacement. Thus if P_1 be the pressure of the exhaust and P_2 the pressure of the compressed air charge admitted to the engine cylinder, the theoretical recoverable work = $(P_2-P_1).v$, where v is the displacement/volume of the engine. Also, if η_t be the pneumatic transmission efficiency, the actual work recovered per cycle will be $\eta_t (P_2-P_1)v$. The transmission efficiency is about 70 to 80 per cent in practice.

In an actual engine the intake valve opens before the top dead centre and closes after the bottom dead centre to ensure the maximum filling of the cylinder. Any air that does not enter the cylinder during the intake stroke, will not perform any useful work, and so no recovery of power is possible to be made out of it. This will also make the air motor efficiency lower.

3.7 Reciprocating Compressor- Blowers of the reciprocating type are used frequently with slow speed engines, but rarely with high speed engines. The efficiency and delivery characteristics of these blowers are good with the only defect that they are bulkier. The delivery is taken from these compressors into a large receiver

which supplies the compressed air to the engine. Normally each cylinder has its own reciprocating blower, thus rendering it possible for the charging to take place under optimum conditions. The phasing of the compressor and power pistons is very important, because if the two are in phase together, immediately on the opening of the inlet valve a dip will occur in the receiver pressure which will continue for the entire charging period, as a result of which on the closing of the inlet valve, the pressure of the charge will be sufficiently low. Thus in order to ensure the maximum trapped charge to the cylinder, the phasing of the two pistons should be done in such a way that in the beginning the pressure is low, while at the closure of the inlet valve, the pressure is the maximum. This has been explained by Fig. 3.4 in which the inlet valve opens 80° before top dead centre position and closes 40°after the bottom dead centre position. A and B are two single acting compressors with different phase angles. It may be seen that the pressure of the air delivered by A reaches a maximum after the inlet valve closes, but, that of the air delivered by B is the maximum at the very instant of the closure of the inlet valve. Thus the phasing of the compressor B for the given valve timings is ideal.

The PV diagram for a reciprocating air compressor is shown in Fig. 3.5 where the air is compressed from a pressure P_1 to P_2. Neglecting the intake surges, valve resistance and temperature effects caused by the valves, we have from the polytropic compression line,

$$P_1 V_4^n = P_1 (V \text{ disp} + V_{cl} - V)^n = P_2 V_{cl}^n.$$

Thus volumetric efficiency,

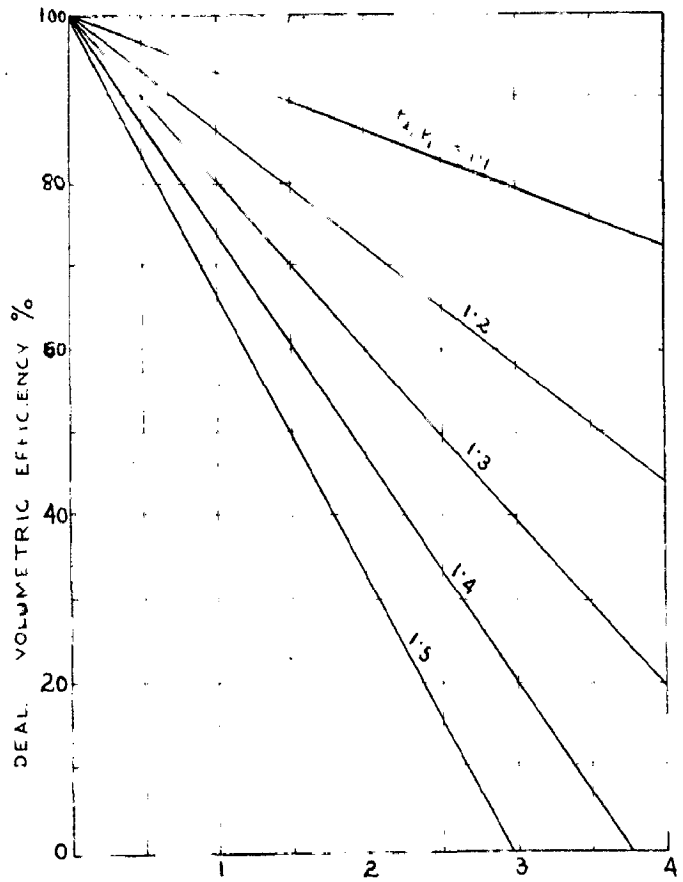

FIG. 3·6.

REF 15.

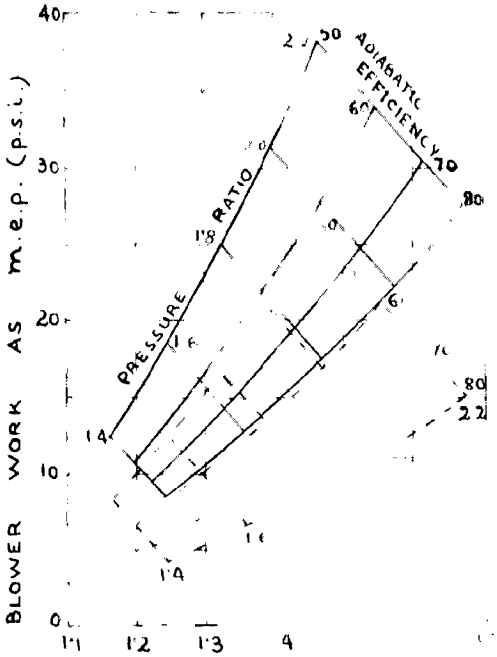

WORK TO DRIVE SUPERCHARGER

FIG 3·8

— — — GROSS WORK

- - - NET WORK

REF 1

$$= \frac{V}{V_{displ.}} = 1 - \frac{V_{cl.}}{V_{displ.}} \left[\left(\frac{P_2}{P_1}\right)^{\frac{1}{n}} - 1 \right] \quad \ldots(3.1)$$

A plot of the volumetric efficiency against the relative clearance volume is shown in Fig. 3.6, assuming n=1.35. It should be noted that the effect of clearance volume upon the volumetric efficiency is very much pronounced at high discharge pressures. From the ideal volumetric efficiency values, about 5 to 10 per cent should be deducted to account for the slippage, which increases with the speed. That is why the volumetric efficiency of reciprocating blowers is sufficiently high at low speeds which justifies its use for the supercharging of slow speed engines. The value of volumetric efficiency varies from 70 - 80 per cent.

The work required per cycle by the compressor is given by

$$W = P_2 V_2 + \frac{P_2 V_2 - P_1 V_1}{n-1} - P_1 V_1$$

$$= \frac{n}{n-1} (P_2 V_2 - P_1 V_1)$$

$$= \left(\frac{n}{n-1}\right) P_1 V_1 \left[\left(\frac{P_2}{P_1}\right)^{\frac{n-1}{n}} - 1 \right] \quad \ldots.(3.2)$$

Thus if N be the number of complete cycles per min. for the compressor the horse-power required to drive the compressor under ideal conditions

$$= \frac{P_1 V_1 \left(\frac{n}{n-1}\right) \left[\left(\frac{P_2}{P_1}\right)^{\frac{n-1}{n}} - 1 \right] \times N}{33{,}000} \quad \ldots.(3.3)$$

Also the adiabatic efficiency of compressor,

$$\eta_{ad} = \frac{P_1 V_1 \left(\frac{\gamma}{\gamma-1}\right) \left[\left(\frac{P_2}{P_1}\right)^{\frac{\gamma-1}{\gamma}} - 1 \right] \times \frac{N}{33{,}000}}{\text{b.h.p. required to drive the compressor}} \quad \ldots(3.4)$$

It should be remembered that the Pv diagram shown i

Fig. 3.5 is for the ideal conditions. For an actual case the indicator diagram will be somewhat similar to the one shown in Fig. 3.7

For a compressor employing multistage compression, say from a pressure P_1 , P_2 to P_3 and P_3 to P_4 etc., with intercooling between the stages, total work done per cycle will be

$$W = \frac{n}{n-1}\left[P_1V_1\left\{\left(\frac{P_2}{P_1}\right)^{\frac{n-1}{n}}-1\right\} + P_2V_2\left\{\left(\frac{P_3}{P_2}\right)^{\frac{n-1}{n}}-1\right\} + P_3V_3\left\{\left(\frac{P_4}{P_3}\right)^{\frac{n-1}{n}}-1\right\}\right] \quad \ldots\ldots(3.6)$$

In case the cooling be 100 per cent efficient, $P_1V_1 = P_2V_2 = P_3V_3$, so that

$$W = P_1V_1\frac{n}{n-1}\left[\left(\frac{P_2}{P_1}\right)^{\frac{n-1}{n}} + \left(\frac{P_3}{P_2}\right)^{\frac{n-1}{n}} + \left(\frac{P_4}{P_3}\right)^{\frac{n-1}{n}} - 3\right] \quad \ldots\ldots(3.6)$$

It may also be shown that for maximum efficiency equal work should be done in all the stages, and the air should be cooled to the initial temperature between the stages.

The effect of recoverable work and of intercooling on the work to drive the supercharger has been shown by Millington (12) in figures 3.8 and 3.9. The gross work expended on the supercharger

$= \frac{1}{\eta_{ad}} \cdot \frac{\gamma}{\gamma-1} \cdot P_1V_1\left[\left(\frac{P_2}{P_1}\right)^{\frac{\gamma-1}{\gamma}}-1\right]$, and the recovered work is $\eta_t(P_2 - P_1)V_2$, where η_t is pneumatic transmission efficiency.

Thus the net work to drive the supercharger

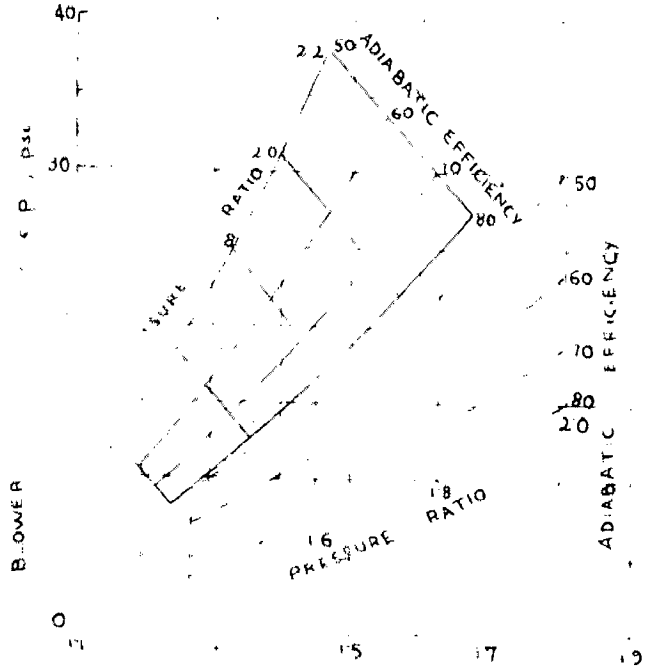

ME RATIO, $\frac{V_1}{V_2}$

R VE SUPERCHARGER

NET WORK

FIG 3·9.

WORK WITHOUT INTERCOOLING

NET WORK WITH INTERCOOLING TO 50°C

REF 12

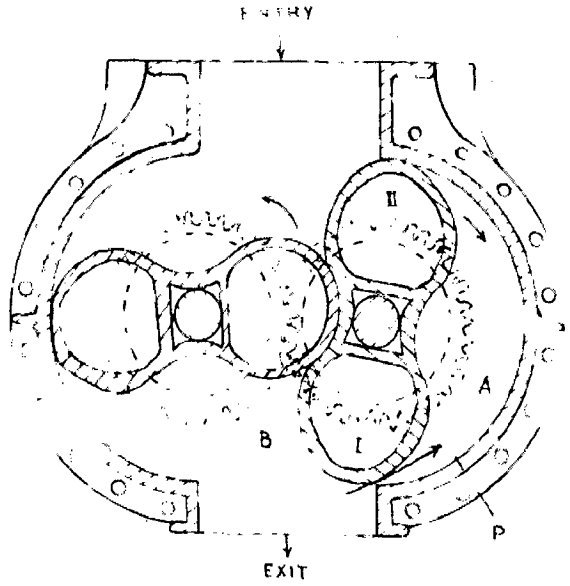

FIG 3·10.

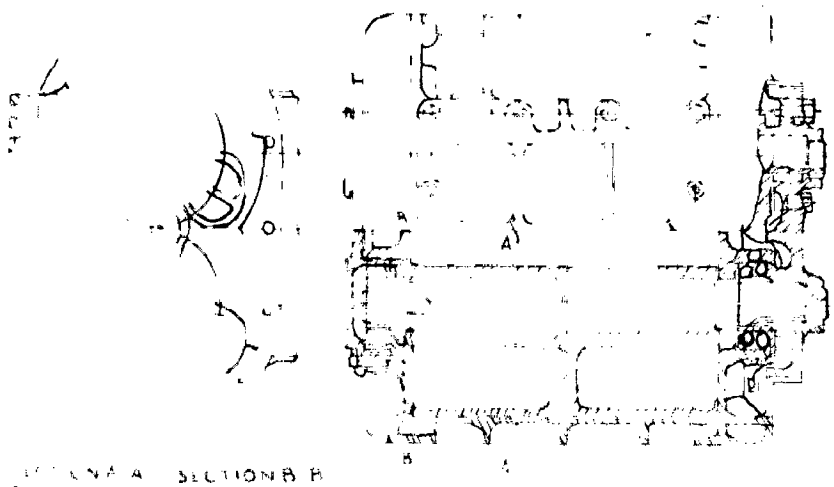

THREE-LOBE BLOWER

FIG 3·11

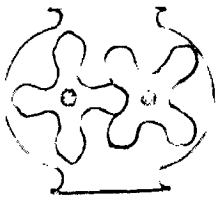

FIG 3·12

$$= \frac{1}{\eta_{ad}} \cdot \frac{\gamma}{\gamma-1} \cdot P_1 V_1 \left[\left(\frac{P_2}{P_1}\right)^{\frac{\gamma-1}{\gamma}} - 1 \right] - \eta_t (P_2 - P_1) V_2,$$

which when expressed in terms of the engine mean effective pressure is given by

$$P_e = P_1 \cdot \frac{V_1}{V_2} \cdot \frac{1}{\eta_{ad}} \cdot \frac{\gamma}{\gamma-1} \left[\left(\frac{P_2}{P_1}\right)^{\frac{\gamma-1}{\gamma}} - 1 \right] - \eta_t (P_2 - P_1) \quad \ldots(3.7)$$

Assuming 70 per cent as the typical value of the transmission efficiency, a plot of the gross and net blower works has been made in Fig. 3.8 for the different volume ratio, pressure ratio and adiabatic efficiency. The volume ratio is also sometimes called the boost ratio, because this in effect is the ratio of air mass flow for the engine supercharged and naturally aspirated. It should be marked that with the increase in adiabatic efficiency, the blower work is considerably reduced. Also the pressure ratio required decreases which will reduce the intake temperature as well.

Fig. 3.9 is similar to Fig. 3.8 with the difference that here intercooling to 50°C (122°F) is also employed. The upper continuous diagram represents the gross work and is exactly the same as shown in the previous figure. The lower dashed diagram also shows the ~~gross~~ net work but with intercooling. It should be noticed that the intercooling reduces the blower work considerably, so it is of much consequence when the blower efficiency is poor. The only difficulty is with the intercooler whose size is fairly large.

3.8 Roots Blower- It is the simplest and the most commonly used of all the positive displacement blowers. Fig. 3.10 illustrates diagrammatically in cross- section a Roots blower which consists

essentially of two displacing elements known as impellers. These are geared externally as shown, and have fine clearances (radial 0.004 to 0.003 in., and end clearance 0.01 to 0.02 in.) between the casing and the lobes of the impellers. The impellers also do not touch each other and are separated by a fine clearance nearly of the same order. The impellers may have two, three or four lobes of the epicycloidal form as shown in figure 3.10, 3.11 and 3.12 respectively. Due to the plain rotation of the independent elements of the Roots blower, the unbalanced inertia forces are completely absent, and so the blower may be operated upto a speed of 7,000 r.p.m.

Here air is drawn into a definite displacement volume between the casing and the lobes, which is then carried around to the discharge port without compression. As soon as the outlet port is uncovered by the impeller, the high pressure medium from the receiver flows back irreversibly and raises the pressure of the displaced air instantaneously to the receiver pressure. With the further rotation of the impeller, the mixture of the trapped air and the back flow from the receiver is discharged into the receiver.

Since the trapped air has not been compressed by the impellers, the volume of the air during its passage through the blower remains constant. This cycle of operation has been represented by ABCD in Fig. 3.13 . But in actual practice it is not so elementary, as pointed out by Tryhorn (11) who studied it by means of a pressure pick-up fitted to the blower casing at P. Thus when the space A is completely filled up with air, and the lobe tip I passes the edge of the delivery port, the pressure

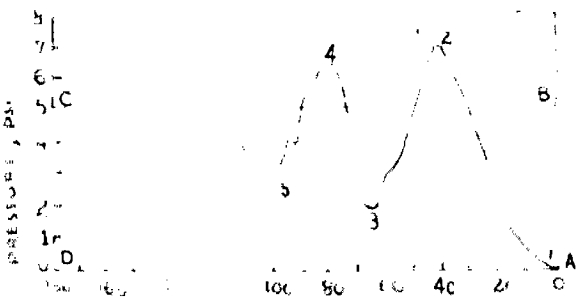

DEGREES IN DEGREES

PRESSURE POSITION DIAGRAM
AT DELIVERY PRESSURE PSI

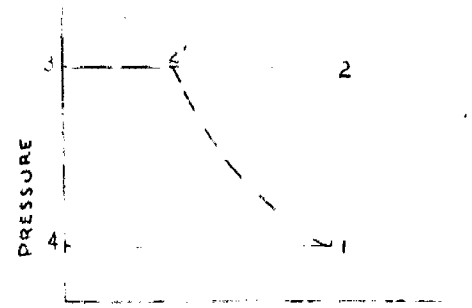

VOLUME

FIG 3-A

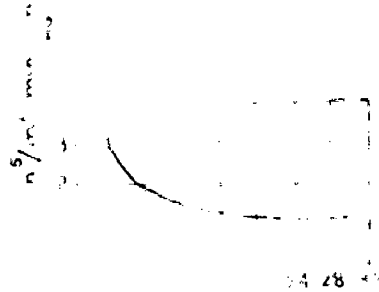

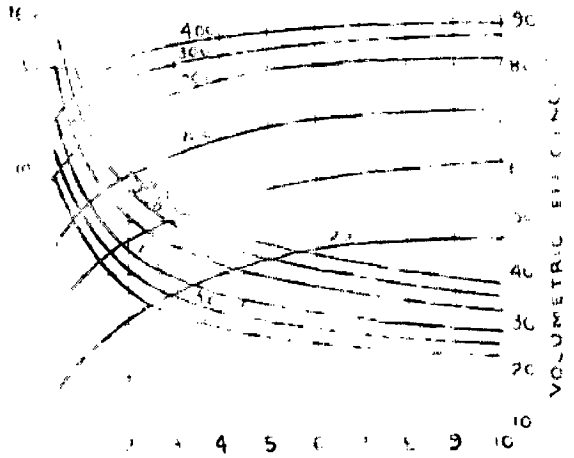

RPM

FIG

INCHES IN HG A

CHARGE INCHES IN HG

REF 13

of the delivery space B being higher than A, a pressure wave is set up. It travels with the velocity of sound in the medium which is a few times greater than the lobe tip speed. Thus during the time the lobe has moved by about 10 - 15 deg., the wave impinges upon the tip II and so is reflected back with an increased intensity. This has been represented by 1 - 2 in Fig. 3.13. After the wave has reached back the space B, it expands and so a depression wave is formed. This also propagates through the space and is reflected back as shown by 2-3. The pressure of the delivery space B being higher again than the space A, another compression wave is set up indicated by 3-4 in the diagram. Again the depression wave is produced (4-5) and the same process is repeated till the lobe tip II passes the pressure pick-up point P. This shows that in a Roots blower, the air is not displaced simply, but is also subject to violent pressure pulsations that are set up within the casing as well as the duct.

As the impellers have to displace the volume v_1 against the pressure difference (p_2-p_1), the theoretical work of a Roots blower is given by the area 1-2-3-4 (Fig. 3.14) and is equal to

$$W_{roots} = v_1 (p_2-p_1) \qquad ..(3.8)$$

Now if the compression were adiabatic with no loss due to eddying or friction, the work done in the ideal isentropic compressor would be given by 1-2+3-4, i.e.

$$W_{comp.} = \frac{\gamma}{\gamma-1} \cdot p_1 v_1 \left[\left(\frac{p_2}{p_1} \right)^{\frac{\gamma-1}{\gamma}} - 1 \right]$$

The ratio of the above two is designated as the <u>type efficiency</u> or adiabatic efficiency of the Roots compressor, so that the type efficiency

$$= \frac{\text{isentropic work}}{\text{actual work in a Roots blower}}$$

$$= \frac{W_{comp.}}{W_{Roots.}} = \frac{\frac{\gamma}{\gamma-1} \cdot p_1 v_1 \left[\left(\frac{p_2}{p_1}\right)^{\frac{\gamma-1}{\gamma}} - 1\right]}{v_1 (p_2 - p_1)}$$

$$= \frac{\gamma}{\gamma-1} \left[\frac{R^{\frac{\gamma-1}{\gamma}} - 1}{R-1}\right] \qquad \text{where } R = \frac{p_2}{p_1} \qquad \text{..(3.9)}$$

It should be noted that as R increases, the type efficiency decreases, which means that the Roots blower is suited only for small pressure ratios, say up to 1.5.

Some amount of leakage always takes place through the clearances between the two impellers and the casing, the effect of which is to reduce the volumetric efficiency. The rate of leakage is proportional to the clearances and the pressure difference, and is more or less unaffected by speed. Schopper (13) has suggested that the leakage may be taken equal to cpk(1+d).. ...(3.10)

where c = radial clearance, in.

p = pressure difference, in. Hg.

l(ℓ) = length of rotor (impeller), in.

d = diameter of rotor, in.

k = a flow coefficient, which has been plotted for various pressure differences in Fig. 3.15.

Now blower displacement per revolution

$$= 2 \cdot \frac{\pi}{4} d^2 \cdot l - 2 \cdot a_r \cdot l$$

$$= \frac{\pi d^2 l}{2} \left(1 - \frac{4 a_r}{\pi d^2}\right) \qquad \text{...(3.11)}$$

where a_r = area of cross-section of the rotor.

Hence the blower capacity per min.,

$$Q = \frac{\pi}{2} d^2 l n \left(1 - \frac{4 a_r}{\pi d^2}\right) - cpk(1+d) \text{ in.}^3 \qquad \text{...(3.12)}$$

n being the rotor speed in r.p.m.

$$\text{or} \quad Q = K_1 \left(\frac{l}{d}\right) d^3 n - K_2 \left[\left(\frac{l}{d}\right) d + d\right] \qquad \text{---(3.13)}$$

where K_1 and K_2 are constants.

Also volumetric efficiency of the blower,

$$= \frac{\text{Volume of air displaced (at intake conditions)}}{\text{blower displacement volume}}$$

Explain

$$\left\{ \begin{aligned} &= \frac{Q}{\frac{\pi d^2 l}{2}\left(1 - \frac{4ar}{\pi d^2}\right)} = \frac{Q}{K_1 \left(\frac{l}{d}\right) d^3 n} \; ? \\ &= 1 - \frac{K_2}{K_1} \frac{1 + \left(\frac{l}{d}\right)}{d^2 n \left(\frac{l}{d}\right)} \qquad (3.14) \end{aligned} \right.$$

Eliminating $\left(\frac{l}{d}\right)$ between equations (3.13) and (3.14) and differentiating the expression for volumetric efficiency with respect to the rotor diameter, and equating to zero, we get

the optimum rotor diameter,

$$d = \sqrt[3]{\frac{Q}{K_1 n} + \sqrt{\frac{Q^2}{K_1^2 n^2} - \frac{K_2^3}{K_1^3 n^3}}} + \sqrt{\frac{Q}{K_1 n} - \sqrt{\frac{Q^2}{K_1^2 n^2} - \frac{K_2^3}{K_1^3 n^2}}} \quad \text{...(3.15)}$$

From equations (3.14) and (3.15), a plot of the volumetric efficiency and the optimum rotor diameter against rotor speed has been shown in fig. 3.16 for different values of the blower capacity. It should be observed that the volumetric efficiency of the blower is fairly constant over a wide range of speeds except at very low speeds, for which the reciprocating compressor is the ideal choice. This determines the suitability of the blower for a fairly large range of speeds on the higher side where the rotor diameter required will also be fairly small.

Fig 3.17 shows the performance curves for a Roots blower. It may be seen that with the increased boost pressures, the temperature of the air goes on increasing. Though the volumetric effi-

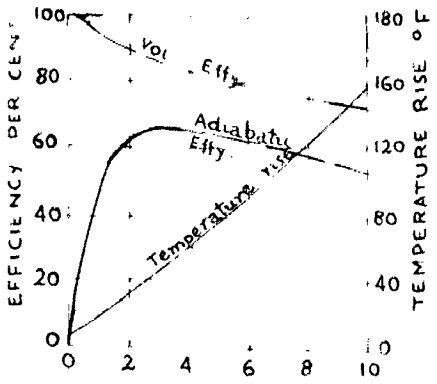

PERFORMANCE OF ROOTS BLOWER

FIG. 3·17

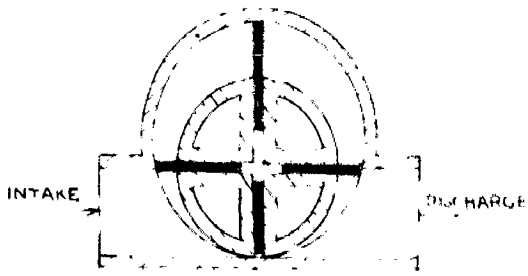

MULTIVANE BLOWER

FIG 3·18

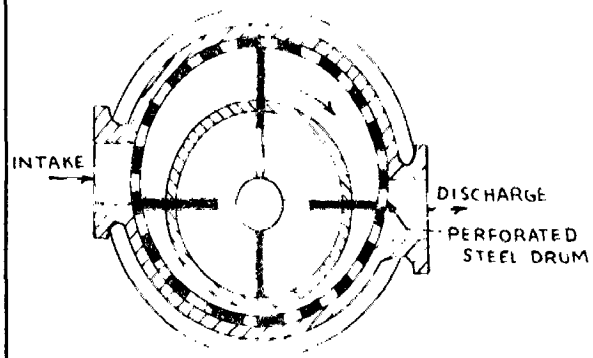

REAVELL COMPRESSOR

FIG. 3·19

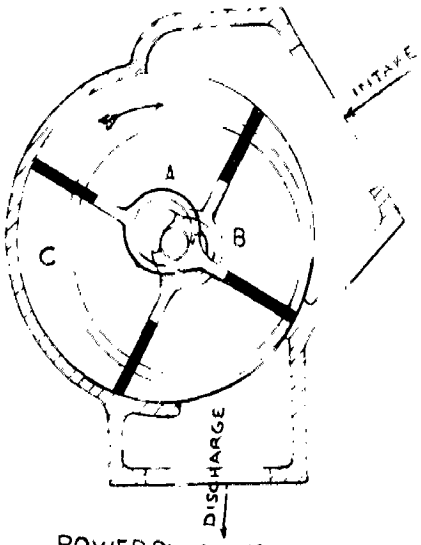

POWERPLUS VANE BLOWER

FIG. 3·20.

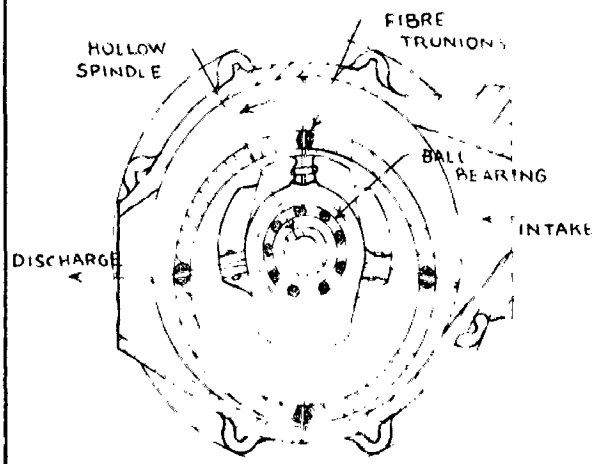

CENTRIC BLOWER

FIG. 3·21.

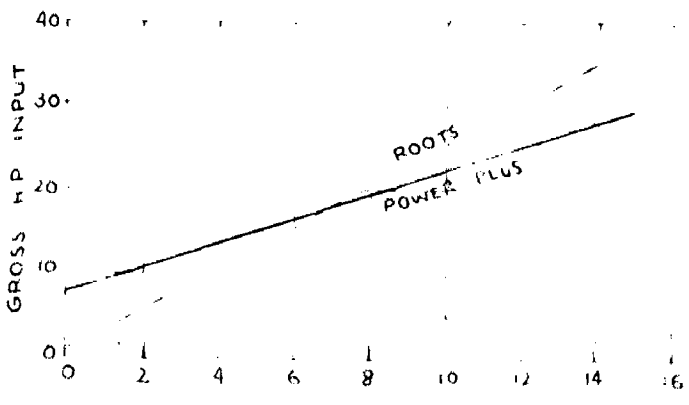

FIG 3·22.

ciency decreases with the degree of supercharging, but the rate is very slow. The lowest value of volumetric efficiency is about 75 per cent for the discharge pressure of 10 psig. The adiabatic efficiency of the blower is also sufficiently high for discharge pressures of 2 to 10 psig.

In practice, Roots blowers have been used most frequently for supercharging of automotive and stationary engines for power outputs of 30 to 50 per cent above the unsupercharged value.

3.9 Vane-Type Blowers- It has been shown that a Roots blower is suited for pressure ratios up to 1.6 only due to the increased leakage loss at higher pressure ratios and the difficulty of maintaining constant clearances at high speeds. To overcome these difficulties, an eccentric drum compressor was introduced. The drum is mounted eccentrically with respect to the fixed cylindrical casing, and has slots cut longitudinally in which the metal blades or vanes can slide. The latter may be either automatic, spring loaded or mechanically actuated. The simplest example of the type is the multivane blower shown in Fig. 3.18. The blower may have either 1,2,3, or 4 vanes. Here, too, after the air is trapped, it is carried around circumferentially within the chambers separated by vanes, such that air undergoes some amount of compression which is more or less insignificant, because the improvement in adiabatic efficiency is too meagre. Thus the device operates mainly like a Roots blower with a fairly uniform delivery and backflow of compressed air upon uncovering the vane space.

In the earliest form of these blowers, the vanes were held in sliding contact with the inner surface of the casing, so they were not found suitable for high speed operation as in

engine supercharging. Thus to overcome this blade friction and wear difficulty, some modifications were introduced. This brought into existence the Reavell Compressor shown in Fig.3.19. Here an additional component is the perforated steel drum which is free to roll on the inner surface of the casing. Thus when the drum rotates, the vanes are also carried along with it, but the relative speed of sliding of the vanes upon the rotating sleeve is lower which obviates to some extent the friction and wear difficulty. This blower is capable of operating at about 2,000 r.p.m. against the multivane blower which runs at 1,000-1,500 r.p.m.

A further modification introduced was in that the vanes were not allowed to contact with the casing, but were held slightly apart so as to preserve a small clearance between the ends of the vanes and the inner surface of the casing. The powerplus vane blower of the type is shown in Fig. 3.20. Here the vanes are mounted on eccentrics A and B which rotate round a fixed point, eccentric to the drum C. The vanes are capable of sliding in the narrow slots cut for them in the drum, their movement being controlled by virtue of the rotation in such a way that a small clearance is always left between the vane tips and the casing surface. Thus the sliding friction has been completely done away with in this case. Such blowers have been employed with success at speeds upto 2,500 r.p.m. on the racing motor-cars, and tried experimentally on the aero-engines as well.

Another example of the above type is the Centric Blower shown in Fig. 3.21. It has a distinguishing feature apart from those described above that the vanes or blades are radial to the fixed cylinder casing. These are supported on trunion blocks

which are slotted cylindrical rods of Fabroil, and permit some amount of rocking and wobble. The drum carrying the vanes is still mounted eccentric on its own ball bearings, and is driven from the hollow central spindle through a pair of external and internal gears. The vanes being diametrically opposite to each other are counter balanced and so produce little load on the ball bearings. The vanes do not touch the casing, but are kept apart from the casing by fine clearances. The casing and end plates are made of aluminium and magnesium alloy, whereas the vanes are of heat treated nickel chrome steel.

This type of blowers give satisfactory operation at speeds upto 3,000 r.p.m., and are capable of maintaining pressures of 30 lb. per sq. in. above atmospheric and even higher. They maintain a good volumetric efficiency even at low speeds.

The vane type of blowers give pulsating discharge, the frequency depending upon the number of vanes in the compressor. As such they cannot be connected directly to the inlet ports of the engine. In practice, they discharge into an air receiver which communicates with the inlet ports of all the cylinders. However, the discharge from a single vane blower is identical to that of a reciprocating compressor, and so the maximum filling of the cylinder can be obtained by proper phasing.

The volumetric efficiency of the vane type of blowers varies between 75 and 96 per cent, and the adiabatic efficiency between 40 to 70 per cent, the nature of the curves being the same as in Fig. 3.17.

The comparison of the performance of a vane type of blower and a Roots blower, was made out in a recent American report (14) given in Figs. 3.22 and 3.23. Both the superchargers-

Roots and Powerplus, were designed for an aero-engine, the latter having a compression ratio of 1.53. Fig. 3.22 shows gross horse-power input to the blowers at 2000 r.p.m. for pressure differences of 0 to 15 in. of mercury. It may be observed here that the power to drive the Powerplus at zero pressure difference was about eight times that for the Roots blower, which is mainly due to its greater mechanical loss and fixed compression ratio. But the rise in the power input is considerably less for the Powerplus than for the Roots, which makes the horsepower input the same at a pressure difference of about 7 in. Hg. for both the superchargers. At higher values of the pressure difference, the Powerplus is decidedly more economical than the Roots blower which justifies the wide spread use of vane blowers for increased pressures.

Fig. 3.23 shows the gross h.p. per lb. of air/per sec. for various pressure differences for these blowers. It should be noted that this takes into account the change of volumetric efficiency as well. At low pressure ratios the Powerplus absorbs more of power due to low mechanical efficiency. But it improves upon its compression efficiency till at a pressure ratio of $(1.53)^4 = 1.81$, corresponding to a pressure difference of 12. in. of mercury, it equals the power input to that of the Roots blower. Higher up the compression efficiency again falls down, thus increasing the mechanical friction at large pressure differences. This shows that whereas the Roots blower yields an economic and satisfactory performance upto pressure ratios of 1.6, the vane type of blower can give good results for pressure ratios upto 1.6 - 2.0.

3.10 Screw-Type Blowers- The axial flow rotary blowers of the

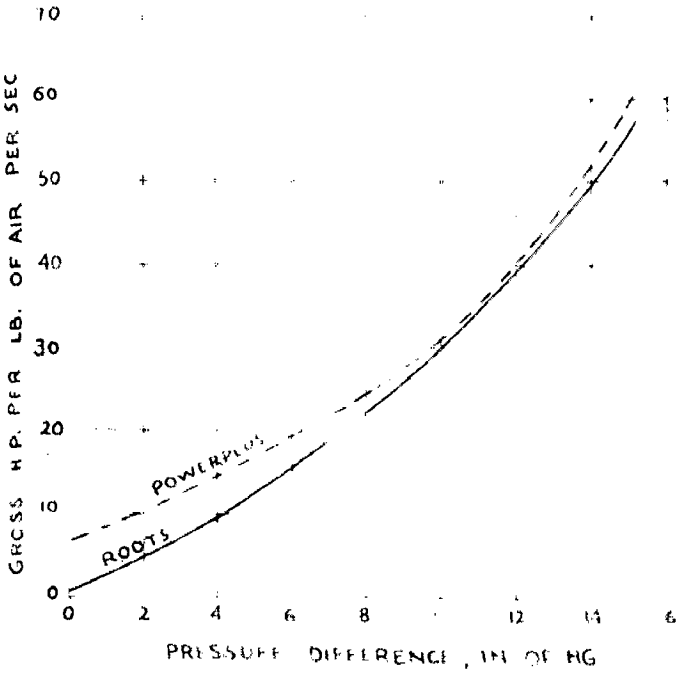

FIG. 3-23

REF. 14

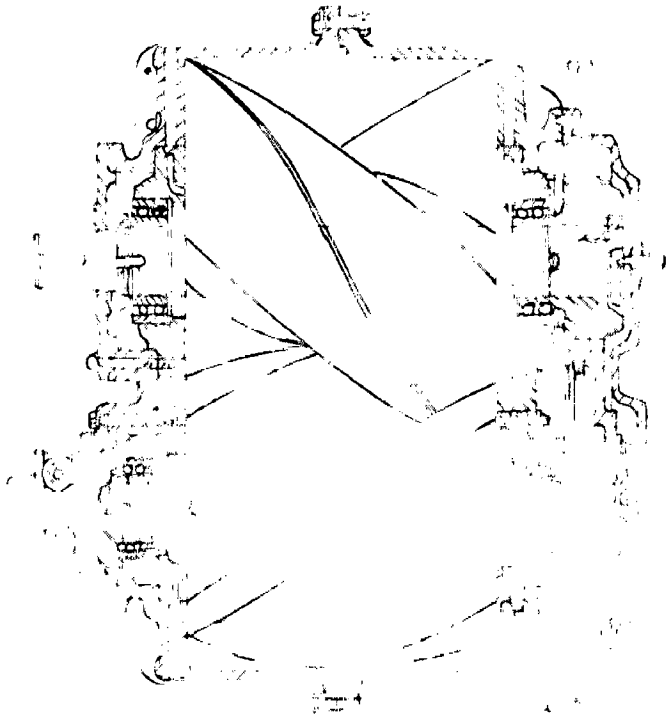

SECTIONAL VIEW OF HAMILTON WHITTIER AXIAL FLOW BLOWER

FIG. 3-24

screw type pertain to more recent developments in the field of lobe-type blowers. They eliminate a few defects of the Roots blowers without affecting their simplicity and operating characteristics. There are two representative blowers of the type- Whitfield blower and the Lysholm blower. Here the displacement of the air is not in the circumferential direction, but along the axis, such that while it is transported from the inlet to the outlet side, the air undergoes progressive positive adiabatic compression. This yields an improved adiabatic efficiency. Also due to the elimination of the sudden back flow of the compressed air into the lobe space, the operation is noiseless.

The Hamilton- Whitfield blower, first manufactured by the General Machinery Corporation of Hamilton, Ohio, in 1943, is shown in Fig. 3.24. There are two rotors in the form of helically threaded members and mounted on ball bearings. They are geared together, but the bulk of the driving effort is transmitted by aerodynamic forces, the timing gears transmitting only 2 to 3 percent of the driving power. The male rotor meshes with the female rotor as explained (15) pictorially in Fig. 3.25, such that there is a continuous sealing line over the whole length of their engagement. The edges of the rotor are sealed by the housing, thus rendering the flow of air (from entry to exist) possible only through the troughs of the threads.

The moment the rotors disengage, the space between the lobes and the casing is left open to suction permitting the air to be sucked in. The space increases gradually, so more and more and of air flows in till it is cut off from the intake side, so that the air is completely trapped within the space. Further rotation of the rotors causes the reduction in the space thus

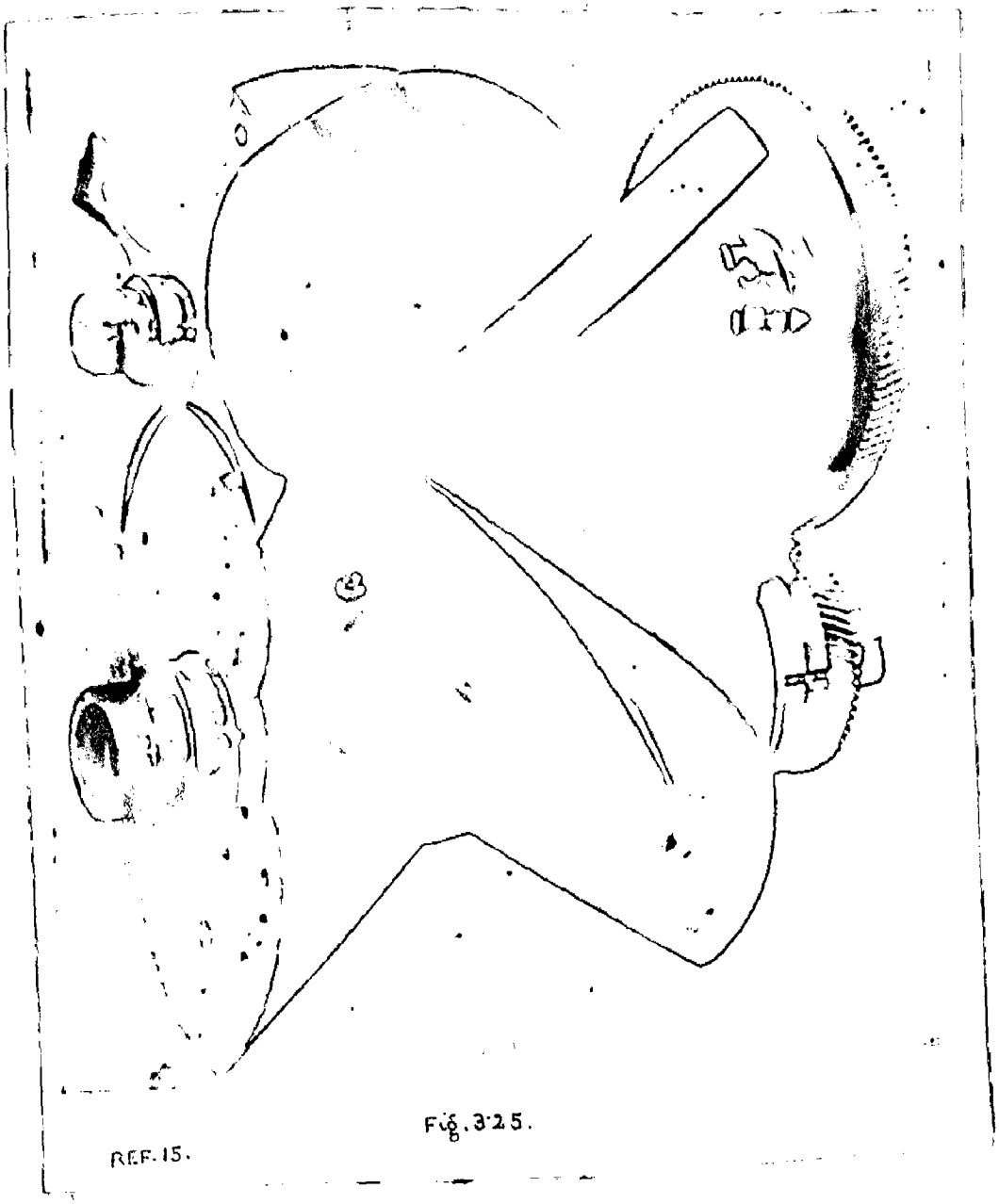

Fig. 3·25.

REF. 15.

producing adiabatic compression of air which is then delivered to the discharge end.

The adiabatic efficiency of these blowers ranges from 70 to 76 per cent and volumetric efficiency from 88 to 92 per cent. Pressure ratios up to 4 are available satisfactorily within the speed range 1,000 to 10,000 r.p.m.

The Elliott - Lysholm Blower, invented in 1943 by Alf Lysholm of the Ljungstrom Steam Turbine Company of Stockholm, Sweden, and manufactured by Elliott Company, Jeannette, Pa., is shown in Fig. 3.26. The intermeshing of the rotors is shown in Fig. 3.27 (16). The working of the blower may be described in the words of Lysholm (15), " A charge is initially enclosed in the space bounded by the tooth flanks, casing bore and end walls. The rotor helices are so chosen that a particular thread space is completely filled and sealed off from the suction just as it is entered at its opposite end by a co-acting lobe of the other rotor. Further rotation establishes an axial seal, which separates this charge from the charge in the succeeding grooves. As rotation proceeds, this seal moves axially effecting a reduction in volume of the charge and a substantially adiabatic compression. When the leading lobes of the grooves pass the boundaries of the discharge port, the compressed medium is brought into communication with the discharge. The location of the port thus determines the built-in compression ratio".

The performance curves (15) of an Elliott Lysholm 3 cuor are shown in Fig. 3.28. The capacity of the blower selected was 10,000 cfm. with a built-in pressure ratio of 1.85. The volumetric efficiency is as good as 100 per cent and the adiabatic efficiency about 82 per cent. The performance of the blower at high speeds and large pressure ratios is better. With Whitfield blowers also,

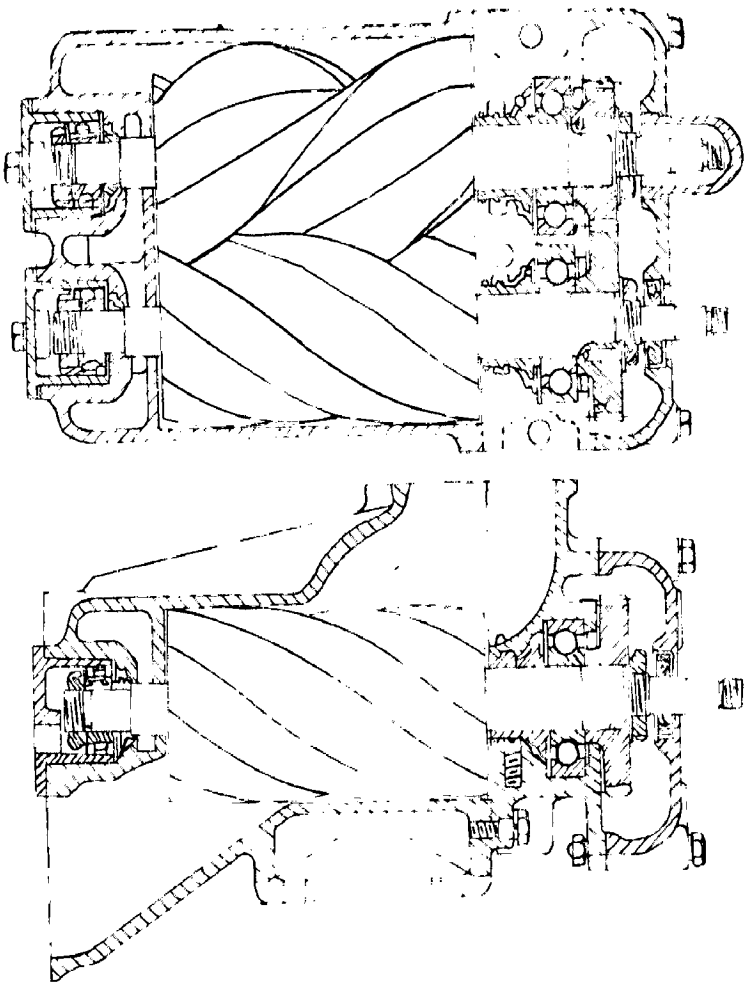

SECTIONAL VIEW OF ELLIOTT-LYSHOLM
AXIAL FLOW BLOWER
FIG. 3.26.

REF 36.

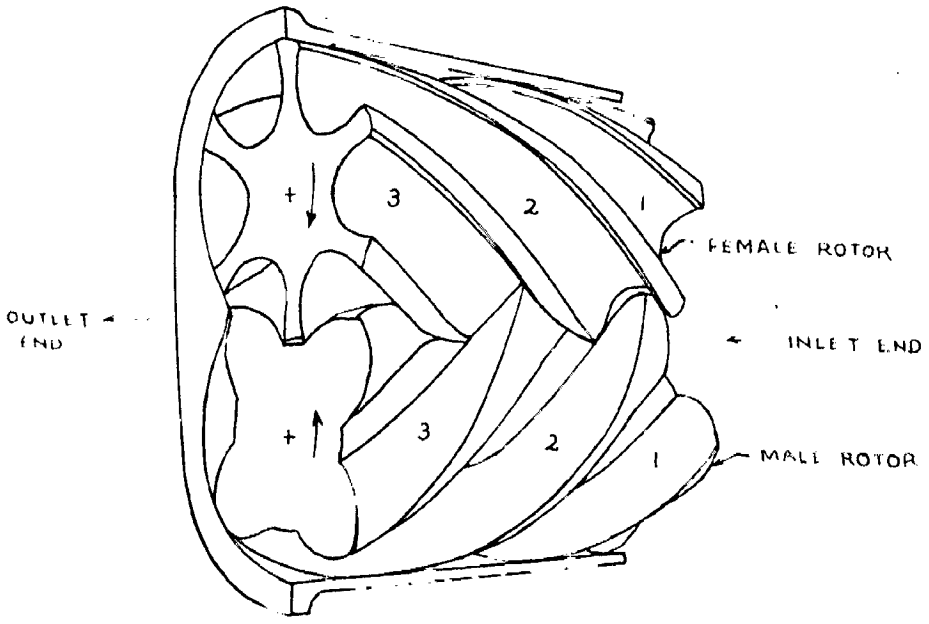

FIG 3.27.

REF 16.

equally good results have been obtained. The Lysholm blower is also suited for pressure ratios upto 4.

3.11 B.I.C.E.R.A. Compressor- The British Internal combustion Engine Research Association has developed recently the Meera compressor for charge pressures of 7 to 20 psi required to increase the engine output by atleast 30 per cent. It is more or less on the Roots blower version, but decidedly more complicated than it is. Unlike the Roots positive displacement blower, here the internal compression of the charge also takes place, so the adiabatic efficiency of the compressor is better.

The construction of the Meera compressor (11) is clear from Fig. 3.20, where there are two cylinders geared to run together within a casing. Each of the cylinders carries two lobes which rotate with a small clearance within the double cylindrical casing. The rotors embrace the slotted tubes, attached to the casing. The tubes function as the stationary members of the rotary valves and serve as ducts to feed the air into and out of the machine.

The cycle of operations may be understood by following the path of a single air charge through the compressor which has been explained in Fig. 3.20. At 1 the intake of air commences, continues during 2 and 3 and is at the point of closing in 4. The charge is now divided in two parts and is undergoing compression by the leakage air which leaks past the leading lobes from the other side where the compression is over. The leakage compression continues till at 7 the direct compression starts due to the dipping of the lobe into the carry-round volume. The reduction of volume continues and so the compression progresses more and more, till at 9 the delivery of the compressed air charge starts which ends at 12. It should be noted that the twelve positions illustrated cover one

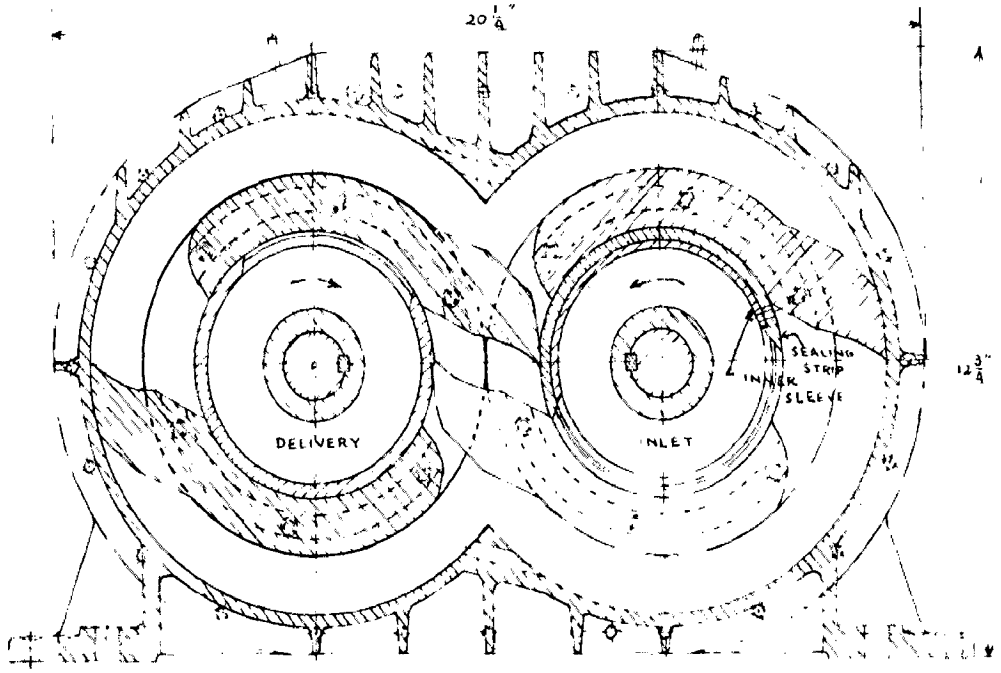

REF. 11

BICERA COMPRESSOR

FIG 3.2)

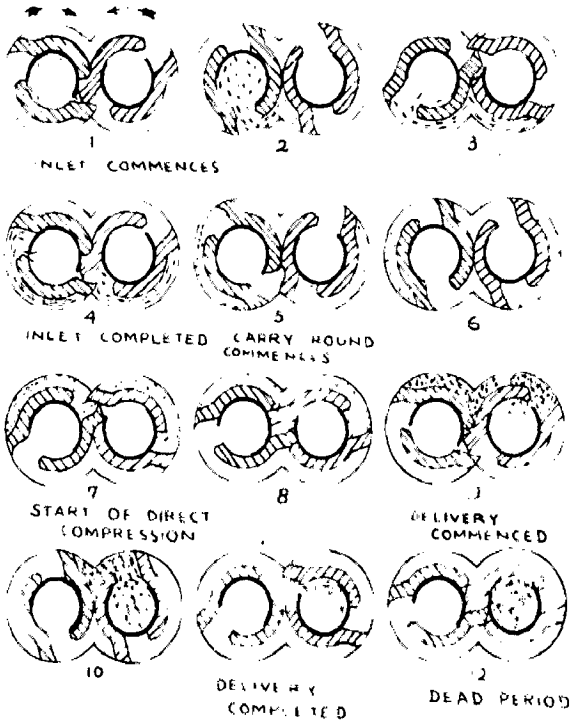

DIAGRAMMATIC PATH OF A SINGLE AIR CHARGE THROUGH BICERA COMPRESSOR

FIG. 3.3C

ATMOSPHERIC AIR
LEAKAGE COMPRESSION
COMPRESSED AIR

REF. 1

and a half revolution, and during this interval the charge has been admitted thrice (at 1 or 2, 5 and 10) and similarly delivered thrice. Thus there are two inlet and delivery periods per revolution.

The above cycle of events has been illustrated on the P-V diagram shown in Fig. 3.31. In order to make the diagram self-explanatory, the same numbers have been marked as in Fig. 3.30 to represent the various cycle events. The suction pressure is a little lower than the atmospheric pressure which represents the inlet depression necessary to create the flow. The flow velocity is kept to a minimum, because it cannot be recouped here as in aerodynamic machines by diffuser action.

The advantage of the tubular valve lies in its facility to alter the port opening periods while the compressor is running. This makes the adjustment of the delivery characteristics of the compressor to suit engine requirements possible. For this purpose the tubular valve is provided with an inner sleeve which supports a sealing strip forming the port edge, as shown in Fig. 3.29 on the inlet side. Same arrangement may be provided on the delivery side as well, but for supercharging of internal combustion engines, the delivery pressure is best controlled by a control of the inlet period. This is illustrated by Fig. 3.32. The full line diagram 1 represents the normal operation of the compressor, where AB is the suction volume which is compressed to CD, the swept volume of the engine per cycle. In the broken-line diagram 2, due to the early closure of the inlet valve, even after full internal compression, the pressure EF is reached which is much lower than CD. In diagram 3 the internal compression being equal to the internal expansion, the engine runs in the unsupercharged condition. For very

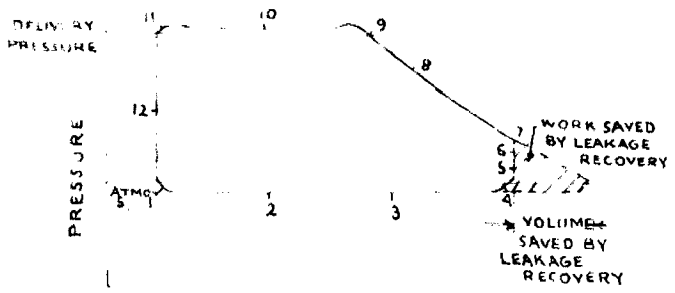

FIG. 3 31.

REF II

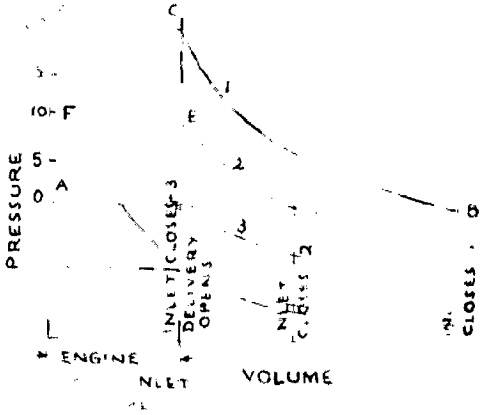

P-V DIAGRAM SHOWING EFFECT
OF CHANGE IN INLET PERIOD

FIG. 3 32.

REF

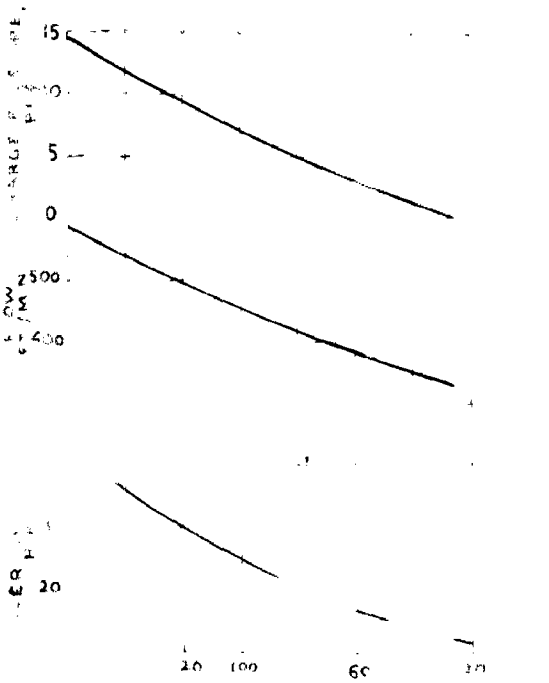

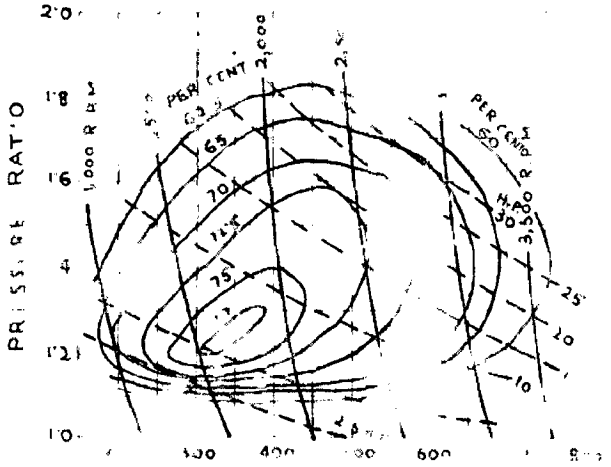

INTERNAL M COMPRESSION
R

FIG. 3 3

REF II.

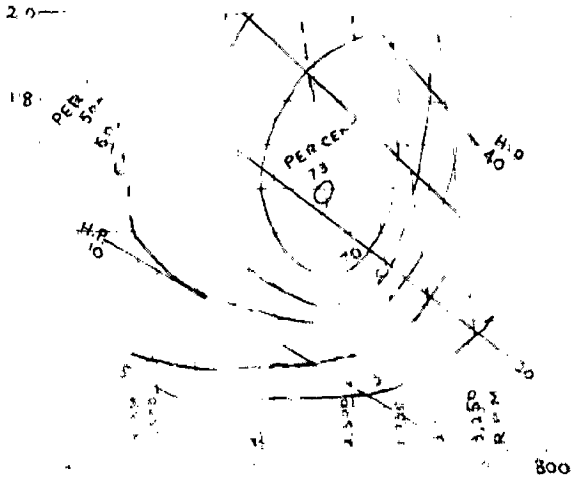

INTERNAL VOLUMETRIC COMPRESSION
RATIO

FIG.

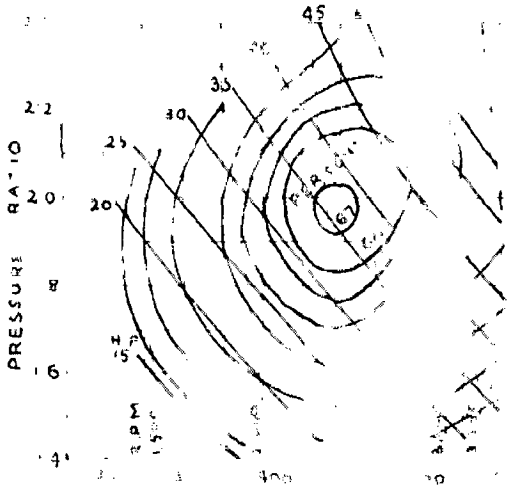

INTERNAL VOLUMETRIC COMPRESSION

light loads, still earlier closure of the inlet valve gives sub-atmospheric ~~inlet~~ outlet pressure as in 4.

The effect of inlet valve setting upon the compressor performance is shown in Fig. 3.33. By closing the inlet valve 139° earlier than normal, the charge pressure was reduced from 15 to 0 lb. per sq. in., reducing the throughput from 535 to 330 cu. ft. per min. and thereby decreasing the power input to the compressor from 44 to 12 h.p.

In practice, the Bicero compressors are provided with three typical internal compression ratios of 1.05, 1.2 and 1.4 which are suited for low pressure, medium pressure and high pressure supercharging respectively. Figures 3.34, 3.35 and 3.36 show the Bicero compressor performance characteristics for these settings where the valve setting was kept fixed. The overall adiabatic efficiency varies from above 50 to 80 percent, and the operation of the compressor is possible over a speed range of 1000 to 3,000 r.p.m. Also delivery pressures as high as 20 lb. per sq. in. (gauge) have been maintained steadily.

3.12. Ricardo Supercharger. Popularly known as wobble-plate compressor, it was devised by Ricardo to meet the requirement of supercharged engines for automotive use, where high torque at low speeds is required. The volumetric efficiency of positive displacement compressors being poor at low speeds, the piston compressor design was the only choice. Thus the Ricardo compressor has seven opposed pairs of compression cylinders. The pistons in the cylinders obtain reciprocating motion by means of a swash or wobble plate as shown (12) in Fig. 3.37. The plate has an articulated joint where a cylindrical bobbin slides in an eye in the piston rod. The driving shaft is supported in the end bearings of

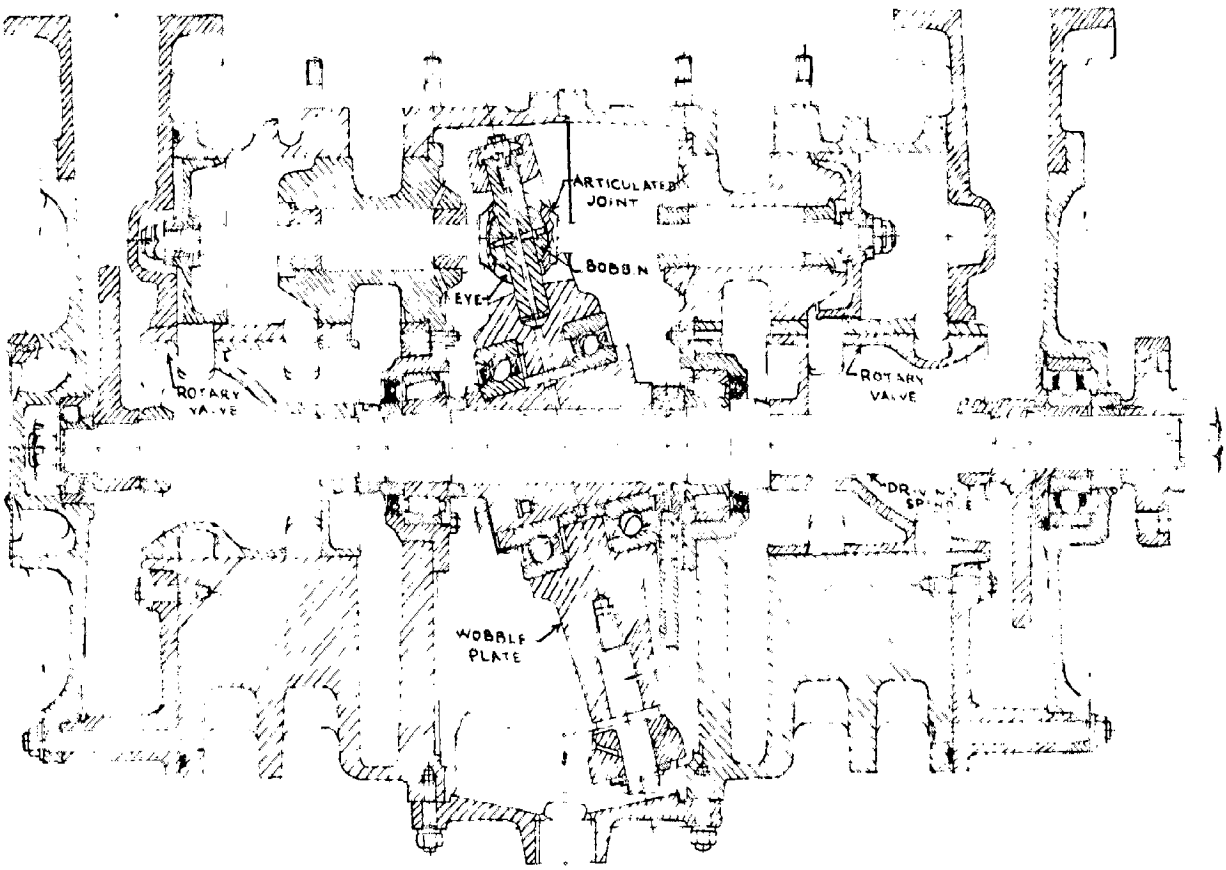

RICARDO SUPERCHARGER

FIG 3 37.

REF 12

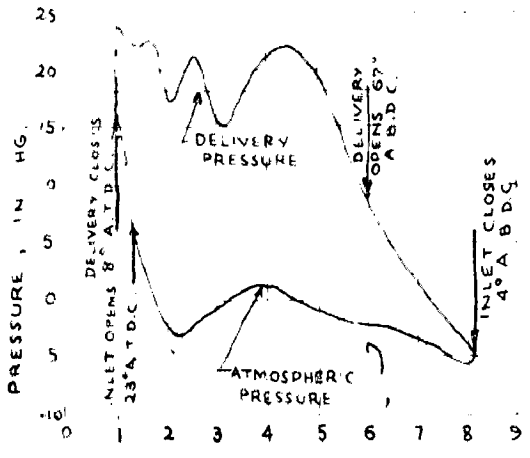

INDICATOR CARD FROM RICARDO SUPERCHARGER FITTED WITH RAT-TAIL VALVE

FIG. 3 38.

REF 12

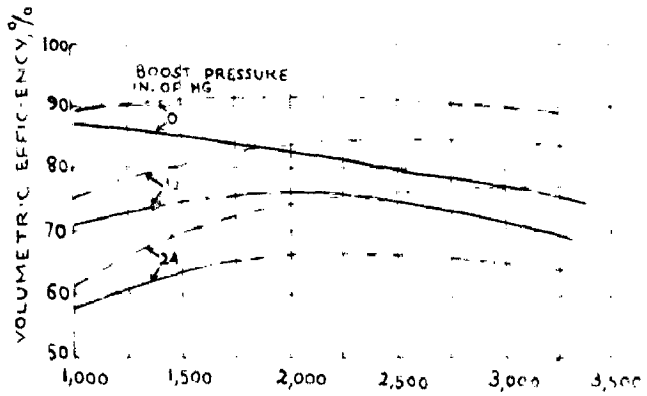

VOLUMETRIC EFFICIENCY OF SUPERCHARGER WITH STANDARD AND RAT-TAIL VALVES

FIG 3 39.

RAT-TAIL VALVE

STANDARD VALVE

the plain roller type and in the main bearing of the taper roller type, and is concentric with all the sets of cylinders. There is a single central rotary valve to control the inlet and delivery both from each of the cylinders. With a view of the compactness of design, high piston speeds were desirable which involved the friction and lubrication problems. To overcome these difficulties, pistons carried on guided piston rods and running clear of the cylinder bores have been used. The type of arrangement adopted gives complete freedom from pressure pulsations in both the suction and delivery lines.

The exact motion of the wobble plate is complex,but it may be understood that in an ideal case, each point on the plate describes a lemniscate, or a figure of eight drawn on a spherical surface. The wobble plate is also restrained against rotation by a piston rod using a pivoted bearing block, running between two straight plates.

The rotary valves of the compressor are carried on the driving shaft. They do not touch the casing at their periphery, but are instead provided with fine clearances to reduce the leakage to minimum,which, to a large extent, governs the over all performance of the supercharger. Both the ports in the body as well as in the valve are provided with sloping edges, where the axial movement of the rotary valve alters the valve timing. This may be effected automatically by loading the valve with air pressure on one side, and restraining it by a spring on the other. Here any change in air pressure will slide the valve and alter the timing appropriately. However, the early partial closing of the inlet valve which, as already discussed, results in an appreciable saving of work, is best obtained by employing the cut-tail port where

the port is narrowed to a slit over half of its length. Fig. 3.38 shows a typical supercharger indicator diagram taken with the rat-tail valve fitted. The pulsations in the suction and delivery strokes represent the surges between the volumes of the cylinder, and the rotary valve and chest. The whole thing acts as a resonant system where the impulse is derived from the acceleration of the air column in the port way due to the port opening.

The variation of the volumetric efficiency with engine speed for a 3.6 litres swept-volume Ricardo supercharger is shown in Fig. 3.39. It may be seen that with the rat-tail valve the volumetric efficiency is higher at lower engine speeds which justifies the suitability of this compressor for use in vehicles where high torque at low speeds is required. Also the compressor has an over-all high value of the volumetric efficiency. Fig.3.40 shows the variation of adiabatic temperature efficiency with engine speed only for the standard valve with the rat-tail type of porting, the adiabatic efficiency is also reduced to some extent with the engine speed. Fig. 3.41 presents a comparative picture with both the types of valves when the compressor has been coupled to the engine. The simplifying assumption made in this case is that the engine volumetric efficiency is constant, its air consumption is 0.035 cu.ft. per engine revolution measured at intake manifold pressure; and the pneumatic transmission efficiency is two-thirds. It may be seen that with the rat-tail valve, at high engine speeds, the saving in gross horsepower required to drive the supercharger is 5.3 h.p. Due to the reduction in recoverable work as well, the equivalent net horse power works out to be 3.2 h.p. Thus in an application where the engine is mostly requ-

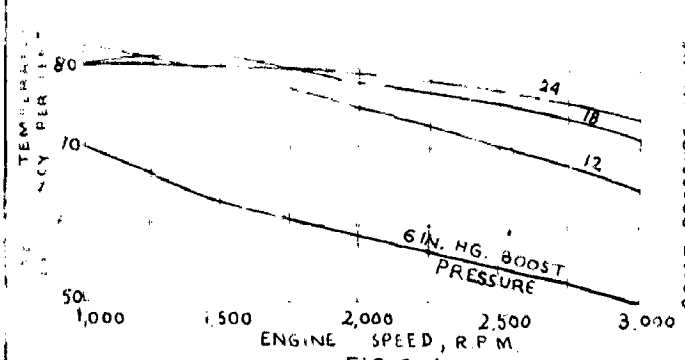

REF 12

FIG. 3·40.

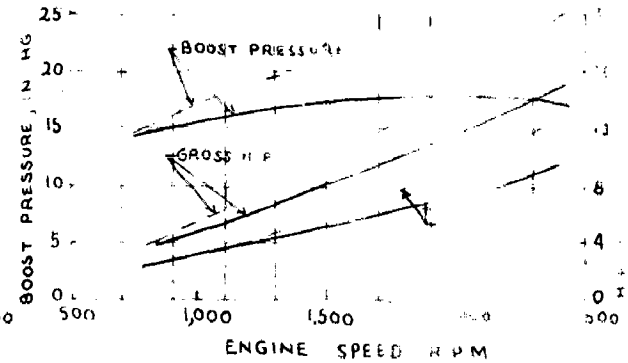

FIG. 3·4

RAT-TAIL VALVE

STANDARD VALVE

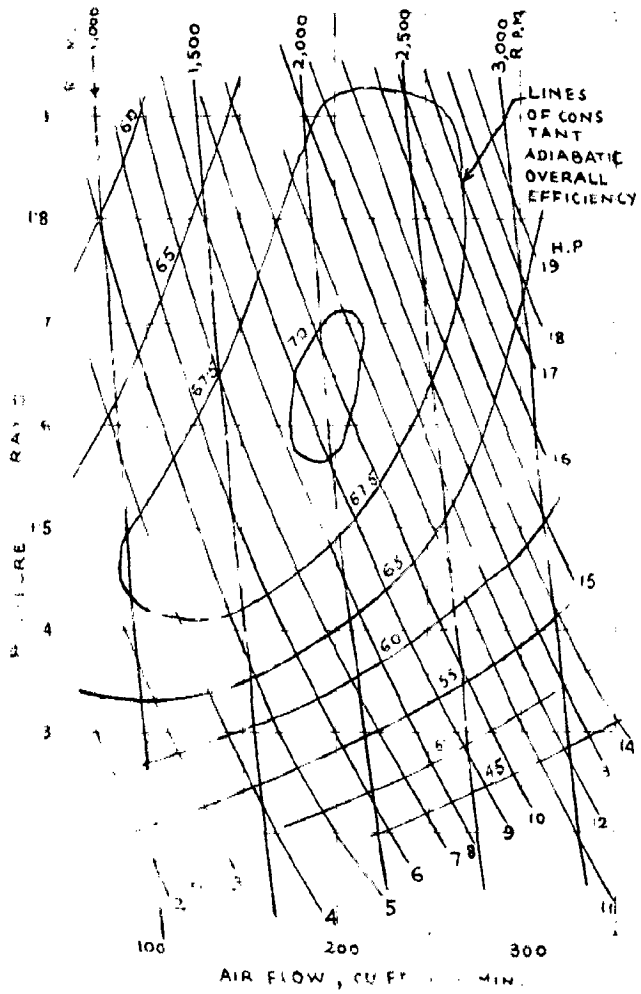

OVERALL PERFORMANCE OF 3·6 LITRE RICARDO SUPERCHARGER

REF 12

FIG. 3·42.

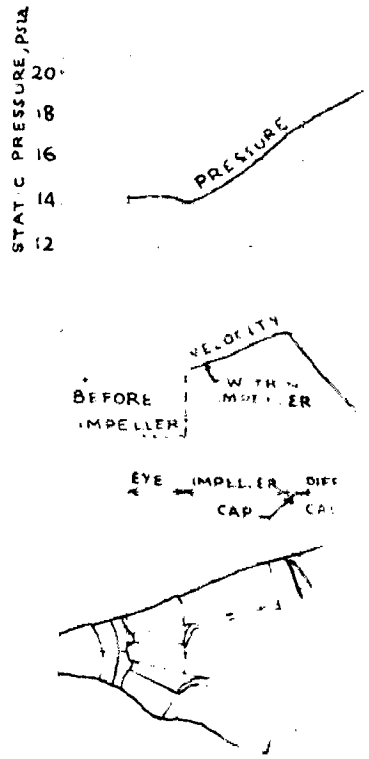

FIG.

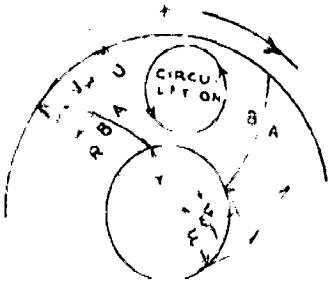

FIG. 3·44.

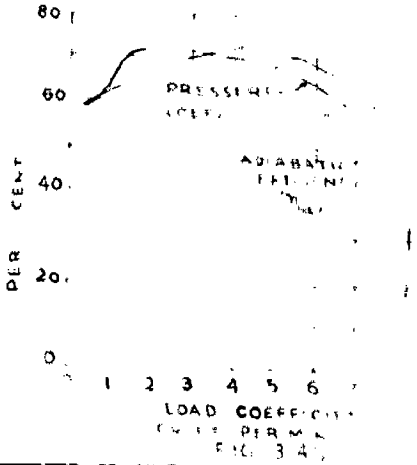

FIG. 3·4

ired to run at high speeds, but where the maximum boost is not required at that speed, this simple modification can bring a substantial economy. Overall performance curves for this supercharger are shown in Fig. 3.42.

3.13. Centrifugal Compressors- With increased knowledge of aerodynamic principles required to analyse the complex nature of flow phenomena, the centrifugal compressors have reached a stage of perfection both in design and performance as a result of which their use is possibly the widest in the field of supercharging. In a centrifugal compressor air is sucked into the impeller eye and, in passing through impeller vanes, is subjected to centrifugal action. This produces outward displacement of air thus producing suction and so inducing more of air to flow in. The compression of fluid being subjected to centrifugal force is called centrifugal compression. This decreases the volume of the fluid which has to pass through the diverging passages between the vanes, as a result of which there is a further rise in pressure called diffuser compression. The fluid leaving the impeller has a high tangential velocity (about 1,000 fps. or more)imparted by the impeller rotating at a speed 3,000 to 25,000 r.p.m. A portion of this kinetic energy of the fluid is converted to static pressure while passing through the diffuser and the volute casing, depending upon the efficiency of the diffusing system. The variation in pressure and velocity of the fluid during its passage through the compressor can be studied from Fig. 3.43 (17).

The impellers (rotors) may be open,closed or semi-closed; the vanes may be radial, straight, angular or curve; and the diffuser may be either one piece volute or of multi-vane type. The compressor may be either single-stage (for 2 to 6 psig. pressure head) or multi-stage (for 7 to 20 psig.) and may be either

motor driven, gear-driven by the engine (speed ratio 3-10:1), or driven by the exhaust turbine.

The velocity diagrams at the inlet and exit end of the impeller can be drawn as shown in Fig. 3.44. Now by Euler's equation,

torque applied to the fluid = rate of change of angular momentum of the fluid

or $T = \frac{RV_w}{g} \pm \frac{rv_w}{g}$, plus or minus sign depending upon the direction of spin, like or opposite, as compared to that of the impeller.

Hence the ideal energy input to the compressor,

$$E = \frac{\omega}{g}(RV_w \pm rv_w) = \frac{UV_w}{g} \pm \frac{uv_w}{g} \qquad (3.15)$$

which is actually the energy acquired by the fluid in passing through the impeller. Due to the losses arising from leakage and skin friction, a factor 'ψ' known as power input factor is introduced to calculate the actual energy input which is

$$= \frac{\psi}{g}(UV_w + uv_w) \qquad (3.17)$$

It is easy to see that the pressure on the forward face A will be greater than on the rear face B. Now the total energy at any radius being constant, the velocity on the rear face will be greater than on the forward face. This causes the circulation in a direction opposite to that of the rotation of the impeller (Fig. 3.44). In practice, this deviation of flow is accounted for by introducing a factor 'σ' known as Slip factor. Thus while calculating the input energy, the value of the whirl velocity should be modified by multiplication with the slip factor.

Stodola on the basis of his study of relative eddy, has given the following expression for slip factor

$$\sigma = 1 - \frac{\pi \sin\phi}{n} \qquad (3.18)$$

where ϕ is the vane outlet angle and n the number of vanes.

Where Fig. 3.5 represents the pressure volume diagram for the centrifugal compressor. The horse-power observed by the compressor in compressing w lb. of air per min. from a pressure p_1 to P_2 and delivering it to an engine, will be given by

$$h.p. = \frac{w C_p T_1 \left[\left(\frac{p_2}{p_1}\right)^{\frac{\gamma-1}{\gamma}} - 1\right]}{33{,}000\,\eta_a \eta_m} \qquad (3.19)$$

where η_a and η_m are the adiabatic and mechanical efficiencies of the compressor respectively. It should be observed that both the equations (3.17) and (3.19) represent the energy input to the compressor.

The energy input is sometimes expressed in terms of the temperature rise directly from eq^n (3.17) as

$$\Delta T^\circ = \frac{\Psi}{gJC_p} \cdot \left(U V_w \pm u v_w\right) \qquad (3.20)$$

The pressure ratio in each stage of the compressor is given by

$$r = \frac{p_2}{p_1} = \left(\frac{T_{2t}}{T_{1t}}\right)^{\frac{\gamma}{\gamma-1}} = \left(1 + \frac{\Delta T_a}{T_{1t}}\right)^{\frac{\gamma}{\gamma-1}} \qquad (3.21)$$

where the subscript 't' denotes the total head value.

Each impeller has a definite maximum work capacity limited by the maximum tangential velocity at exit, which will evidently give the maximum delivery pressure of P_2 max. Thus the measure of the effectiveness of the actual impeller in producing pressure is given by a ratio 'η_p' called pressure co-efficient.

$$\text{Thus } \eta_p = \frac{C_p T_1 \left[\left(\frac{p_2}{p_1}\right)^{\frac{\gamma-1}{\gamma}} - 1\right]}{C_p T_1 \left[\left(\frac{p_{2\max}}{p_1}\right)^{\frac{\gamma-1}{\gamma}} - 1\right]} = \frac{\left[\left(\frac{p_2}{p_1}\right)^{\frac{\gamma-1}{\gamma}} - 1\right]}{\left[\left(\frac{p_{2\max}}{p_1}\right)^{\frac{\gamma-1}{\gamma}} - 1\right]} \qquad (3.22)$$

The performance of a centrifugal compressor is shown in Figs. 3.45, 3.46 and 3.47. In Fig. 3.45 (7) the variation of the adiabatic efficiency and the pressure coefficient with the load coefficient $\frac{Q}{N}$ is shown where Q is the inlet volume in cubic feet per minute and N the r.p.m. As soon as $\frac{Q}{N}$ exceeds some critical value there is a sudden drop in both η_p and η_a. On the other side there is a sudden drop in pressure coefficient, and at this point the surge usually starts. Fig. 3.46 (18) shows the behaviour of the delivery pressure with inlet air flow. It may be seen that if too great a flow is demanded out of the compressor, the pressure ratio may even approach unity. The curves also show that any machine is good enough only for a definite range of flow, from the surge line to the critical value of flow. This range of satisfactory operation narrows down with increasing speeds. Complete performance characteristics of a centrifugal compressor at various speeds are given in Fig. 3.47 (19). The mechanical efficiency of a well designed centrifugal supercharger is 90 to 95 per cent. Also the weight of a single stage compressor (integral with the engine) is 0.6 to 1 per cent of the dry engine weight.

The comparative idea of the engine torque developed at a particular speed with the Roots blower as well as the centrifugal compressor is illustrated in Fig. 3.48. It may be seen that at low speeds the Roots blower is decidedly advantageous, but at high speeds the centrifugal compressor is superior than the Roots blower because of the drooping characteristics of the latter with the engine speed.

3.14 Axial Compressor- This type of aerodynamic compressor consists essentially of two parts- the rotor and the stator. The former

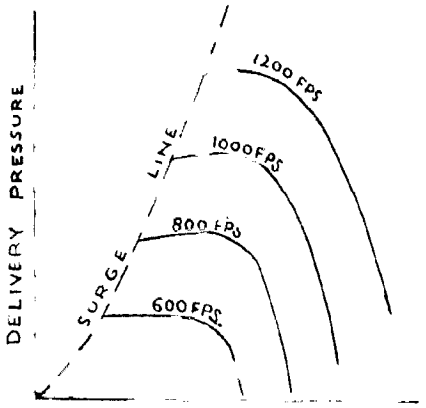

FIG 3 46.

REF. 18.

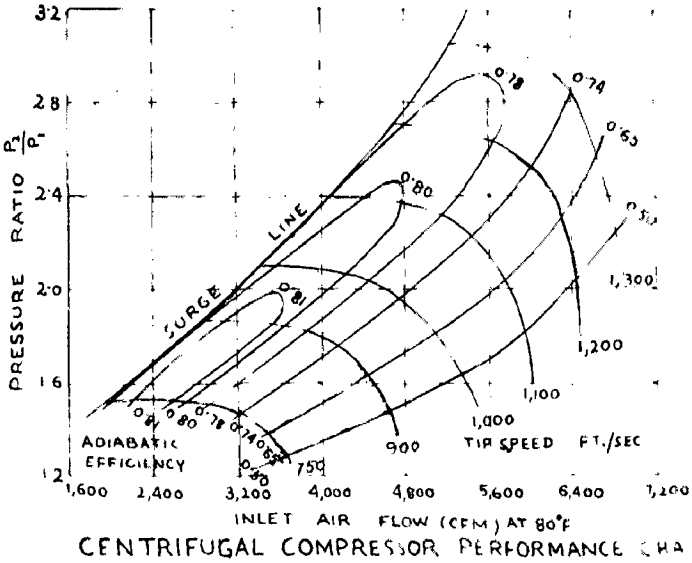

CENTRIFUGAL COMPRESSOR PERFORMANCE CHA

FIG 3 47

REF

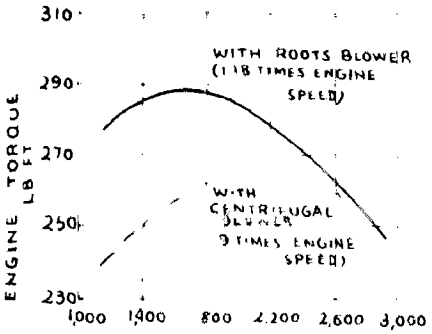

FIG 3·48.

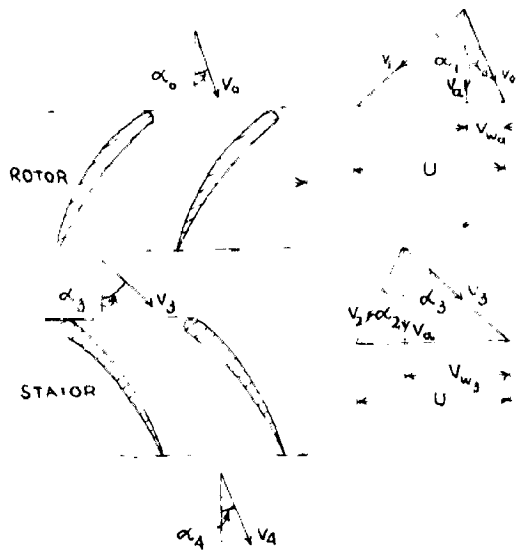

VELOCITY TRIANGLES FOR ONE STAGE

FIG. 3·49

REF 17

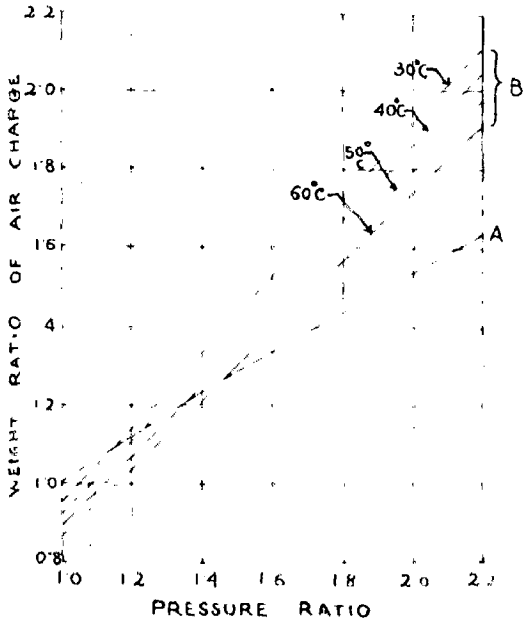

REF 20

FIG 3 51

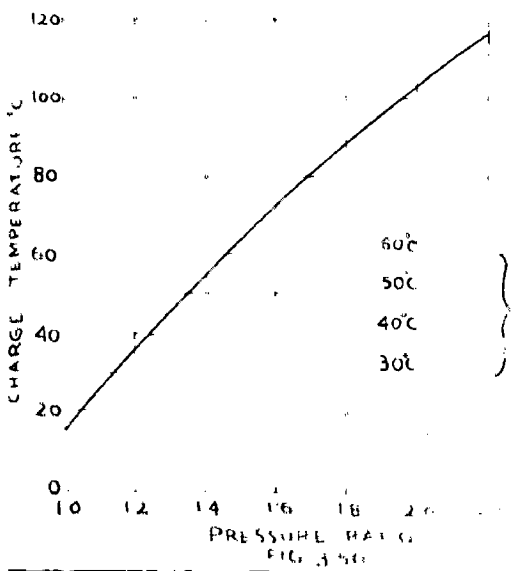

FIG 3 52

carries the moving blades on its periphery and the latter the stationary rows of blades which recover part of the kinetic energy possessed by the fluid into the pressure energy and also redirect it at a suitable angle into the next stage. The blades are true aerofoil sections designed from aerodynamic considerations. This serves to minimise the losses and avoids the stalling troubles which arise when the angle of incidence between the flow direction and the blades becomes excessive- a difficulty frequently encountered at off-design operations.

The rotor is either of the drum type or of the disc type, or a combination of the two. Either of the stator or the rotor is flared to provide a successively contracting passage so as to keep a constant axial velocity throughout with the gradual increase in density. This materially simplifies the design problem, because the same design is applicable for all the stages. The flow through the compressor is essentially decelerating or diffusing, so that the pressure rise is obtained during the passage of the fluid through the expanding spaces of the stator and the rotor.

The fundamental process of the acceleration of the fluid followed by diffusion is carried out in a number of stages, each stage comprising a rotor ring followed by a stator ring. The velocity diagrams for a stage of the compressor are shown in Fig. 3.49, where V_0 and V_3 are the absolute velocities and V_1 and V_2 the relative velocities at the points referred. U is the peripheral velocity, V_a the axial velocity assumed constant throughout, and α_s the angles at the respective places. (Check for angles!)

From the velocity triangles,

$$\frac{U}{V_a} = \tan\alpha_0 + \tan\alpha_1 = \tan\alpha_2 + \tan\alpha_3 \qquad (3.23)$$

The work done per lb. of air per second

$$W = \frac{U}{g}(V_{w_3} - V_{w_0})$$

$$= \frac{U}{g} V_a (\tan \alpha_3 - \tan \alpha_0)$$

$$= \frac{U}{g} V_a (\tan \alpha_1 - \tan \alpha_2) \text{ from eq}^n (3.21) \qquad (3.24)$$

The work so absorbed by the fluid will produce a stage temperature rise,

$$\Delta T_{st} = \frac{U V_a}{g J C_p} (\tan \alpha_1 - \tan \alpha_2) \qquad (3.25)$$

In an actual case the stage temperature rise is slightly less than that found theoretically and given by the above equation. This is due to the variable nature of the axial velocity across the annulus and the adverse effect of the boundary layer and tip clearance. To account for this loss, a factor Ω called the 'work-done factor' is introduced in the theoretical equation for stage temperature rise. The mean value of the work-done factor Ω(1) as found by tests is about 0.86.

Thus the actual stage temperature rise,

$$\Delta T_{st} = \frac{\Omega . U V_a}{g J C_p} (\tan \alpha_1 - \tan \alpha_2) \qquad (3.26)$$

The adiabatic efficiency of the compressor is given by

$$\eta_{ad} = \frac{\text{adiabatic temperature rise corresponding to pressure ratio.}}{\text{Actual temperature rise}}$$

$$= \frac{(R)^{\frac{\gamma-1}{\gamma}} - 1}{(T_{2t} - T_{1t})/T_{1t}} \qquad (3.27)$$

The characteristics of an axial compressor along with the surging and choking phenomena are discussed in terms of non-dimensional parameters in the section on matching.

In eq^{n}(3.27) R is the pressure ratio, and T_{1t} and T_{2t} the absolute total head temperatures at inlet and exit of the compressor respectively.

3.15 Temperature Rise in Superchargers- The temperature of air rises during its passage through the supercharger. This temperature rise is due to the heat produced by compression as well as by friction. Thus if the subscripts 1 and 2 refer to the intake and delivery conditions, the temperature rise due to the adiabatic compression is given by

$$\frac{T_2}{T_1} = \left(\frac{p_2}{p_1}\right)^{\frac{\gamma-1}{\gamma}} = \frac{T_1 + (\Delta t)_{comp.}}{T_1}$$

$$\text{or } (\Delta t)_{comp.} = T_1\left(\frac{p_2}{p_1}\right)^{\frac{\gamma-1}{\gamma}} - T_1 = T_1\left[\left(\frac{p_2}{p_1}\right)^{\frac{\gamma-1}{\gamma}} - 1\right]$$

$$= 530\left[(r)^{\frac{\gamma-1}{\gamma}} - 1\right] \text{ where } r = \frac{p_2}{p_1}\ ;\ T_1 = 530^{\circ}R \quad (3.28)$$

If Q be the quantity of heat added due to friction and v the specific volume of air at intake, the temperature rise due to friction is given by

$$(\Delta t)_{fr.} = \frac{Q}{\frac{v_1}{v} \cdot C_p} \quad (3.29)$$

Now the mechanical efficiency of the supercharger,

$$\eta_m = \frac{\text{useful work}}{\text{useful work + friction loss}}$$

$$= \frac{1}{1 + \frac{\text{Friction loss}}{\text{useful work}}}$$

$$= \frac{1}{1 + \frac{\frac{v_1}{v} \cdot C_p \cdot (\Delta t)_{fr} \cdot 778}{p_1 v_1 \cdot \frac{\gamma}{\gamma-1}\left[\left(\frac{p_2}{p_1}\right)^{\frac{\gamma-1}{\gamma}} - 1\right]}}$$

$$= \frac{1}{1 + \frac{\frac{1}{13.8} \times 0.243 \ (\Delta t)_{fr.} \ 778}{3.5 \times 14.7 \times 144 \left[(r)^{\gamma-1} - 1\right]}}$$

Where v = 13.8 cu.ft. per lb. at 14.7 psia and 70°F, and $r = \left(\frac{P_2}{P_1}\right)$

$$= \frac{1}{1 + \frac{(\Delta t)_{fr.}}{540 \left[(r)^{\gamma-1} - 1\right]}}$$

$$\therefore (\Delta t)_{fr.} = \left(\frac{1}{\eta_m} - 1\right)\left[(r)^{\gamma-1} - 1\right] \cdot 540 \qquad (3.30)$$

Thus the total temperature rise

$$= (\Delta t)_{comp.} + (\Delta t)_{fr.}$$

$$= T_1 \left[(r)^{\gamma-1} - 1\right] + 540 \left(\frac{1}{\eta_m} - 1\right) \left[(r)^{\gamma-1} - 1\right]$$

$$= \left[(r)^{\gamma-1} - 1\right] \left[530 + 540 \left(\frac{1}{\eta_m} - 1\right)\right] \qquad (3.31)$$

So for different delivery pressures, the total temperature rise of air can be calculated for a compressor whose mechanical efficiency is known.

3.13 <u>After-cooling</u>- We have seen that the higher the pressure ratio or lower the mechanical efficiency, the greater is the temperature rise. This implies that in case of high pressure supercharging which is the modern trend these days, the intake temperature being considerably high, the charge weight or the power output will not be proportionally increased. For every reduction of 10°c in compressed air temperature the engine output increases by about 3 per cent. Under these conditions the importance of after-cooling is recognized, and as a matter of rule, for pressure ratios above 1.5:1, the use of intercoolers between the compressor

delivery and engine intake has become a regular practice.

Based on the calculations of Berger (20) of Brown-Boveri Co., the charge temperatures for the various pressure ratios for an ambient temperature of 15.°c are shown in Fig. 3.50. The corresponding increase in the weight of supercharging air is shown by the curve A in Fig. 3.51. The effect of cooling the charge to various temperatures on the air charge weight is also shown on the same diagram. It may be observed that cooling increases the weight of the air charge much more rapidly.

Because of the extra accessory required in the form of after-cooler and the inevitable pressure reduction due to path resistances, intercooling proves to be an economic proposition only if the charge can be cooled by a minimum of 20°c. The corresponding increase in power will be about 6 to 7 per cent. For effective cooling, the temperature of the cooling water should be atle at 35°c lower than that of the charging air for a fall of about 15°c through the after-cooler.

3.17. Air Coolers- The charge-air coolers are made of standard cooling elements, each composed of a number of round water tubes, threaded through several thin fin-plates. For effective heat transfer, the water tubes are made of aluminium brass, the fin plates of copper and the tube plates of each element of naval brass. The frontal area and the charge velocity through the intercooler may be adjusted by increasing the number of elements in parallel.

For coolers of small sizes, single-flow water system is employed. Here water enters the bottom header and leaves through the top header. For coolers of larger sizes, double-flow system is preferrably used, because the quantity of water required otherwise will be too large. Here the top header is divided in two parts,

the water entering through the first half and leaving through the other half. To reduce the air pressure loss and increase the effectiveness of the cooler, the entry to the cooler is divergent and the duct connecting the engine inlet manifold is convergent, so that the velocity of air through the cooler passages is tolerably low.

SECTION B

EXHAUST GAS TURBOCHARGING

Theory of Turbocharging

3.18 Principle of Turbocharging- The exhaust from a diesel engine possesses about 27 to 33 per cent of the energy of combustion. When the engine is supercharged, the residual energy increases to about 40 per cent due to the fact that the air mass flow is increased and the effective cylinder expansion ratio is reduced. If a mechanically driven compressor were used, the whole of the exhaust energy would have been wasted. But if this energy could usefully be employed to drive a turbine, part of the energy would be harnessed due to the compensation of the reduced cylinder expansion rate by a further expansion stage. The power so recovered may be employed to drive the rotary compressor which in turn feeds the high pressure air to the engine. This increases the power output and so the resultant overall efficiency by about 5 to 15 per cent, and is responsible for the origin of turbocharging.

The arrangement of exhaust gas turbocharging is shown in Fig. 3.52. Here the exhaust from an engine discharges through a pipe on the blades of the turbine, and thence to atmosphere. The exhaust driven turbine is coupled to the rotary compressor, the latter drawing air from the atmosphere, compressing it, and delivering it to the engine, either direct or through an intercooler. Thus there is no mechanical connection between the turbocharger and the engine. The turbocharger being run by the exhaust adjusts itself to the loading conditions of the engine.

3.19 Development of the Buchi System- The development of turbocharging is largely due to the pioneer work of Dr. Alfred Buchi (21,22) of Winterthur who performed his first experiments on turbocharging in 1911. The Buchi system of turbocharging has been

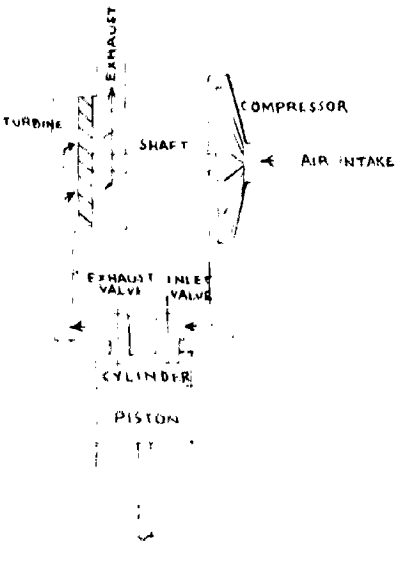

FIG 3 52

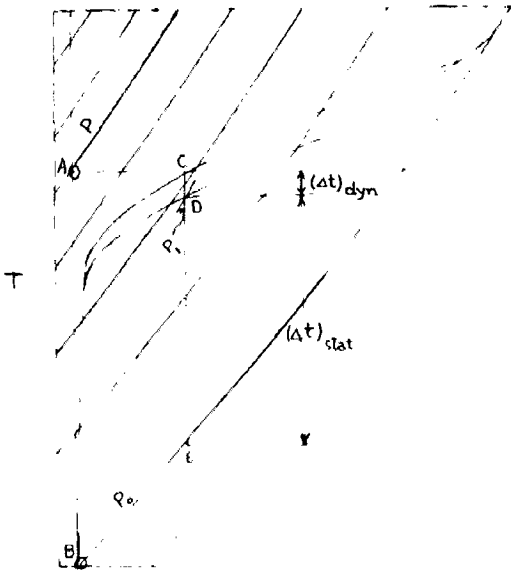

ENTROPY DIAGRAM FOR EXHAUST PROCESS

FIG. 3 55

REF 24

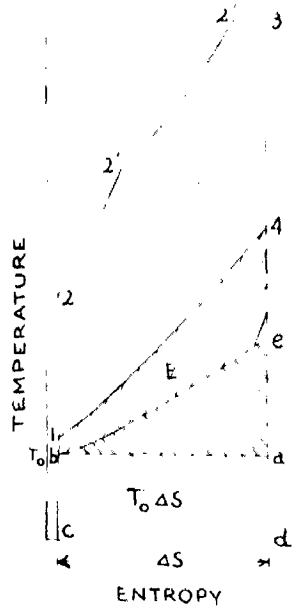

FIG. 3·53.

REF. 24

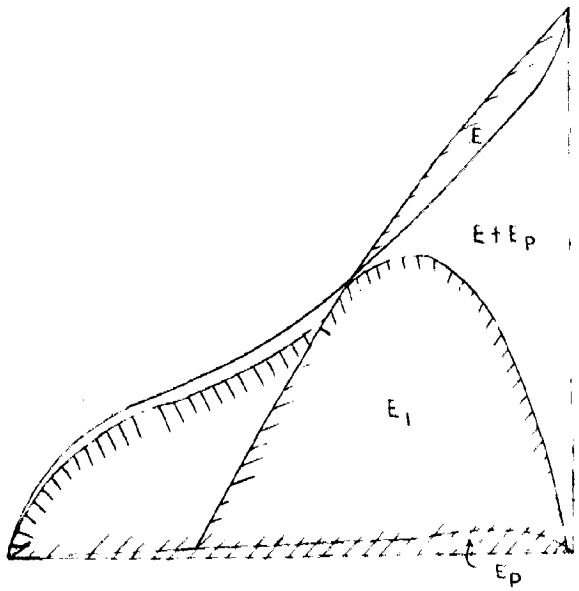

ENERGY IN PRESSURE WAVE

FIG 3·56

REF 24

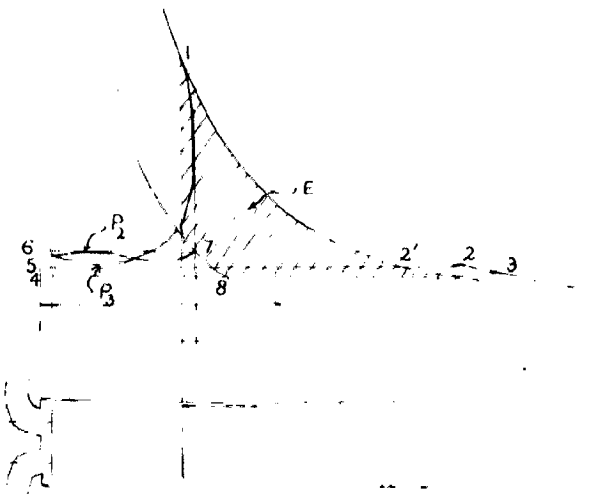

FIG. 3·54

REF 24

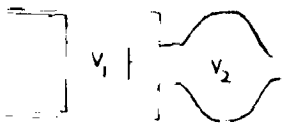

FIG. 3·57.

REF 24

universally adopted for the supercharging of four stroke and two stroke engines, The first turbocharged engines were used in some German motor ships in 1923, and later in 1928 were installed in U.K.

In the early stages, constant pressure system, guided probably by the steam turbine practice, was used. Here a large capacity exhaust piping was incorporated between the engine exhaust and the turbine so as to act as a receiver, and thus the pressure pulsations were damped down to a minimum. The system was not found suitable because of the poor scavenging and the high exhaust temperatures, these being the direct result of high back pressures. This was not a healthy situation, because the exhaust temperature crossed the permissible limit for the satisfactory operation of the turbine blades. Later work revealed that the pulse system was capable of giving better results. Here small narrow exhaust pipes were used to give rise to appreciable pressure waves caused by the rapid opening of the exhaust valves. The turbocharger turbine was thus of the impulse type. This very scheme of operation is employed in the popularly known Buchi system of to-day.

3.20 Energy in the Exhaust- In an internal combustion engine about 40 per cent of the energy supplied in fuel is lost in the exhaust. This exhaust gas loss consists of three parts.-

(1) Due to the introduction of heat at a finite temperature, only the part corresponding to the Carnot cycle efficiency can be converted into heat. Thus the unavailable energy $T_0 \Delta S$ is always rejected to the surroundings. This loss is about half of the exhaust losses.

(2) 10 per cent of the exhaust loss takes place due to the irreversible process by which the temperature is brought back to

its initial value.

(3) The remaining 10 per cent loss takes place, because the expansion in the cylinder cannot be carried down to the atmospheric pressure which requires a very long cylinder. Thus to conserve this loss the engine weight per b.h.p. is terribly high. An exhaust gas turbine can, however, be used to utilise this energy efficiently.

The schematic representation of the above losses has been made in Fig. 3.53 which represents the engine cycle on the temperature-entropy diagram. The heat loss ToΔS is represented by a-b-c-d, the loss due to irreversible process by a-b-c , and the loss due to restricted expansion capable of being utilized by the turbine is given by c-b-1-4.

Thus 10 per cent of the chemical energy supplied by the fuel is present in the form of available energy (E) at the beginning of exhaust. This is also known as the 'blowdown energy'. This can be utilized in two ways, either by pressure wave scavenging or by exhaust gas turbocharging. Since for charging of internal combustion engines, isentropic compressor power equivalent to 10 to 35 per cent of E is required, turbo-charging appears to be a feasible operation. But, in practice, due to the throttling loss in the exhaust valve and friction and heat conduction losses, it is not easy to obtain the requisite quantity of energy for pressure charging.

The available energy (E) is also represented by the shaded area on the p-v diagram given in Fig. 3.54. Here p_2 represents the charging pressure and p_3 the exhaust pressure. Since, for purposes of scavenging, there should be sufficient pressure drop available, p_3 cannot be raised at will. This will mean that the head available at low charging pressures for use in the turbine will be small.

Thus the energy available in the turbine corresponds to the area 2-3-4-5 which is not quite sufficient to cover the losses and input to the blower given by the area 8-7-6-4. The energy input to the turbine may, however, be increased by reducing the throttling (which is the bulk of all the losses), and by producing in the exhaust pipe an intense pressure shock during the initial exhaust period.

3.21 Loss in Exhaust Energy due to Throttling. The outgoing exhaust loses a large part of its available energy due to the inevitable throttling suffered on the exhaust valves. The greater the pressure difference and the smaller the constriction, the larger is the loss. So it can substantially be reduced by making the valves open instantaneously and by reducing the pressure difference. The latter can be achieved by increasing the back pressure by ram effect.

To understand the things quantitatively, let us consider the exhaust gas leaving the cylinder at a pressure p. If the pressure in the exhaust pipe be P_1 and at the outlet of the turbine P_o, then the drop in pressure suffered by the exhaust will be AB as shown in Fig. 3.55. But due to throttling taking place at the exhaust valves, the entropy of the gases increases, say by an amount AC. Now the exhaust will be having the kinetic energy CD, together with an energy drop DE which will be utilized in the turbine. Here P_1 designates the pressure in the exhaust pipe.

These energies have been shown quantitatively in Fig. 3.56 The total energy available in the exhaust through complete expansion has been shown by the area I, and the area I_1 represents the useful energy that is recovered by expansion through the turbine. The energy imparted to the outgoing exhaust gases by the

piston is E_p. Thus the total energy that could be obtained in an ideal case from the exhaust has been shown by the area $E_1 + E_p$ on the same base. Thus the ratio $\frac{E_1}{E + E_p}$ represents the efficiency of the exhaust turbine process.

Due to the inertia forces, the instantaneous opening of the valve cannot be achieved. However, the effective flow cross-section can be enlarged without proportional increase in the inertia forces by providing a good aerodynamic form of the exhaust valves so that the flow separation does not take place. This will reduce the losses due to turbulence.

3.22 Measures for Increased Utilization of the Exhaust Energy-

Nonek (23) and Rijswijk investigated the phenomena of dynamic pressure shock and found that in order to obtain the maximum usable energy, narrow exhaust pipes should be employed. This may be explained by Fig. 3.57 where V_1 represents the cylinder volume and V_2 the exhaust pipe volume. In case the equalization of pressure on the two sides be instantaneous on the opening of the exhaust valve, it is easy to see that $\frac{V_2}{V_1}$ being small, the mean pressure pm and so the usuable energy will be large. Also V_2 being small, there will be a rapid rush of the exhaust gases resulting in intense scavenging of of the cylinder. For larger values of $\frac{V_2}{V_1}$, the conditions will not be so favourable. The curve I of Fig. 3.58 (a) corresponds to the case when $\frac{V_2}{V_1}$ is small, and the dotted curve II relates to the condition when $\frac{V_2}{V_1}$ is large. The scavenging is definitely better in the former case.

In an actual case, the valves do not open instantaneously, and the equalization of pressure takes some time. The curves in Fig. 3.58 (b) are shown for such an actual case for both the cases enumerated above i.e., when $\frac{V_2}{V_1}$ is small and when it is large.

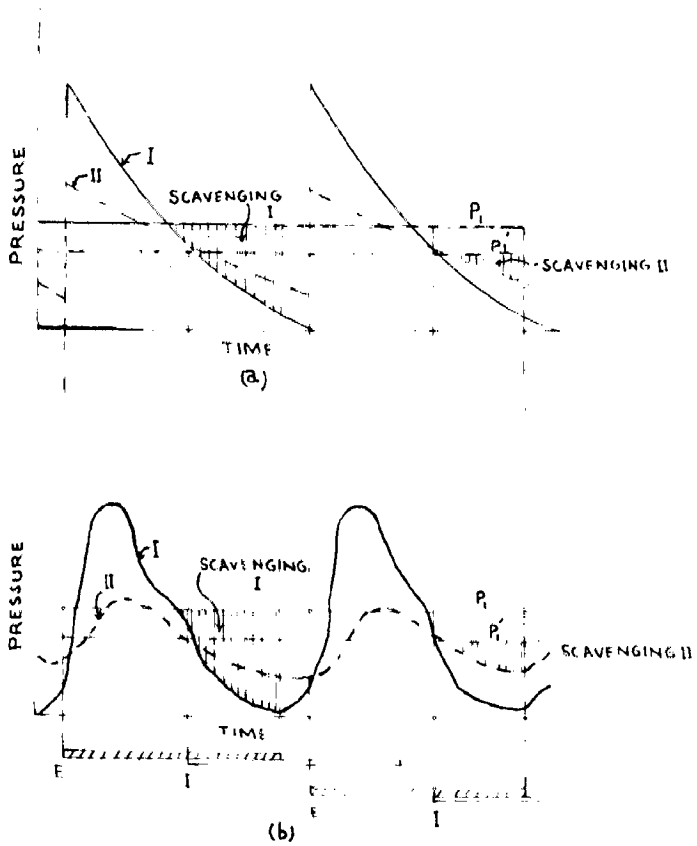

FIG. 3·58.

P_1 – CHARGING PRESSURE WITH SMALL VALUE OF $\frac{V_2}{V_1}$

P_2 – CHARGING PRESSURE WITH LARGE VALUE OF $\frac{V_2}{V_1}$

E – PERIOD DURING WHICH EXHAUST VALVE OPEN

I – PERIOD DURING WHICH INLET VALVE OPEN

REF 24

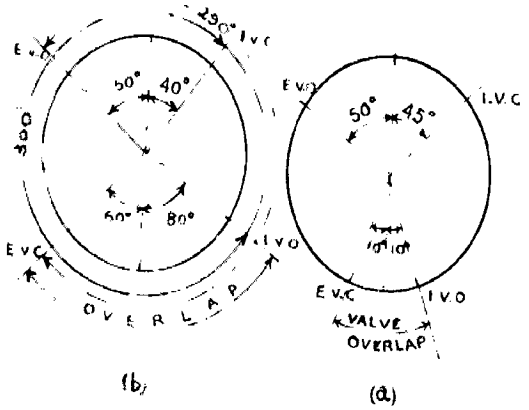

FIG. 3·59.

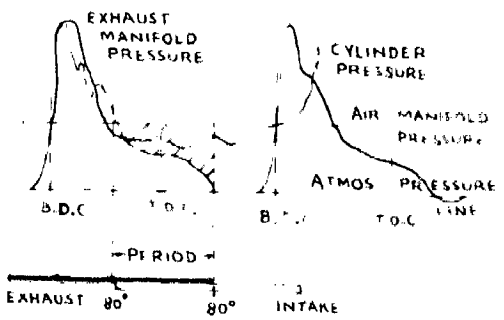

FIG. 3·60

REF 25

Here too improved scavenging results in the former case.

If ϕ designates the ratio of the cross-section of exhaust pipe to the effective cross-section of the exhaust valve, it has been found by Jenny (24) that reduction of ϕ from 1.46 to 1.18 produces a gain in energy of about 15 per cent. Also the increase in ϕ from 1.46 to 1.85, reduces the energy by the same amount. Thus the cross-section of the exhaust pipe should not be appreciably larger than the effective cross-section of the exhaust valve. However, unfortunately the loss free flow ($\phi = 1$) is not possible because of the flow separation around the valve stem.

The other possibility of increasing energy utilization is to raise the initial pressure in the exhaust pipe. It can be achieved by arranging the reflection of the previous pressure wave arriving at the cylinder coincident with the beginning of the exhaust. Thus the amplitude of the resulting pressure wave will be considerably increased.

For optimum utilization of exhaust energy, the exhaust pipes should preferrably be tuned so that the interference of the pressure waves does not take place. With short exhaust pipes, the reflected waves reach the cylinder a few crank degrees before the beginning of the exhaust. This may affect proper scavenging and transmission of energy to the nozzle. With long pipes, there is a large pressure difference between the cylinder outlet and the turbine inlet. This reduces the energy utilization of the turbine. However, in practice, the influence of pipe length on energy gain has not been found to be very large at ground level, but at high altitudes it becomes considerable.

3.20. Scavenging- Any supercharged engine must be scavenged adequately so that the proportion of the residual exhaust gases is

reduced to a minimum and cooling is provided to the piston dome, cylinder and exhaust valves. This will help to diminish the cycle temperatures so that in the case of highly supercharged engines, the exhaust temperature will not be tremendously high so as to suffer from the limitations upon its use in the turbine blading.

Scavenging is achieved by increasing considerably the overlap of the inlet and exhaust openings and by providing the pressure difference between the air and exhaust manifolds. This is explained in Fig. 3.59 where for a Napier exhaust turbo-charged C.I. engine (b)the valve overlap provided is 140° in contradistinction to that of a naturally aspirated engine (a) having a valve overlap of 20° only. The larger overlap will increase the throughput of scavenge air considerably.

To illustrate the scavenging operation in Fig. 3.60 the exhaust manifold pressure and the cylinder pressure have been plotted (25) against the crankshaft rotation. Due to the valve resistance, the cylinder pressure is always higher than the corresponding exhaust manifold pressure. During the latter part of the exhaust opening, the exhaust pressure droops down considerably below the air manifold pressure. This provides the pressure head for the charging air to effect scavenging until the exhaust valve is closed.

The effect of scavenging on the exhaust temperature was found by Hecht (21) and is shown in Fig. 3.61. It may be seen that the temperature of the exhaust at the turbine entrance drops down considerably (670°C to 512°C) during the scavenging operation. Also the pressure past the exhaust valve is lower than the pressure at the turbine entry due to the high kinetic energy

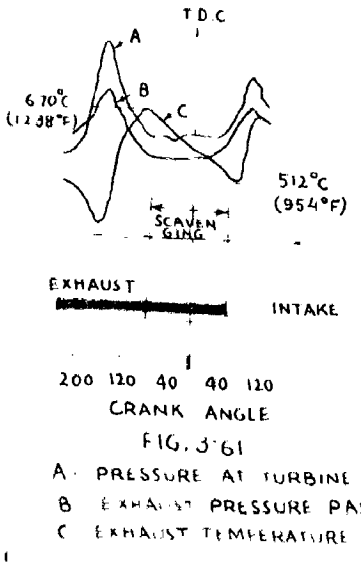

FIG. 3·61

A PRESSURE AT TURBINE ENTRANCE
B EXHAUST PRESSURE PAST DIESEL ENGINE
C EXHAUST TEMPERATURE AT TURBINE ENTRANCE

REF 21

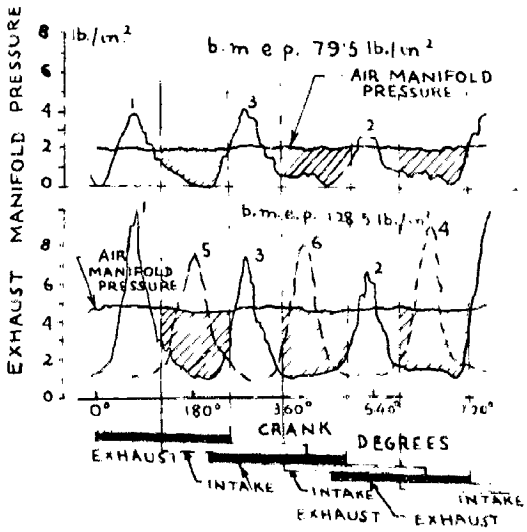

FIG. 3·62

REF 21

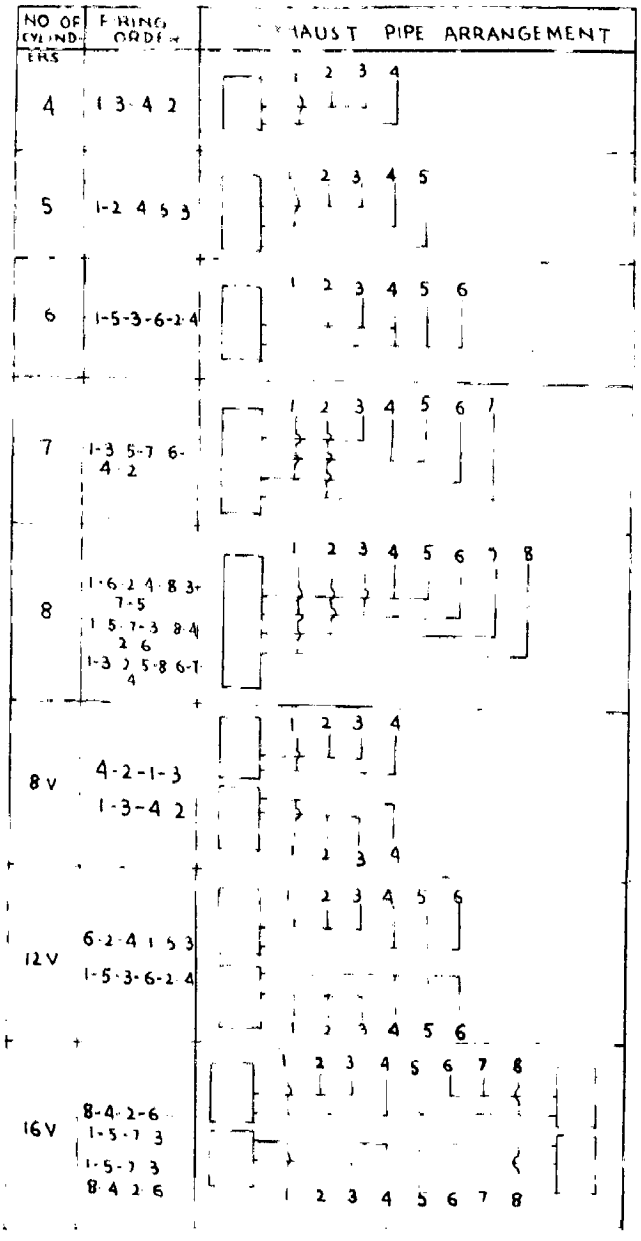

FIG. 3·63.

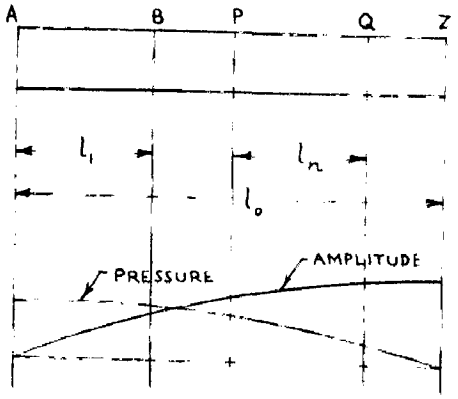

FIG. 3·64.

REF 21

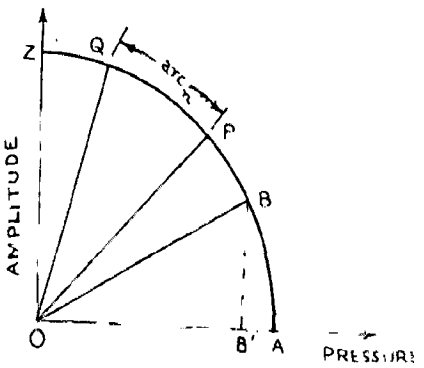

FIG. 3·65.

of the gases leaving the valve.

3.24 Exhaust Manifold of a Turbocharged Engine- In case of a single cylinder turbocharged engine, there is no difficulty, provided the exhaust system has been designed on the consideration of the pressure disturbances. But in a multi-cylinder engine, it may so happen that while one cylinder is exhausting, the other is being scavenged out of the exhaust gases. If the two cylinders have a common exhaust pipe, the pressure in the exhaust line being considerably high due to the exhaust from one of the cylinders, the scavenging of the other cylinder will be seriously impaired. This implies that to avoid the interference, either separate or sub-divided exhaust pipes should be used. As it may involve too much of complication to accomodate a number of exhaust pipes on the engine in a restricted space, in practice, the latter alternative is normally used.

It has been found that if the exhaust from two cylinders takes place in the same exhaust pipe within a crank angle of 240°, interference with scavenging takes place. This imposes a restriction that more than three cylinders firing consequently cannot be made to exhaust into a common manifold. Thus in a multi-cylinder engine either more than one turbo-charger, or turbine of the multi-entry type will be used.

Fig. 3.62 shows the exhaust manifold conditions of a six-cylinder turbo-charged diesel engine, obtained by Dr. Buchi (21) with the help of electric indicators and oscillographs. Superimposed on the exhaust pressure curve is shown the charging air pressure. The valve timing is shown at the bottom of the figure. The upper curve corresponds to 79.5 psi. b.m.e.p. and the lower one to 123.6 psi. b.m.e.p. The pressure peaks are much higher

in the latter case than in the former, whereas the roots of the troughs are nearly equally low. The pressure in the latter half of the exhaust opening is much b low the charging pressure, so that by properly adjusting the opening of the intake valve, effective scavenging is being achieved. The pressure oscillations of the exhaust from the remaining three cylinders, exhausting into a separate manifold, have also been shown by dotted lines in the lower diagram. The displacement in phase will obviously be 120°. It is clear that if all the cylinders would have been exhausting into the same manifold, scavenging would have been rendered entirely impossible. It is therefore, absolutely essential to divide the exhaust, typical exhaust 'steering-schemes' having been shown in Fig. 3.63.

3.25 Tuning of Exhaust Pipes- The sharp impulse initiated due to the discharge of the high pressure gases into the exhaust pipe set up pressure waves which travel back and forth with the velocity of sound in the pipe. Thus the pressure at any point in the pipe will rise and fall depending upon the natural frequency of the system. The amplitude of oscillation will be progressively reduced, till a new impulse from the subsequent exhaust puff is superimposed on the system. The pressure oscillations may be favourable or unfavourable depending up n the period or the frequency of the waves. If the natural frequency of oscillation (f) is equal to or is a multiple of the frequency of exhaust impulses ($f = \frac{N}{60}$ per sec. where N engine revs./ min.) , the conditions will be the most unfavourable. This is so because the rise in the pressure wave will regularly coincide with the exciting impulse. On the contrary, the conditions are the most favourable if the period of the waves is equal to the period of the exhaust valve opening

(i.e. $f = \frac{1}{\frac{a.60}{360.n}} = \frac{6n}{a}$ per sec. where a is the valve opening in crank degrees.) This will assist to create a partial vacuum during the latter part of the scavenging period, and also the depression will taper out while approaching the exhaust closure, thus enabling a large quantity of the high pressure charge to be entrapped within the engine cylinder.

The natural frequency of oscillation of the pressure waves in the exhaust system is determined by the length and diameter of the pipe and the volumes interposed in the system. The diameter of the pipe may be determined from a common formula

$$Q = 72 \sqrt{\frac{\Delta p\, d^5}{\rho L}} \qquad (3.27)$$

where Q = volume of exhaust in cu. ft. per min.

Δp = pressure drop in psi, which should normally be less than 5 in. of water.

d = diameter of the exhaust pipe, in.

ρ = specific weight of the exhaust gas, cu.ft./lb.

L = length of the pipe in ft.

Alternatively, the pipe diameter may be determined from the equation

$$Q = \frac{\pi}{4} d^2 . V \qquad (3.28)$$

where the velocity of the exhaust gases in the pipe may be taken as 250 fps. In practice slightly smaller diameter pipes give better performance.

The tuning is done by adjusting the length and the volumes interposed in the system. The main factor controlling the tuning is the natural frequency of the pressure waves. Both ana-

lytical as well as graphical methods are available to determine the frequency, but the former are too complicated to apply to the actual branched systems used in turbo-charged engines. Hence a graphical method evolved by Harning will be discussed below.

3.26 Natural Frequency of Pressure Waves in a Uniform Pipe- Let us consider a system (Fig. 3.64) consisting of an exhaust pipe with constant area and open at one end. The natural frequency of this system is

$$f = \frac{a}{4l_o} \cdot 60 = \frac{15a}{l_o} \quad (3.27)$$

where l_o is the length of the pipe in inches and a the velocity of sound (in /sec.) in the exhaust pipe. As a fair approximation, exhaust may be treated as atmospheric air for evaluating the sonic velocity. Hence

$$a = \sqrt{\gamma g RT} = 595 \sqrt{t + 460} \text{ in/sec.} \quad (3.28)$$

where t is the temperature in ^oF.

Due to the oscillation of exhaust gas in the pipe, the pressure and amplitude of the wave will vary from place to place as shown in Fig. 3.64. The values of the pressure and amplitude at different points may, therefore, be plotted on a polar diagram as in Fig. 3.65. Thus at any point B, the pressure is equal to OB' and the amplitude to BB'. These values may be represented to any scale.

Now arc AB (in terms of degrees of angle) $= \frac{l_1}{l_o} \times 90 \text{ deg.} \quad (3.30)$

Thus considering any length PQ $= l_n$, the corresponding arc PQ $=$ arc $_n = \frac{l_n}{l_o} \cdot 90$ deg. Substituting $l_o = \frac{15a}{f}$ from eq (3.28), we get

$$\text{arc}_n = \frac{l_n \cdot f}{15a} \cdot 90 = \frac{6 l_n f}{a} \text{ deg.} \quad (3.31)$$

The polar diagram may now be constructed of constantarea pipe by employing equations (3.29) and (3.31). However, to start with the value of the natural frequency has to be assumed. This leads to a method of trial and error. With the correct value of the frequency, the point Z on the polar diagram will be on the ordinate, because the pressure at the open end is zero (gauge).

3.27 Natural Frequency of Pressure Waves in a Pipe of Varying Cross- Section- The system shown in Fig. 3.66 represents an exhaust system composed of several pipes of different cross-sectional area. Eq.ns (3.29) and (3.31) will hold good for each pipe of constant area separately. It should be noted that where two pipes of different area are connected, pressure cannot change due to the simultaneous acceleration of air throughout the whole pipe, but the amplitudes, a_n and a_{n+1} at the point of connection will be inversely proportional to the areas, S_n and S_{n+1}. Thus we get

$$\frac{a_{n+1}}{a_n} = \frac{S_n}{S_{n+1}} \qquad (3.32)$$

The polar diagram for this system may now be constructed using eqns (3.29), (3.31) and (3.32) as given in Fig. 3.67. At end A of the pipe (the end being closed), the amplitude of the pressure wave is zero. So the corresponding point A, will be chosen arbitrarily on the abscissa. The temperature of the exhaust being known, the velocity of propagation of the pressure wave may now be calculated from eq.n (3.29). Thus arc $A_1B_1 = \frac{6l_1 f}{a}$, where l_1 being known, the arc length in degrees may be calculated, provided some suitable value of the frequency is assumed. As a first approximation, we may take, $f = \frac{15a}{l_o} = \frac{15a}{l_1 + l_2 + l_3 + l_4}$. Thus arc A_1B_1 is known. With centre O and radius OA_1, the arc may

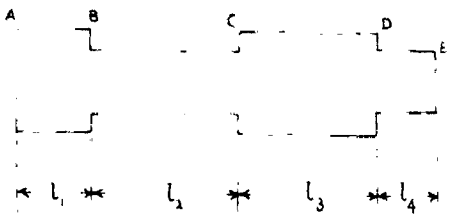

FIG 3·66.

REF 26

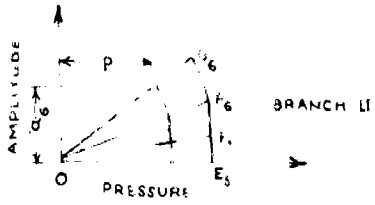

FIG 3·69

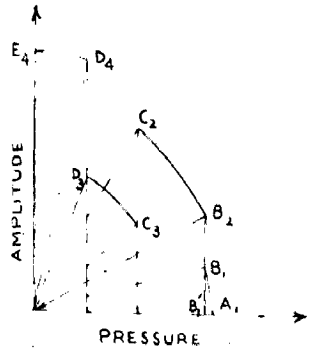

FIG 3·67

REF. 26

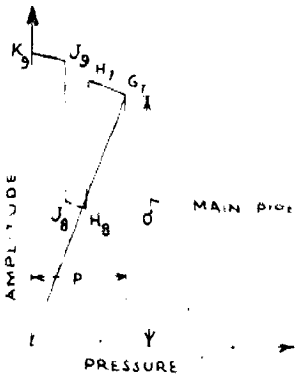

FIG 3·69

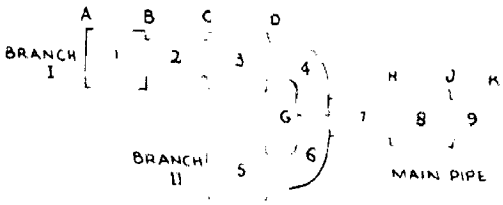

FIG 3·68.

REF. 26.

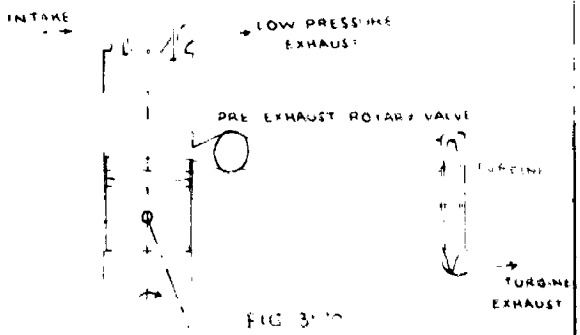

FIG 3·

REF 27

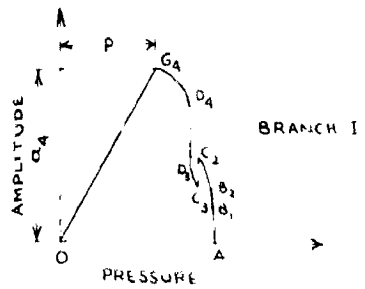

FIG 3·69

REF 26

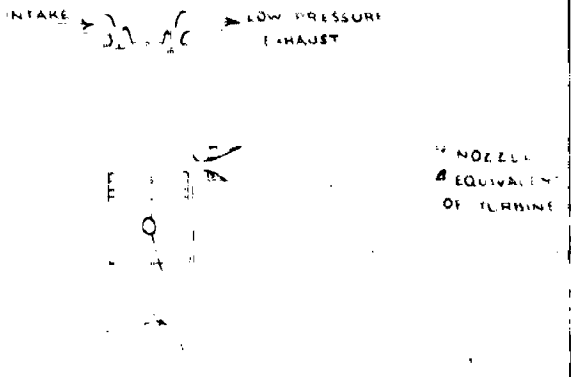

FIG 3·7

REF

now be drawn equal to its calculated length, so that B_1 is fixed. Since at the junction of pipes AB and BC, the pressure is the same, draw $B_1 B_2$ perpendicular to the abscissa where B_2 will be determined from eqn (3.32) i.e.

$$\frac{S_2}{S_1} = \frac{B_1 B_1'}{B_2 B_1'}$$

Now arc length $B_2C_2 = \frac{6\ell_2 f}{a}$, so C_2 is fixed. Again from the amplitude equation C_3 may be fixed up. Thus continuing this process, the diagram is completed where if the frequency assumed is correct, E_4 must be on the ordinate. Otherwise, the most approximate value of frequency should be determined by extrapolation. It will be found that normally after making two trials, the value of the frequency interpolated comes out to be fairly accurate.

3.30 Natural Frequency of Branched system of Turbo-charged Engines- In exhaust turbocharging, the same exhaust pipe is not be connected to more than three cylinders to avoid interference of the exhaust pulses. In case of a 4- cylinder engine, normally two exhaust pipes will be provided each receiving exhaust from two of the cylinders (Fig. 3.67). In a 6-cylinder engine, there will again be two exhaust pipes, each receiving exhaust from three of the cylinders. So as a typical case, a branched system of the type shown in Fig. 3.33 will be discussed here, and the method may be extended for the analysis of any other system.

The polar diagrams for different branches will be started from the ends of the branches and will be worked out towards the junction. The pressure p at this point being the same in both the branches, the diagram for the branch II will be reduced accordingly. The diagram for the main pipe will be started from the junction point. Here the amplitude a_7 will be determined from

the relationship,

$$a_7 \cdot S_7 = a_4 \cdot S_4 + a_6 \cdot S_6 \qquad (3.33)$$

The diagram will then be completed for the main pipe, whose if the last point will fall on the ordinate, the natural frequency of the branched system will be known. Otherwise, a few trials may have to be made as already discussed. The polar diagrams for the two branches as well as the main pipe are shown in Fig. 3.69.

In case of exhaust turbocharging, the main pipe will be connected to the turbine. For purposes of this analysis the turbine may be replaced by a nozzle, the effect of which will be to lower the natural frequency. The end of the pipe connecting the turbine will be treated as an open end. To account for the nozzle, a pipe of the same diameter (d) as that of the nozzle, and equal in length to 0.4d, should be connected on both sides of the nozzle.

3.29. Calculation of Exhaust Pulse Energy. It has been established that it is the blow-down energy which is utilized in the turbine of the exhaust turbo-charger. To facilitate its calculation, Pullman (27) suggested that the exhaust from an engine may be split up in two parts - the first part of the blow-down gases or pre-exhaust leading to a turbine, and the main exhaust (with reduced energy) discharged directly to atmosphere. This type of system is too advantageous in view of scavenging and is shown in Fig. 3.70.

To apply the analytical methods for the calculation of the exhaust pulse energy available to the turbine, let us resolve a system equivalent to that given in Fig. 3.69. By replacing the rotary valve, with a vena contracta, the problem is simplified, because now the cylinder may be considered to be discharging

directly into the exhaust pipe. The turbine may also be replaced by a nozzle of known area ratio. Such an equivalent system is shown in Fig. 3.71. This system will now be analysed to determine the amount of energy transported down the pipe and delivered to the turbine.

3.30 Analysis of the Equivalent System- Let us consider a pipe (Fig. 3.72) of cross-sectional area A_2, terminated by a nozzle of area $A2\phi$ where ϕ is the ratio of the nozzle area to the pipe area. The conditions of pressure, particle velocity and density at the throat of the nozzle are designated by P_t, u_t and ρ_t, and at the turbine outlet by P_o, u_o and ρ_o respectively. Now if a wave of amplitude p_2 and velocity u_2 be assumed to traverse a pipe, it will get reflected at the nozzle outlet with the values p_r and u_r. Thus the pressure p_n and particle velocity u_n, at any point in the pipe, resulting from the superimposition of the waves, are obtained from the summation laws (Appendix I) of Rucklos (28) which are

$$\left(\frac{p_n}{p_o}\right)^{\frac{1}{7}} = \left(\frac{p_2}{p_o}\right)^{\frac{1}{7}} + \left(\frac{p_r}{p_o}\right)^{\frac{1}{7}} - 1 \qquad (3.34)$$

and $$u_n = 5a_o\left[\left(\frac{p_2}{p_o}\right)^{\frac{1}{7}} - \left(\frac{p_r}{p_o}\right)^{\frac{1}{7}}\right]$$

or $$\frac{u_n}{a_o} = 5\left[2\left(\frac{p_2}{p_o}\right)^{\frac{1}{7}} - \left(\frac{p_n}{p_o}\right)^{\frac{1}{7}} - 1\right] \qquad (3.35)$$

on substitution from eq^n (3.34)

The laws of isentropic flow may now be applied to analyse the effect of nozzle upon the mass flow. Further for the subsonic range, it may be assumed that $P_t = P_o$ (back pressure), $a_t = a_o$, $\rho_t = \rho_o$.

The continuity eqn gives

$w_n \rho_n A_2 = w_t \rho_t A$ where $\frac{A}{A_2} = \phi$

so that $w_n \rho_n = \phi w_t \rho_t$ (3.36)

For isentropic flow of gas through the nozzle, we have

$$\frac{p_n}{\rho_n^\gamma} = \frac{p_0}{\rho_0^\gamma}$$

or $\frac{\rho_0}{\rho_n} = \left(\frac{p_n}{p_0}\right)^{\frac{1}{\gamma}} = \left(\frac{a_0^2 \rho_0}{\gamma} \cdot \frac{\gamma}{a_n^2 \rho_n}\right)^{\frac{1}{\gamma}}$ from $a^2 = \frac{\gamma p}{\rho}$

$= \left[\left(\frac{a_0}{a_n}\right)^2 \cdot \frac{\rho_0}{\rho_n}\right]^{\frac{1}{\gamma}}$

or $\left(\frac{a_0}{a_n}\right)^{\frac{2}{\gamma}} = \left(\frac{\rho_n}{\rho_0}\right)^{\frac{1}{\gamma}} \left(\frac{\rho_0}{\rho_n}\right) = \left(\frac{\rho_0}{\rho_n}\right)^{1-\frac{1}{\gamma}}$

i.e. $\left(\frac{a_0}{a_n}\right)^{\frac{2}{\gamma-1}} = \frac{\rho_0}{\rho_n} = \frac{\rho_t}{\rho_n}$ (for subsonic flow).

Substituting in (3.36),

$$\frac{\rho_t}{\rho_n} = \frac{1}{\phi} \cdot \frac{w_n}{w_t} = \left(\frac{a_0}{a_n}\right)^{\frac{2}{\gamma-1}}$$

or $w_t = \frac{1}{\phi} \cdot w_n \left(\frac{a_0}{a_n}\right)^{\frac{2}{\gamma-1}}$ (3.37)

Now the energy equation is

$$\frac{1}{2} w^2 + C_p T = C_p T_0$$

or $\frac{1}{2} w^2 + \frac{\gamma}{\gamma-1} RT = \frac{\gamma}{\gamma-1} RT_0$ where $a = \sqrt{\frac{\gamma p}{\rho}} = \sqrt{\gamma RT}$

Therefore, $w^2 = \frac{2}{\gamma-1} \left[a_0^2 - a^2\right]$

Applying this equation to the system,

$$w_t^2 - w_n^2 = \frac{2}{\gamma-1} \left[a_0^2 - a_t^2 - a_0^2 + a_n^2\right]$$

$$= \frac{2}{\gamma-1} \left[a_n^2 - a_t^2\right]$$

But for subsonic flow $a_t = a_0$, so that

$$w_t^2 - w_n^2 = \frac{2}{\gamma-1} \left[a_n^2 - a_0^2\right] \quad (3.38)$$

Eliminating w_t from (3.37) and (3.38)

$$\frac{1}{\phi^2}\cdot\frac{w_N^2}{a_0^2}\left(\frac{a_N}{a_0}\right)^{\frac{4}{\gamma-1}} - \frac{w_N^2}{a_0^2} = \frac{2}{\gamma-1}\left[\left(\frac{a_N}{a_0}\right)^2-1\right]$$

$$\text{or}\quad \left(\frac{w_N}{a_0}\right)^2 = \frac{\frac{2}{\gamma-1}\left[\left(\frac{a_N}{a_0}\right)^2-1\right]}{\frac{1}{\phi^2}\cdot\left(\frac{a_N}{a_0}\right)^{\frac{4}{\gamma-1}}-1} \qquad (3.39)$$

Since $\frac{\rho_0}{\rho_N} = \left(\frac{p_0}{p_N}\right)^{\frac{1}{\gamma}} = \left(\frac{a_0}{a_N}\right)^{\frac{2}{\gamma-1}}$. (already derived),

(3.39) may also be written as

$$\left(\frac{w_N}{a_0}\right)^2 = \frac{2}{\gamma-1}\cdot\frac{\left[\left\{\left(\frac{p_N}{p_0}\right)^{\frac{\gamma-1}{2\gamma}}\right\}^2-1\right]}{\left[\frac{1}{\phi^2}\left\{\left(\frac{p_N}{p_0}\right)^{\frac{\gamma-1}{2\gamma}}\right\}^{\frac{4}{\gamma-1}}-1\right]} \qquad (3.40)$$

The above equation describe the behaviour of the gas in the nozzle, in the subsonic range only when the particle velocity will become sonic, $w_t = a_t = a_0$. Thus to determine the sonic limit state, substituting

$\frac{w_t}{a_0} = 1$ in eqn (3.37),

$$a_0^2 - w_N^2 = \frac{2}{\gamma-1}\left[w_N^2 - a_0^2\right]$$

$$\text{or}\quad 1 - \left(\frac{w_N}{a_0}\right)^2 = \frac{2}{\gamma-1}\left[\left(\frac{a_N}{a_0}\right)^2-1\right]$$

$$\text{or}\quad \frac{2}{\gamma-1}\left(\frac{a_N}{a_0}\right)^2 + \left(\frac{w_N}{a_0}\right)^2 = \frac{\gamma+1}{\gamma-1} \qquad (3.41)$$

The intersection of the curve (3.41) with (3.39) will give the critical values. Thus combining the two equations and putting

$$3\cdot5 - 5\left(\frac{a_N}{a_0}\right)^2_{crit} = \frac{5\left[\left(\frac{a_N}{a_0}\right)^2_{crit}-1\right]}{\frac{1}{\phi^2}\left(\frac{a_N}{a_0}\right)^{10}_{crit}-1}$$

$$\text{or}\quad 6 - 5\left(\frac{a_N}{a_0}\right)^2_{crit} = \frac{5\left[\left(\frac{a_N}{a_0}\right)^2_{crit}-1\right]}{\frac{1}{\phi^2}\left(\frac{a_N}{a_0}\right)^{10}_{crit}-1} \qquad (3.42)$$

From eq^{n} (3.39) for a fixed value of ϕ, the value of $\left(\frac{w_N}{a_0}\right)$ may be calculated for different values of $\left(\frac{a_N}{a_0}\right)$. Thus for ϕ = constant (a fixed value), a curve can be plotted between $\left(\frac{w_N}{a_0}\right)$ and $\left(\frac{a_N}{a_0}\right)$. But since from the continuity equation,

$$\frac{\rho_N}{\rho_0} = \left(\frac{a_N}{a_0}\right)^{\frac{2}{\gamma-1}} = \left(\frac{p_N}{p_0}\right)^{\frac{1}{\gamma}}$$

$$\text{or} \quad \frac{p_N}{p_0} = \left(\frac{a_N}{a_0}\right)^{\frac{2\gamma}{\gamma-1}} \qquad (3.43)$$

so alternatively the curve may be plotted between $\left(\frac{w_N}{a_0}\right)$ and $\left(\frac{p_N}{p_0}\right)^{\frac{1}{\gamma}}$ as has been done in Fig. 3.73. By taking different values of ϕ, a number of such curves may be obtained.

From eq^{n} (3.35) it may be seen that for a given value of $\left(\frac{p_2}{p_0}\right)^{\frac{1}{\gamma}}$, there exists a linear relationship between $\left(\frac{w_N}{a_0}\right)$ and $\left(\frac{p_N}{p_0}\right)^{\frac{1}{\gamma}}$. These inclined lines have also been drawn in Fig. 3.73 intersecting the ϕ curves. Thus it is now possible to determine the variation of p_N and w_N with time, that is, the net conditions obtaining in the pipe. For a fixed value of γ and a particular value of $\left(\frac{p_2}{p_0}\right)^{\frac{1}{\gamma}}$, the values of $\left(\frac{w_N}{a_0}\right)$ and $\left(\frac{p_N}{p_0}\right)^{\frac{1}{\gamma}}$ may be read out from the figure. Also from eq^{n} (3.43) the corresponding value of $\left(\frac{a_N}{a_0}\right)$ may be calculated. These value will be required in the next article for the calculation of the energy drop available in the exhaust turbine.

3.31. Exhaust Energy Utilized in the Turbine. The area of the exhaust pipe being A_2 and the net particle velocity and density of the exhaust gas being w_N and ρ_N, the mass flow into the turbine at any instant is given by, $G = A_2 \cdot w_N \cdot \rho_N$.

Energy of the exhaust gas per unit mass flow rate (in unit time)

$$= \frac{1}{2} w_N^2 + C_p T_N$$

$$= \frac{1}{2} w_N^2 + \frac{\gamma}{\gamma-1} RT_N = \frac{1}{2} w_N^2 + \frac{\gamma}{\gamma-1} \cdot \frac{p_N}{\rho_N}$$

Hence energy supplied into the nozzle or turbine in a time interval Δt

$$E_N = \left(\frac{1}{2}\frac{G}{g} w_N^2 + \frac{G}{g} \cdot \frac{\gamma}{\gamma-1} \cdot \frac{g p_N}{\rho_N}\right) \Delta t$$ where 'g' has been introduced in the numerator of the last term to keep consistent units.

$$\therefore E_N = \frac{G}{2g}\left[w_N^2 + \frac{2\gamma}{\gamma-1} \cdot \frac{g p_N}{\rho_N}\right] \Delta t \qquad (3.44)$$

Now $\frac{2}{\gamma-1} \cdot \left(\frac{g\gamma p_N}{\rho_N}\right) = \frac{2}{1.4-1.0} (a_N)^2 = 5a_N^2$

Thus eq^n (3.44) is

$$E_N = \frac{G}{2g}\left[w_N^2 + 5a_N^2\right] \Delta t$$

$$= \frac{A_2}{2} \cdot \frac{w_N \rho_N}{g}\left[w_N^2 + 5a_N^2\right] \Delta t \qquad (3.45)$$

Now for isentropic flow

$$\frac{\rho_N}{\rho_0} = \left(\frac{a_N}{a_0}\right)^{\frac{2}{\gamma-1}} = \left(\frac{a_N}{a_0}\right)^5 \qquad \text{(already derived)}$$

Hence eq^n (3.45) may be written as

$$E_N = \frac{A_2}{2} \cdot w_N \cdot \left(\frac{a_N}{a_0}\right)^5 \cdot \frac{\rho_0}{g}\left[w_N^2 + 5a_N^2\right] \Delta t$$

$$= \frac{A_2}{2} \cdot \left(\frac{a_N}{a_0}\right)^5 \cdot w_N \gamma p_0 \left(\frac{\rho_0}{\gamma g p_0}\right)\left[w_N^2 + 5a_N^2\right] \Delta t$$

$$= \frac{A_2}{2} \cdot \gamma p_0 a_0 \left(\frac{w_N}{a_0}\right) \cdot \left(\frac{a_N}{a_0}\right)^5 \left[\left(\frac{w_N}{a_0}\right)^2 + 5\left(\frac{a_N}{a_0}\right)^2\right] \Delta t \qquad (3.46)$$

Assuming outlet velocity to be negligibly small, energy remaining after expansion

$$E_T = G C_p T_0 \Delta t = G \frac{\gamma}{\gamma-1} R T_0 \Delta t$$

$$= \frac{G}{2g} \cdot 5(a_0)^2 \Delta t$$

Hence the energy drop available in the turbine,

$$E = E_N - E_T = \frac{A_2}{2} \gamma p_0 a_0 \left(\frac{w_N}{a_0}\right)\left(\frac{a_N}{a_0}\right)^5 \left[\left(\frac{w_N}{a_0}\right)^2 + 5\left(\frac{a_N}{a_0}\right)^2 - 5\right] \Delta t \qquad (3.47)$$

Since the values of $\left(\frac{w_N}{a_0}\right)$ and $\left(\frac{a_N}{a_0}\right)$ at any instant may

be found from Fig. 3.73, the total energy delivered to the turbine may be calculated. Hence the actual amount of energy utilized by the turbine can be determined, provided the efficiency of the turbine is known. According to the latest information for full periphery admission a typical value of turbine efficiency is 70%.

3.32 Factors Affecting the Blowdown Pulse Energy- In practice friction in the exhaust pipe is encountered, which may be neglected for preliminary calculations. The effect of friction (29) is to reduce the particle-velocity, as a result of which the mass of the exhaust gases swept out of the engine is reduced. The expressions derived while taking friction into consideration are very complicated. The available energy is also influenced by the port area and the pipe area. Thus the available energy has been found to be the maximum when the port area is equal to the pipe area. At larger values the energy transmitted in the first pulse is greater than in the succeeding pulses.

3.33 Low Pressure Turbocharging- This is the most widely applied form of turbocharging giving a power increase of about 50 per cent over the naturally aspirated version, at a pressure ratio of 1.5:1. The mean effective pressure produced is 75-95 psi, and may even go to 125 psi in high speed rail traction engines. The maximum pressure produced in the cylinder is about 900 psi, and the maximum temperature at the valves is 900°F. The values of pressure and temperature are nearly the same as would be obtained in case of a naturally aspirated engine at full load. Hence if an ordinary four-stroke engine is to be converted into a low pressure turbo-charged engine, the engine need not be re-designed. However, the following modifications will have to be made-

(1) A valve overlap of about 140° in order to provide an effective

air of about 30 per cent for scavenging and cooling the piston head, cylinder barrel and the valves. This will require specially designed cams and recesses in the piston head.

(2) In a multi-cylinder engine, the exhaust gases from the groups of cylinders firing at less than 240° to be led through separate or sub-divided pipes to the turbine nozzle.

(3) Due to larger quantity of fuel required per cycle, the fuel injection equipment will have to adjusted. The lengthening of the injection period being objectionable, it will be done by the use of larger fuel pump plungers and slightly larger orifices in the injector nozzle.

(4) Sometimes, the valve lift may have to be increased for better volumetric efficiency conditions. Also the valve diameters, the shape of the piston head, or the size of the intake and exhaust manifold may require modification.

3.34 Altitude Turbocharging- This yields a power increase of about 50 per cent in engines operating at altitudes above 1000 ft., compared to the power developed by the engine in the naturally aspirated form at sea level. To develop this power the pressure ratio will be of the order of 1.8-2 : 1, and the mean effective pressures about 75 to 120 p.s.i. Due to the high compression pressure, the pressurised air will be cooled before passing to the engine cylinder. Also a high pressure turbocharger will have to be used.

The maximum pressure and temperature limits being the same as in the case of a low pressure turbo-charged engine, the same modifications will have to be introduced for conversion into the supercharged form.

3.35 High Pressure Turbocharging- This is used for power increase up to 120 per cent with as high compression ratio as 2.2, resulting

in a b.m.e.p. of 200-220 lb. per sq. in. the maximum ignition pressure for a high pressure turbocharged engine may be 1200-1500 psi. Hence high pressure turbocharging requires, an engine specially designed for the purpose. Due to high compression of the charging air, its temperature will be sufficiently high (say 170°F) so that cooling becomes indispensable in order to achieve any substantial power increase. Furthermore, due to low scavenging efficiency (30) at higher pressure ratios cooling is the only resort to keep down the exhaust temperature below the limiting value of 1500°F for use in the turbine.

3.33 Characterised Features of High Pressure Turbo-charged Engines- Due to very high maximum pressures produced, the highly stressed parts of the engine have to be correspondingly strengthened. Sometimes, instead of a cast iron frame, a welded steel monobloc frame may be employed. Due to high thermal loading on the engine, cooled pistons may be used. The cooling arrangements for the top end of the liner should provide the temperature gradient for the heat to flow away from the piston and combustion space through the piston rings. The number, size and location of the piston rings should be so adjusted that the excessive heat produced does not produce the ring seizure.

The engine must have the necessary arrangement for the after-cooling of air, so that the temperature of the charging air is not over 100-110°F. This will require specially designed water circulated coolers of small bulk, less weight and low pressure drop.

The engine should be fitted with a modified fuel injection equipment capable of supplying adequate quantity of fuel for the high pressure turbocharged condition. The conventional fuel pumps require very long injection periods which is objectionable. The

other alternative is to fit larger plunger and more massive elements, but this results in the overloading of the drive gear. So the only possible recourse is to increase the rate of fuel injection which, in practice, is obtained by servo-operation. The method was recently developed by the British Internal Combustion Engine Research Association.

Fig. 3.75 shows a servo-operated fuel injection system, where a gear pump A, driven at several times the engine speed, feeds the fuel to a chamber C through a control valve B. The pressure of the fuel in the chamber is about 1,000 psi. Below this chamber is another chamber E, charged with high pressure air, and separated from the above by a rubber diaphragm D. The piston valve F is operated against the spring force by a Cam G. The displacement of the piston valve will make the high pressure fuel communicate with H through the moving piston F and thence with the fuel - pump plunger J. The effort to the fuel will be supplied by the expansion of air in the chamber E. Next the displacement of the piston valve back to the left due to the spring force will release oil from chamber H, and so the fuel-pump plunger will be thrown back to its initial position. It should be noted here that if the ratio of the areas of the piston H to the plunger J is 5, the oil injection pressure will then be 500 psi. in the fuel line. The high pressure so developed accelerates the rate of fuel injection. The maximum injection pressure can also be varied by presetting the servo pressure at the control valve B.

3.37 <u>After-Cooling</u> It has been observed that in an engine developing a b.m.e.p. of about 140 lb. per sq. in. at a pressure ratio of 1.4:1, the exhaust gas temperature at the turbine inlet is nearabout 1200°F. This implies that further increase in b.m.e.p.

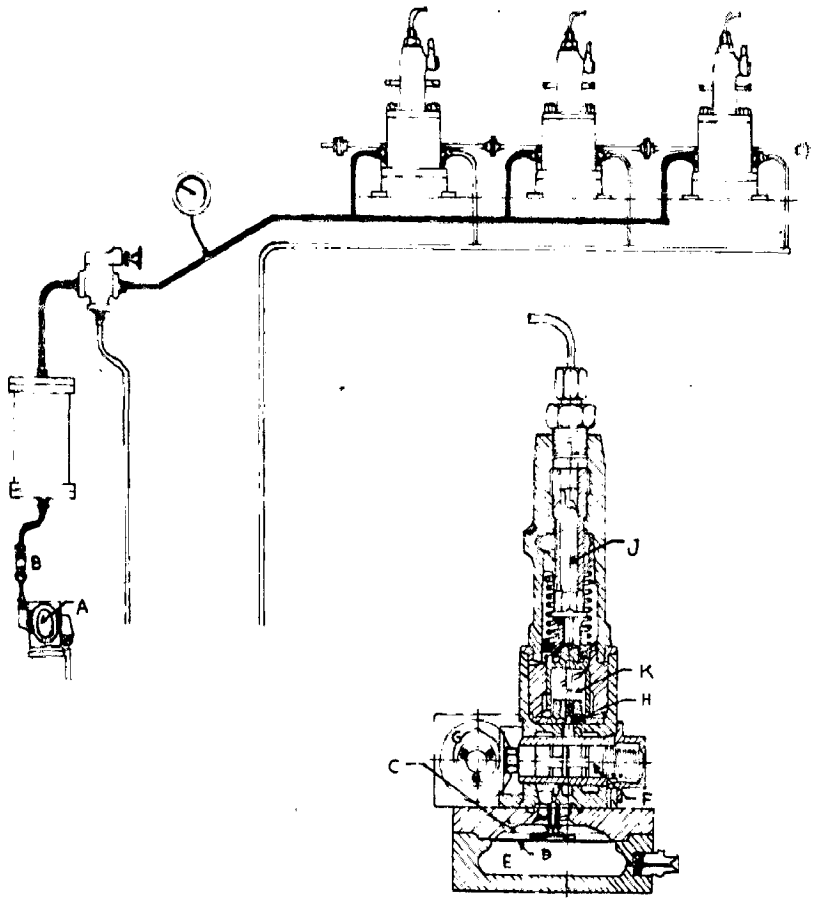

REF. 31.

SERVO-OPERATED FUEL INJECTION SYSTEM.
FIG. 3·75.

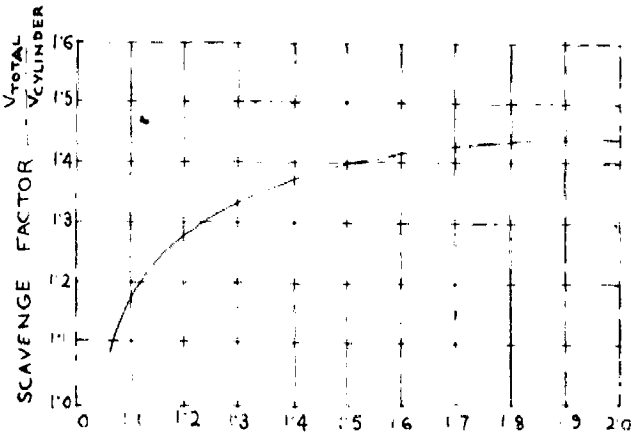

FIG. 3·74.

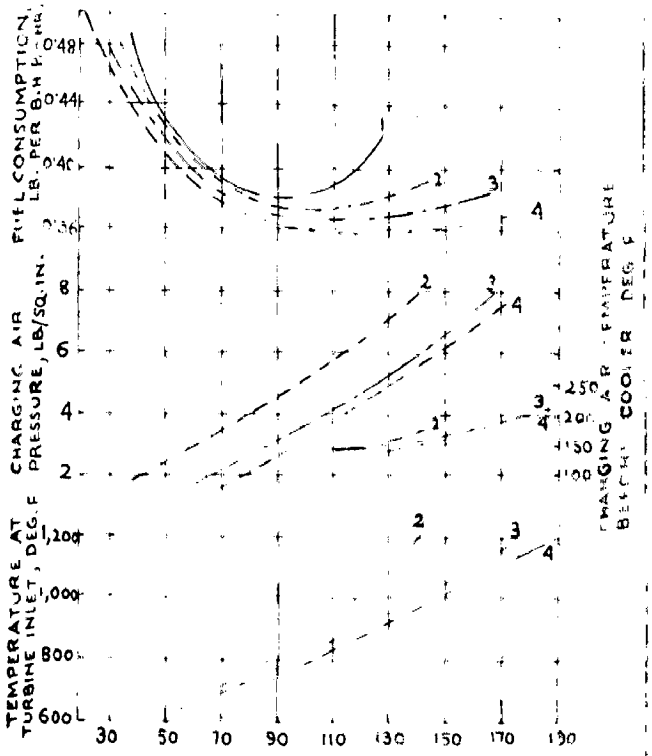

NOTATIONS OF FIG. 3·76

1 - NOT SUPERCHARGED.
2 - TURBO-CHARGED, NO AFTERCOOLING
3 - TURBO-CHARGED, AFTERCOOLING TO 64°F
4 - TURBO-CHARGED, AFTERCOOLING TO 36°F

REF. 30

PERFORMANCE CURVES SHOWING EFFECT OF AFTER COOLING
FIG. 3·76

or the pressure ratio will necessitate the aftercooling of air i.e., between the blower delivery and the engine inlet valve. However, with moderate pressure charging (manifold pressure upto 5 psi and power outputs upto 50% extra) it is not considered economical to cool the air charge.

In order to assess the possibilities of high output coupled with charge cooling, Bradbury (31) subjected an 8.5 litre six-cylinder engine running at 1500 r.p.m. to test under naturally aspirated and turbocharged conditions. With the latter varying degrees of aftercooling was also employed. The only limit imposed on power output was the limiting temperature of 1200°F at the exhaust gas turbine inlet.

Fig. 3.76 gives the curves plotted from the results obtained during the test. It may be seen that the specific fuel consumption of the un-supercharged engine is the highest, and it goes on decreasing with increased after-cooling for a turbocharged engine. Curve 2 shows that in the simple turbocharged case (no after-cooling), the maximum b.m.e.p. was 140 psi. with a specific fuel consumption of 0.39 lb. per b.h.p.hr. Also the charging air pressure and temperature for this case were 8 psi. and 175°F respectively. In case 3 with aftercooling to a temperature of 64°F, the b.m.e.p. increased to 175 psi for the same specific fuel consumption. In case 4 with aftercooling to 33°F, there was a further increase in b.m.e.p. to 180 psi. for a reduced specific fuel consumption of 0.372 lb. per b.h.p.hr. The parallel shape of the charging air pressure lines leads to the conclusion that, for the same maximum charge pressure, increased output could be obtained with the further lowering in temperature, this being impracticable. Hence power increase is only possible with moderate aftercooling

coupled with higher and higher charge pressures.

The effect of aftercooling and scavenging on power output for pressure ratios up to 4 may be studied from Fig. 3.77 which is based on the investigations of Dr. A.J. Buchi (2) on a multi-cylinder engine. The keys to the various curves are given below the caption in the figure. It may be seen that both scavenging and aftercooling improve the power output of the engine, the best results being obtained with (cs co 100), which refers to turbocharging with scavenging and cooling of the charge back to ambient temperature.

Of the various factors that govern the upper limit of supercharging, smoke limit is also an important factor. At this output limit profuse smoking occurs. It corresponds to an excess of air, the latter being about 1.3 times the theoretical quantity of air required for complete combustion. This is represented by (SL) in the figure.

The charge coolers generally used in turbocharging are water-cooled air coolers already described in article 3.17. The effectiveness of a cooler is defined as the ratio of charge air temperature drop to available temperature drop between charge air inlet temperature and cooling water inlet temperature. Thus the effectivness of the cooler used must be atleast 80 per cent. The coolers are normally designed for air velocities of about 35 ft./Sec. and water velocities of 2 ft./Sec. The performance of a typical air cooler is given in fig. 3.78.

3.33 Development of Cooling Methods in High Pressure Exhaust Gas Turbocharging. Efforts are being made to explore all the measures by means of which as high a power output as possible may be obtained out of an engine. Higher pressure ratios combined with cooling have shown promising results. But for effective cooling, the temperature

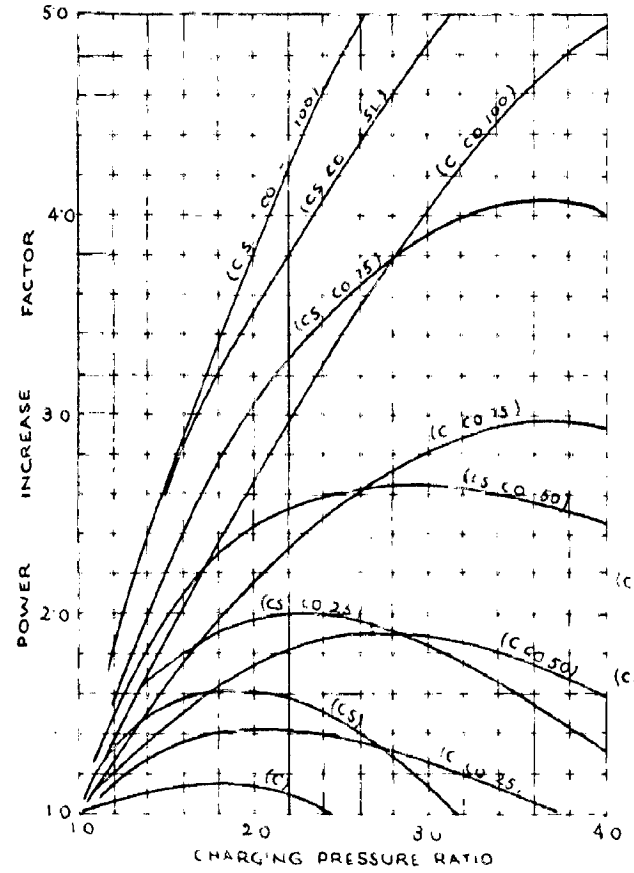

REF 2

FIG 3·77

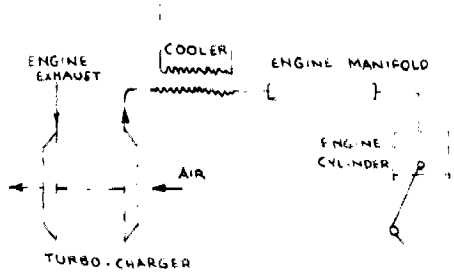

MILLER SYSTEM OF TURBO CHARGING

FIG 3·79

REF 31

NOTATIONS FOR FIG. 3·79

(C) – TURBO CHARGING WITHOUT SCAVENGING

(C CO 50) – TURBO CHARGING WITHOUT SCAVENGING BUT WITH AIR COOLED TO 50 PER CENT OF THE TEMPERATURE INCREASE IN COMPRESSOR

(CS) – TURBOCHARGING WITH SCAVENGING

(CS CO 50) – TURBO CHARGING WITH SCAVENGING AND CHARGING AIR COOLED TO 50 PER CENT OF THE TEMPERATURE INCREASE IN COMPRESSOR

(SL) – SMOKE LIMIT AS 98 86 PER CENT [illegible]

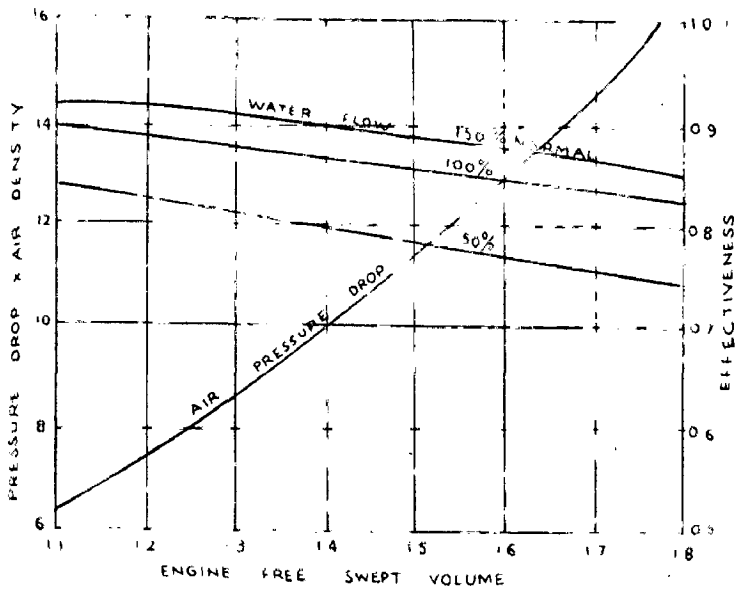

CHARGING AIR COOLER PERFORMANCE

FIG. 3·78

REF 17

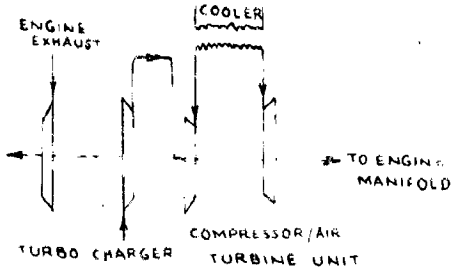

COOPER BESSEMER SYSTEM OF TURBO-CHARGING

FIG 3·80

REF 31

of the coolant should be considerably lower than the temperature of the air charge. Hence watercooling has not proved efficacious for the lowering of temperature beyond a particular limit. Several schemes have, therefore, been proposed for the cooling of the air charge to make high pressure turbo-charging possible. These schemes are the Miller, the Sone and the Buchi Duplex.

The Miller System of Turbo-charging (Fig. 3.79)- Here the compressed air from a high pressure turbo-charger is delivered to a conventional after-cooler. The cooled air then passes to the engine cylinder at a temperature of about 140°F. Partial expansion of the air is made to take place in the engine cylinder by closing the inlet valve a few crank degrees before the bottom dead centre. This makes the temperature of the air to fall down at the beginning of the compression. The system is complicated because variable valve timing is required for different load conditions which is achieved by swinging the inlet valve cam roller.

The Sone System or the Cooper-Bessemer System of Turbo-charging (Fig. 3.80)- Here air is first compressed into a compressor driven by the exhaust turbine and delivered to the second compressor. Air coming out of the second compressor is then cooled in a conventional cooler and fed to an air turbine. Here the expansion of air takes place resulting in the lowering of its temperature. Thus the motive power to the air turbine is supplied by the expanding air which in turn drives the second compressor. Since the intercooler is used here after the second stage of compression, cooling medium at a relatively high temperature may be employed. This makes the system suitable for automotive engines where radiator water (120-160°F) is used.

The BuchiDuplex System of Turbocharging- Here compression of the

air takes place in two stages. The power is supplied by a mechanical drive to the first compression stage, whereas the second stage compressor is driven by the exhaust turbine. Cooling of air is effected either between each of the stages or only at the end of second stage compression. While starting the second stage compressor is usually by-passed. However, this system has not offered any particular advantages when applied to four stroke engines, and is definitely of great use in two stroke engine turbocharging.

3.39 Economic Aspects of Turbocharging-

1. For a turbocharged engine, the weight and space requirements are smaller. The weight of the charger together with the exhaust manifold and air pipes may be expected to be about 3 per cent of the weight of a medium speed engine. The specific weight of an uncharged engine is about 45 per cent greater than that of the turbo-charged engine for the same power; the dimensions of the uncharged engine are also 40 to 45 per cent greater.

2. Pressure charged engines cost less than the ordinary engines for the same power output. Further the operating costs of supercharged diesel engines are lower, because heavier fuels can be burnt.

3. The specific fuel consumption of pressure charged diesel engines is lower.

4. The consumption of lubricating oils in turbocharged diesel engines is lower.

5. The closed circuit water-cooling plant of turbo-charged engines is smaller, but the heat content of exhaust gases is greater.

6. Maintenance and overhauling costs of turbocharged engines are lower.

7. Turbo-charged engines can be readily overloaded, because the turbocharger speed alters automatically with load variations.

8. The exhaust of a turbocharged engine is quieter because of the uniform discharge of gases from the turbine. Hence no special silencing is required.

EXHAUST GAS TURBOCHARGERS

3.40 Turbocharger construction- Most of the turbochargers have a centrifugal compressor and an axial flow turbine, run on ball bearings. Recently turbochargers have also been developed with radial-flow turbines and bush bearings for the low power range. Some high pressure turbochargers may have the axial compressors as well.

The largest manufacturers of the turbochargers are the Brown Boveri Company and the British Napier Turbochargers. As a typical illustration Fig. 3.81 gives the constructional details of the Brown Boveri Buchi type turbocharger (20). It has a single-stage centrifugal compressor on the left, driven by a single-stage axial flow turbine on the right. The engine exhaust enters the turbine at A and leaves at B. The centrifugal compressor, whose inner and outer casings are marked by C and D, draws air through the suction and silencer hood E. The composite unit of the compressor and the turbine is fitted on the engine by the foot mountings F-F.

Between the compressor and the turbine, there is sufficient air space which serves to heat-insulate the compressor from the turbine. There is also a heat insulating barrier G provided for the purpose. The common drive shaft is provided with a protective sleeve shown in the figure. The turbine rotor carries the blades on its periphery, on which flow the hot exhaust gases ejecting from the nozzle ring K. Thus the exhaust gas turbine drives the shaft which, on the other end, has an impeller J mounted upon it. While passing through the impeller, the air is accelerated, and after flowing through the diffuser, the high pressure air comes out of the spi-

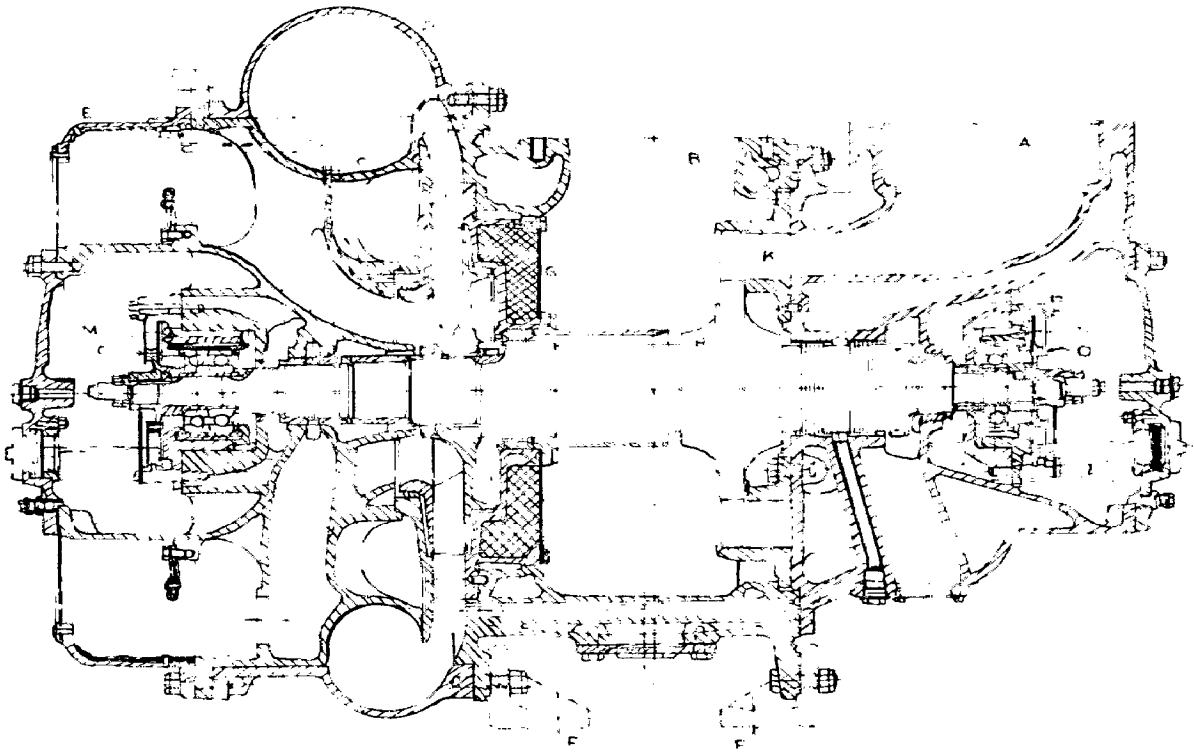

BROWN - BOVERI BUCHI TYPE TURBO-CHARGER
FIG 3 81.

ral volute.

The steel shaft is supported on two resiliently mounted high speed bearings. The bearing on the compressor outlet casing is a thrust bearing located in an aluminium- bronze housing. The turbine-end bearing 3 is a ball bearing encased in a mild-steel housing. Both the housings serve as oil reservoirs where the lubricating oil to the bearings is supplied by the oil-throw disc 0. These oil sumps are provided with drain plugs, oil filler cap, oil-level sight glass and an internally screened breather.

The turbine inlet and outlet casings are made of special heat-resisting cast iron. These are provided with removable covers for inspection and cleaning. The wheel is forged out of high temperature material. The blades which are of high heat resistant alloy make a sliding fit in the rotor. These are provided with very fine radial tip clearances on the periphery. The compressor casing is cast in sea-water-resisting aluminium alloy and the impeller is a machined aluminium forging.

Turbochargers employing high compression ratios, have an open sided centrifugal compressor and are provided with shorter turbine blades, the external dimensions remaining unchanged. The unit shown in Fig. 3.80 is meant for low pressure supercharging for boost ratios of 1.5:1.

For universal applicability of the turbocharger, the compressor and the turbine casings are so designed that these may be fitted at any angle. The mounting feet are also adjustable so that the turbocharger may be installed at any desired place on the engine.

3.41 Axial Flow Turbine- Till recently axial flow turbines were exclusively used in exhaust gas turbochargers. Here exhaust from the engine enters the fixed guide vanes acting as nozzles, so that

th gases are accelerated whic when impinge upon the moving blades advancing in an axial direction, are deprived of the bulk of their kinetic energy. This imparts the tangential momentum to the baldes. In a multistage turbine this process will be repeated in a number of stages. Thus the gases leaving the first stage will enter the nozzles of the second stage and thence on to the next moving blade ring, and soon. In case of exhaust, sufficiently rich in energy, a multistage turbine should preferably be used, otherwise the outlet velocity loss is appreciable. The variation of pressure and temperature due to the passage of gas along the fixed and moving blades of a stage is shown in Fig. 3.82. The velocity triangles at the inlet and exit ends of the moving blade are also shown in the diagram. Obviously,the work done per lb. of gas on the blades is given by

$$W = \frac{u(V_{W_1} - V_{W_2})}{2} \qquad (3.48)$$

The p-v diagram for the wor done in the turbine is shown in Fig. 3.83 where the expansion take place alon 3-4 in the ideal case. The actual expansion will take place along some curve 3-4,/ in which case the work obtained by expansion in the turbine will decrease by the amount of the area 3-4-4'.

The work done in turbine in an ideal case

$$= p_3 V_3 + \frac{p_3 V_3 - p_4 V_4}{\gamma - 1} - p_4 V_4$$

$$= \frac{\gamma}{\gamma - 1} (p_3 V_3 - p_4 V_4)$$

$$= \frac{\gamma}{\gamma - 1} p_3 V_3 \left[1 - \left(\frac{p_4}{p_3}\right)^{\frac{\gamma-1}{\gamma}}\right] \qquad (3.49)$$

The temperature drop in the turb ne in an ideal case

$$= T_3 - T_4 = T_3 \left[1 - \left(\frac{p_4}{p_3}\right)^{\frac{\gamma-1}{\gamma}}\right] \qquad (3.50)$$

So the work done per min. in the turbine in an ideal case

$$= w C_p (T_3 - T_4) = w C_p T_3 \left[1 - \left(\frac{p_4}{p_3}\right)^{\frac{\gamma-1}{\gamma}}\right] \qquad (3.61)$$

where w is the weight of gas passing through the turbine per min.

Now adiabatic efficiency of the turbine,

$$\eta_{at} = \frac{\text{actual work done}}{\text{ideal work done}}$$

Hence the turbine power, which must equal the compressor power, is given by

$$\text{H.P.} = \frac{w C_p T_3 \left[1 - \left(\frac{p_4}{p_3}\right)^{\frac{\gamma-1}{\gamma}}\right] \eta_{at} \cdot \eta_m}{33,000} \qquad (3.62)$$

where η_m is the overall mechanical efficiency of the turbo-charger.

3.42. Radial Flow Turbine. The use of radial turbines as exhaust gas turbines is a recent development, and has resulted due to its potential advantages of cheapness, higher efficiency and ease of manufacture. These are especially suited in certain applications, because the vanes can be swivelled by an external mechanical linkage which increases their suitability from the matching point of view.

In construction a radial turbine may be conceived as a centrifugal compressor running backwards that is the hot gases enter at the periphery, pass through the nozzle blades, thence through the impeller, and finally leave in an axial direction at the impeller eye.

Because of the recent appearance of the radial flow turbine, too little information is available about its effective design

and performance data. It is yet undecided whether straight or curved nozzle vanes should be used. There may also be a possibility of dispensing with the nozzles and using the volute or the equivalent of the vaneless diffuser of a compressor. The operation of the turbine has been found to be more satisfactory within the speed range 40,000 to 45,000 r.p.m. Speeds up to 80,000 r.p.m. have been tried by Judson and Kellitt (32)using plain bearings, angular contact bearings and ball bearings, but the speed being very high bearings have given trouble. A close study of these troubles has revealed that the bearings themselves are not likely to impose design limits.

The design of radial-flow turbine is based upon the thermodynamic and aerodynamic design criteria of centrifugal compressors. Some useful information on the radial machinery has been supplied by Balje (33) whose test results show that efficiencies up to 85 per cent for pressure ratio of 3, and 75 percent for pressure ratio of about 4 are obtainable with intake Reynolds number 3.0- 5.5 x 10^6 and U_a from 0.57 to 1.04. Here U_a is the ratio of the tip speed to the acoustic velocity at the critical temperature corresponding to inlet total temperature.Results of Von der Nuell (34) show that efficiencies up to 86 per cent can be obtained for the radial vaned turbines. Also for an inward flow turbine of 45 h.p. output, the efficiency (35) of 78 per cent has been obtained. This leads to the conclusion that radial flow turbines can be successfully designed to give efficiencies ranging from 75 to 85 per cent.

The difficulty that has been encountered with the radial turbines is with the thermal stress problems, as the whole rotor structure is bathed by hot gases. In the small sizes that

have been developed so far, it has been avoided owing to the effective heat conduction. In future it is very likely that some suitable cooling method may be developed for the purpose. Since compounding of this turbine is not possible, it will not be suitable for power outputs greater than 600 h.p. So far it has only been tried with small engines, and because of its cheapness and easy manufacture, along with its high efficiencies, has exhibited its potentialities for use in the automotive field.

It should be noted that except for eq^{n}(3.48) all others given in the previous article for axial flow turbine will apply to this type of turbine as well.

3.43. Pulsating-Flow and Steady Flow-Turbines- In the Buchi system of turbocharging, the exhaust gases on being discharged from the cylinder, travel back and forth in the form of pressure waves in the exhaust manifold. Thus the high pressure exhaust which already contains a high content of kinetic energy, is led to the turbine nozzle ring where it is accelerated, thereby further increasing its kinetic energy. Thus during the passage of this high velocity gas over the moving blade ring, the latter absorbs tangential momentum and so reduces its kinetic energy. In such a case the turbine receives a pulsating discharge and so the operation of the turbine is non-steady.

If the exhaust of the engine is at a sufficiently high pressure(as is the case with high pressure turbo-charged engines), it may be led to a receiver, so that the pulsations are damped down. The only energy possessed by the exhaust gas is now by virtue of pressure and not due to pressure pulsations. Thus the turbine will now receive a steady supply of the gas, which, as usual, will expand through the nozzle and will then pass over the

moving blade ring. Such system of working is known as constant pressure system. The Buchi System could not prove effective in the beginning, because due to constant pressure working then employed, the energy of the exhaust was short by the energy due to pressure pulsations, and so was not sufficient to drive the turbine.

In turbo-charging practice, the pulsating flow turbine is commonly termed the impulse turbine. From the fundamental theory, the impulse turbine must not have any reaction atall (i.e. the increase of kinetic energy over the moving blade ring)but, in practice, there is always some degree of reaction, say 15 per cent. This contributes to the efficiency of the turbine, because the efficiency of the reaction turbine is higher than that of the impulse turbine. The turbines employing constant pressure system are known as the 'reaction turbines'. In this case there is a possibility of the simplified exhaust system.

3.44 Turbocharger Analysis- The analysis of the compressor was performed in article 3.13, and that of the turbines in 3.41 and 3.42. Here the turbo-charger will be analysed taking both the compressor and the turbine as a composite unit.

Thus if T_1= absolute temperature of air at compressor inlet,

T_2= absolute temperature of air at compressor outlet,

C_p= specific heat of air at constant pressure.

W_a= flow of air through the compressor, lb./sec.

we have the work done by the compressor on the gas

$$W_c = J.W_a.\ C_p\ (T_2-T_1) \quad \text{ft- lb. per sec.} \qquad (3.53)$$

Again, if T_3= absolute temperature of exhaust gas at turbine inlet,

T_4= absolute temperature of exhaust gas at turbine outlet,

C_{pg}= specific heat of exhaust gas at constant pressure,

W_f = weight of fuel used per lb. of air passing through the compressor,

we have the work developed by the turbine.

$$W_t = J.W_a\,(1+W_f)\,C_{pg}\,(T_3-T_4). \qquad (3.54)$$

Since, turbine shaft output = compressor shaft input

$$J.W_a\,(1+W_f)\,C_{pg}\,(T_3-T_4)\,\eta_{mt} = \frac{J.W_a.\,C_p\,(T_2-T_1)}{\eta_{mc}}$$

where η_m represents the mechanical efficiency for the compressor and the turbine with proper subscripts affixed.

$$\therefore \quad T_3-T_4 = \frac{C_p}{C_{pg}}\left(\frac{T_2-T_1}{1+W_f}\right).\frac{1}{\eta_{mc}\eta_{mt}} \qquad (3.55)$$

CHAPTER 4

PERFORMANCE AND APPLICATION OF SUPERCHARGED ENGINES

4.1. Effect of Supercharging on Engine Performance- The effect of supercharging on the fundamental factors that govern the operation of an engine has already been discussed in chapter 2. The engine performance is also very much influenced by the degree of supercharge. Whatever may be the method adopted for obtaining higher boosts, supercharging will invariably have the following effects:-

(1) Increase in brake mean effective pressure and therefore increase in power output of the engine. A pressure ratio of 1.5:1 increases the b.m.e.p. from 70-80 lb. in.^{2} to 110-130 lb./in.^{2}, and that of 2.2: 1 raises it to 200-220 lb/in.^{2}. The mean effective pressure of 350 lb./in.^{2} have also been obtained continuously during tests, and of about 440 lb./in.^{2} for a short time.

(2) Increase in mechanical efficiency, because the increase of friction losses compared to the power gain is much smaller.

(3) Reduction of specific fuel consumption. The reduction is due to the increased turbulence, better mixing of the fuel and air and increased mechanical efficiency. In some cases specific fuel consumption may not reduce.

The performance curves presented in the subsequent discussion show the effect of supercharging quantitatively upon these variables.

4.2 Effect of Supercharging on Heat Balance- The heat balance for $11\frac{13}{16}$ in. × 15 in. N.A.C.A. 6 cylinder engine is shown in Table 4.1 below. To have the comparative idea the heat balance was obtained for both the naturally aspirated and the supercharged condition. With atmospheric induction the engine developed 690 h.p. at 700 r.p.m.

with a specific fuel consumption of 0.337; the corresponding values in the supercharged condition being 950 h.p. at 700 r.p.m. and a specific fuel consumption of 0.373.

Table 4.1 (36)

	Supercharged(Turbo-charged) B.T.U. per hr.	Per cent	Naturally aspirated B.T.U.per hr.	per-cent
Shaft output	2,420,000	37.0	1,760,000	33.0
To radiator	1,020,000	15.0	1,220,000	25.0
To oil cooler	180,000	3.0	160,000	3.3
To exhaust	2,730,000	42.5	1,630,000	33.5
Radiation	120,000	2.0	100,000	2.2

It may be seen that in a supercharged engine the portion of heat going into the exhaust is greater. Also, due to better scavenging, the heat rejected to cooling water is much less which means that the cooling equipment may be smaller. This is of great importance in rail traction and automotive service where space and weight are at a premium.

4.3. Performance of Mechanically Supercharged Engines- To present the representative performance of engines with all the mechanical superchargers, a typical example for each category has been selected. Thus the performance of a Fell locomotive (12), employing Roots blower for supercharging is given in Fig. 4.1. which is representative, more or less, of the whole class of positive displacement blowers. With blowers of improved adiabatic efficiency e.g. the screw blowers, the performance may be expected to be slightly on the higher side.

The Fell diesel locomotive comprises four 530 h.p. propulsion units supercharged by two Roots blowers, each driven by a separate 160 h.p. auxiliary engine. The characteristic required for a locomotive engine is that the power should remain fairly constant

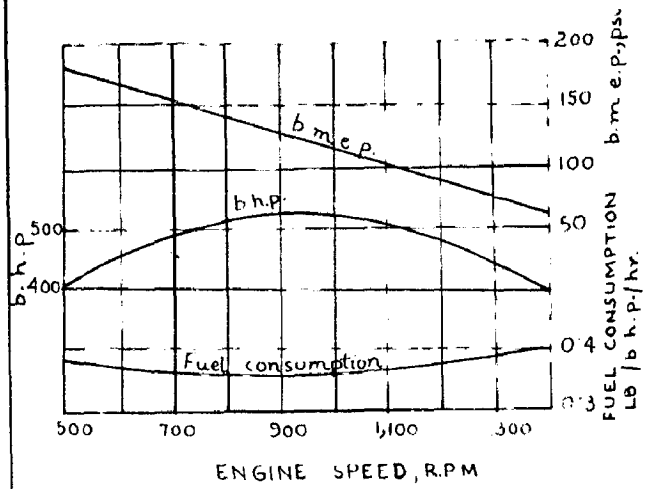

(a) POWER AND CONSUMPTION

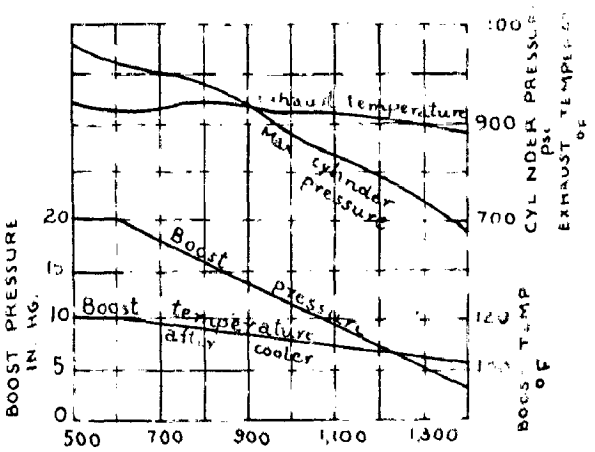

(b) OPERATING CONDITIONS

FELL LOCOMOTIVE ENGINE PERFORMANCE CURVES

REF. 12

FIG 4·1.

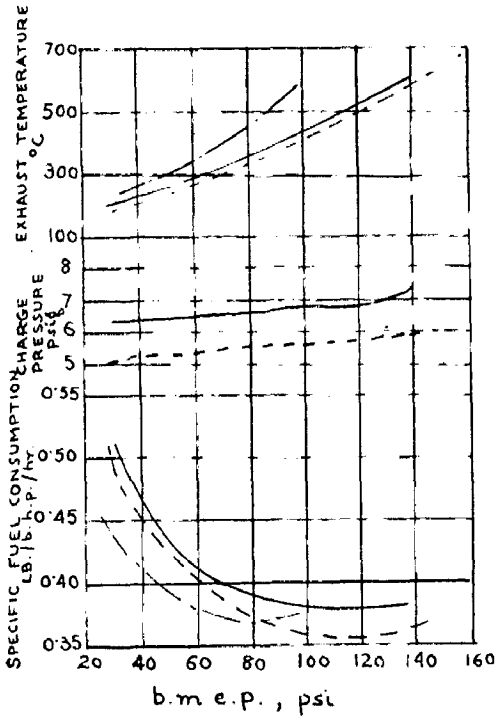

PERFORMANCE CURVES OF ENGINE CHARGED BY BICERA COMPRESSOR

FIG. 4·2.

——— UNCOOLED] PRESSURE
- - - - WITH COOLER] CHARGED
—·—·— NATURALLY ASPIRATED

REF 11

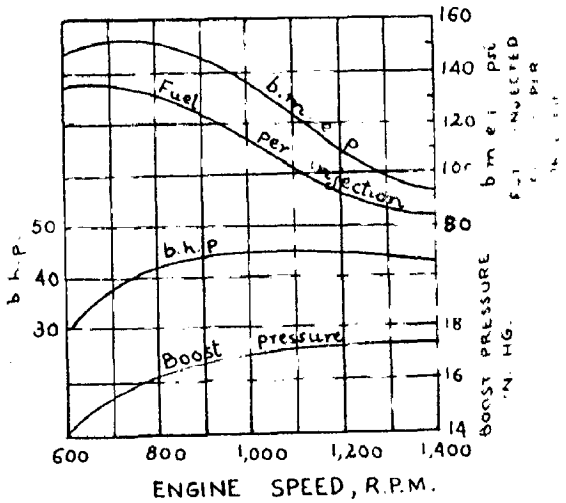

PERFORMANCE CURVES OF EXCAVATOR ENGINE SUPERCHARGED BY RICARDO COMPRESSOR

FIG 4·3

REF 12

over the entire speed range. This is being achieved here, because the engine is maintaining a b.h.p. of 400 over a wide speed range of 500-1400 r.p.m. For constant power the specific air consumption (lb. of air per b.h.p. per hr.) will also be nearly constant. Consequently the supercharger has to run at a constant speed irrespective of the speed of engine. This can only be accomplished when the blower is driven externally. Here the boost pressure is automatically adjusting itself to the engine speed. When this decreases, the air temperature, the exhaust temperature and the cylinder pressure fall down.

Fig. 4.2 gives the typical comparision of the performance (11) of the engine under different conditions-naturally aspirated and supercharged by Bicera compressor (the compressed air being fed directly as well as through the intercooler to the engine). The charge pressure is lower when delivered via the cooler because of the pressure drop taking place into it. Also the specific fuel consumption and the exhaust temperature are the lowest in the pressure charged and cooled cases.

The performance of a 4.4 litre excavator engine is given in Fig. 4.3. Here the requirement is a high torque at low speeds as is clear from the b.m.e.p. curve where the b.m.e.p. at 1400 r.p.m. is the same as that of the normally aspirated engine. This engine was supercharged by a Ricardo wobble plate compressor, because of its high volumetric efficiency at low speeds. Due to low b.m.e.p. requirement at high speeds, the quantity of fuel injectedhas also been decreased.

In figure 4.4. the sea level performance of a 5.75x 6 in. 14 cylinder aircraft engine (37) with geared centrifugal supercharger is given. The line b-c represents the maximum allowable b.m.e.p.

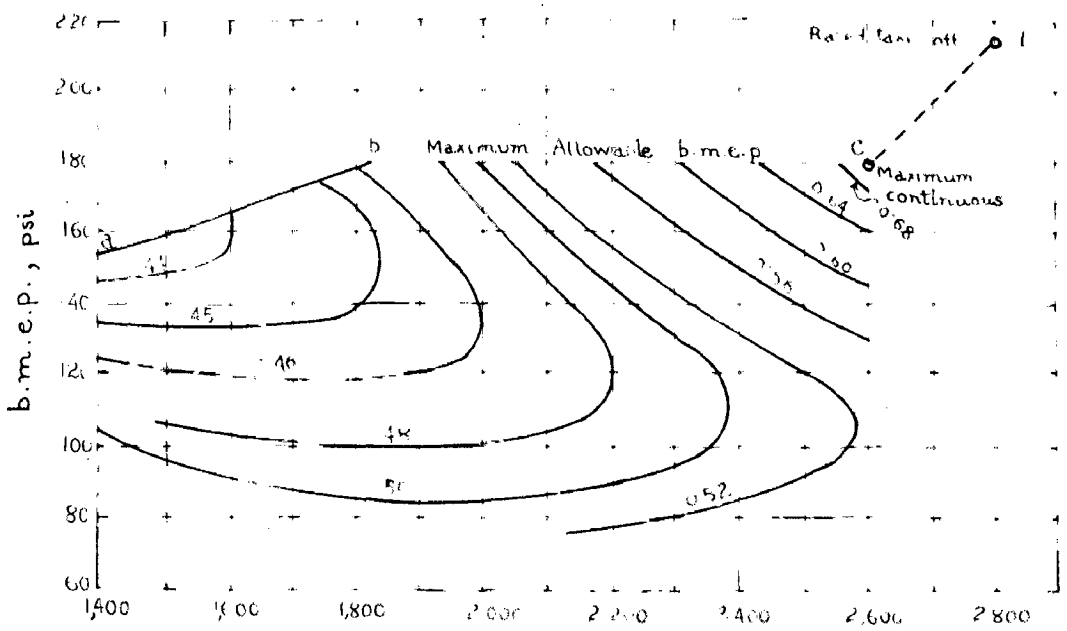

PERFORMANCE CURVES OF AN AIRCRAFT WITH GEAR-DRIVEN SUPERCHARGER

FIG 4·4.

REF. 37.

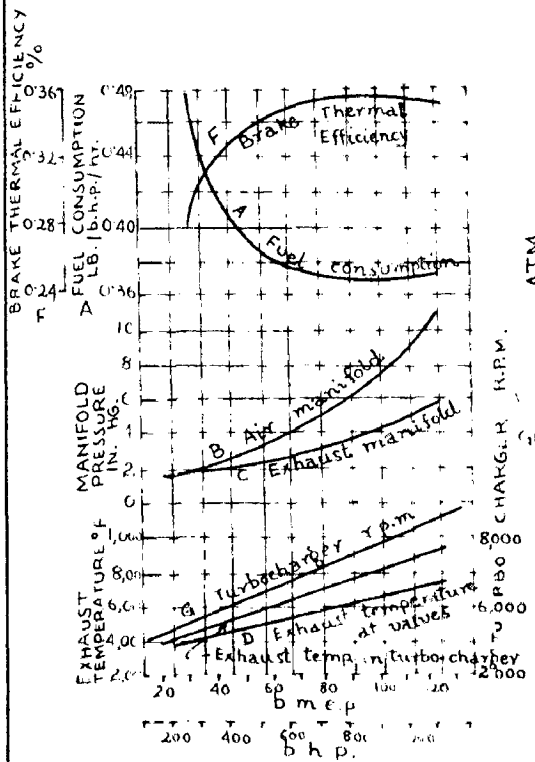

PERFORMANCE CURVES OF A LOW PRESSURE TURBO CHARGED ENGINE

FIG 4·5.

REF 38

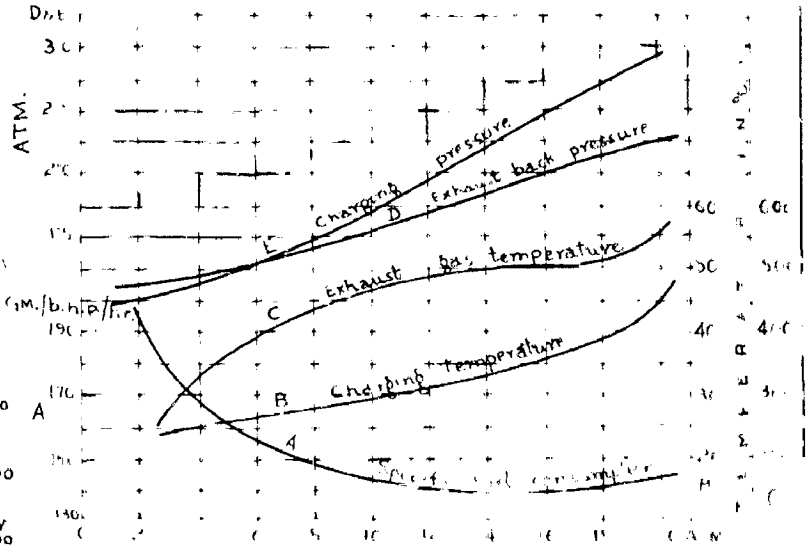

PERFORMANCE CURVES OF A HIGH PRESSURE TURBO CHARGED ENGINE.

FIG 4·6

REF

restricted from considerations of design, and controlled by the throttle. This can safely cruise continuously at c, but it normally does so at the point of best economy. The point gives the limit for maximum output possible for very short periods with a very rich mixture strength.

4.4 Performance of Turbo-charged engines- The typical performance curves of a low pressure turbocharged 6 cylinder 12½ in. x 13 in. Alco Oil engine (33) are shown in Fig. 4.5. The engine was rated to develop 1,000 b.h.p. at 740 r.p.m. Curve A shows the specific fuel consumption which has the lowest value of 0.37 lb. per b.h.p. hr. at a brake mean effective pressure of 100 psi, and a charge pressure of about 4 psi. Curve L gives the exhaust temperature at turbine-inlet which is higher than the corresponding temperature at the exhaust valves. This is so because there is a certain amount of temperature rise due to frictional reheat in the exhaust manifold. The supercharger speed goes on increasing with the power which reflects on the supercharger adjustment with engine speed.

Fig. 4.6 presents the comprehensive performance of a high pressure turbo-charged 6 cylinder 300 mm. X 450 mm. M.A.N. engine (17). The engine has a fabricated frame with aluminium pistons and cast cylinders. The unit comprises a five-stage exhaust gas turbine and a ten stage compressor, nine stages of which are axial and the last one radial. An intercooler was also inserted between the ninth and tenth stages of the compressor. Curve A shows the specific fuel consumption with the lowest value of 0.31 lb. per b.h.p. hr. at a brake mean effective pressure of 225 lb. per sq. in. when the charging air pressure is 35 lb. per sq. in. With increased charge pressures, the charging air temperature increases rapidly which marks the necessity of cooling of the charge in case of supercharged engines.

The exhaust temperature is also very high, the maximum being 1050°F.

4.5. Comparison of Performance for Mechanically Supercharged and Turbo-charged Engines- The actual performance curves obtained with three different pressure chargers on similar engines are shown in Fig. 4.7. It may be seen that the specific fuel consumption is the lowest with turbo-charged engines except at very low b.m.e.p.s.With low pressure turbocharged engine the b.m.e.p. increases with the engine speed which is a common characteristic of all turbocharged engines. With Roots blower the engine has got a drooping characteristic for the b.m.e.p., a property common with all mechanically supercharged engines. By providing a simple governor in the fuel system, the fuel supply has been so adjusted that it gives the higher values of torque at low engine speeds. Thus the drooping torque curve has been obtained with high pressure turbo-charged engine as well.

The results obtained with a locomotive Daimler Benz 12-cylinder 800 h.p. engine (33) with both mechanically driven as well as the exhaust turbine driven centrifugal blower are given in Fig. 4.8. Here the fuel supply was adjusted to give outputs required by the propeller at different speeds. The speed range shown is so limited because these engines are driven through hydraulic or electric transmission in practice. The specific fuel consumption is although lower with turbocharging. As expected, the exhaust back pressure is higher, the maximum value being 2.5 psi. With mechanical supercharging the exhaust temperature is slightly higher in the higher speed range which is due to the rapid increase of power, absorbed by the blower with speed.

In Fig. 4.9 are illustrated the results based upon the

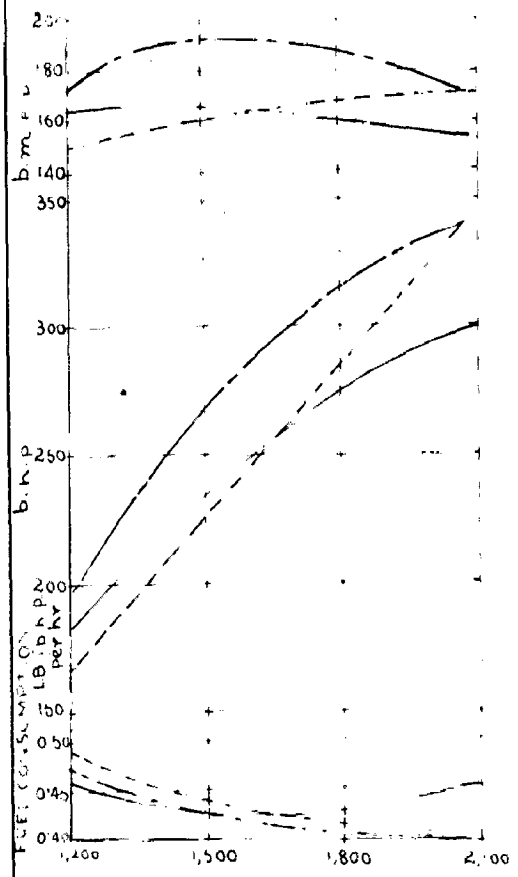

COMPARATIVE PERFORMANCE CURVES

FIG. 4·7

—— ROOTS CHARGED ENGINE

– – – TURBO CHARGED ENGINE (½ L)

· · · · TURBO CHARGED ENGINE (2 L)

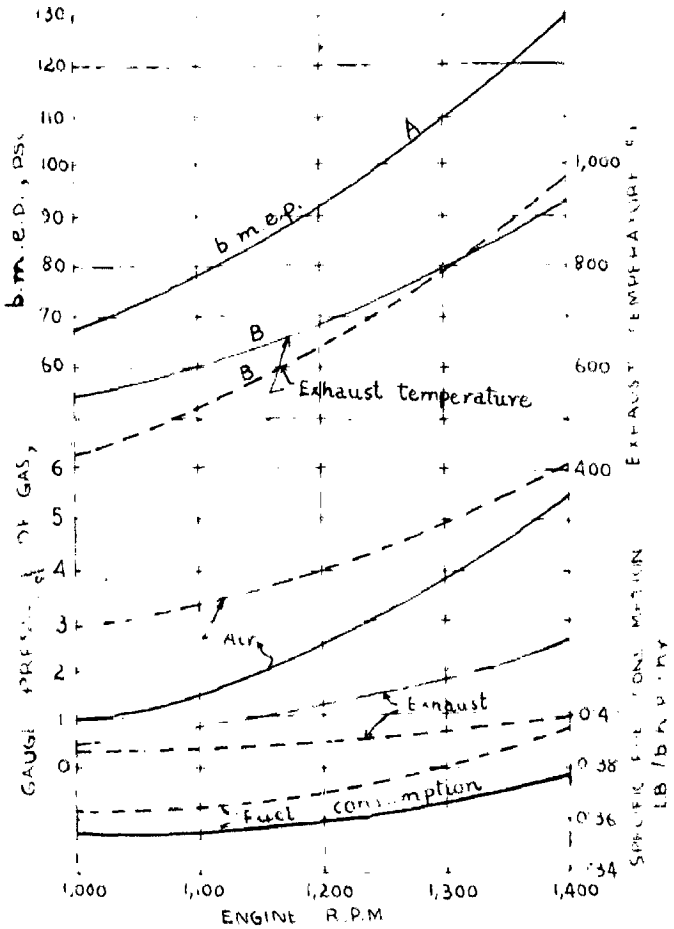

COMPARATIVE PERFORMANCE CURVES

FIG 4·8.

GEARED CENTRIFUGAL

TURBO BLOWER

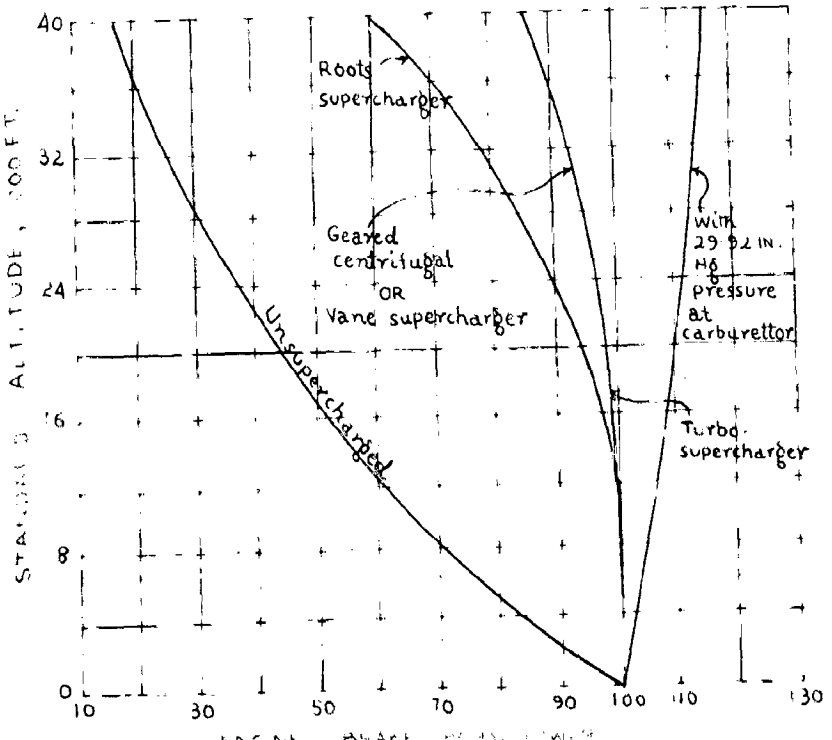

COMPARATIVE PERFORMANCE OF DIFFERENT SUPERCHARGERS

FIG 4·9

investigations of O.E.Schey (39) on the aircraft engines supercharged in three different ways. All the engines delivered 100 b.h.p. at ground level. At an altitude of 40,000 ft. the naturally aspirated engine could deliver only about 17 per cent of its ground level power; the corresponding power developed by the engine with Roots blower was about 60 per cent, and with geared centrifugal or vane type of supercharger was about 86 per cent. With exhaust gas turbo-charging, the net power output was the same as at the ground level. Provided the pressure maintained at the carburettor suction would have been atmospheric, the engine would have delivered about 115 b.h.p. due to its operation against a low back pressure equal to the atmospheric pressure at that altitude. Upto a height of about 15,000 ft., there exist only small differences between the curves, but beyond this the superiority of turbocharging is self evident.

4.3 Application of Supercharged Engines- On the basis of the performance discussed above, a critical study of the suitability and adoptability of a class of supercharged engines to a particular application may now follow. For pressure charged engines used in locomotives marine propulsion, power stations, aircrafts, and industrial installations, both mechanical supercharging and turbocharging have been applied. There persists, however, a lot of controversy about the supercharging of engines used in automotive applications and earthmoving machinery. For such applications a drooping torque characteristic is the essential requirement, which means that the engine should be capable of developing high torques/b.m.e.p. at low speeds. A turbo-charged engine will not ordinarily fulfil this requirement, because the turbo-charger depends for its operation directly upon the engine. At low engine speeds the energy

supplied in the exhaust will be less, so that the compressed air supply from the turbo-charger will also be poor. These limitations hampered the development of turbocharging for such applications and have led to the mechanically supercharged engines dominating in this field.

The growing consciousness of lower specific fuel consumption in turbo-charged engines could not restr in the use of turbocharged engines in the automotive field as well. Consequently turbocharged engines have been used for such applications as well, but their validity is challenged by the positive driven chargers e.g., Lycholn blower, Bicera and Richardo compressors on the following two points:

1. lackof drooping torque characteristics
2. on-set of smoke during acceleration .

It is true that the turbocharged engines lack in drooping torque characteristics , but it can definitely be achieved (Fig. 5.7) by providing a simple control in the fuel supply. The conventional turbocharger matched to give optimum conditions at low engine speeds will serve the purpose. Also with the expanding use of torque converter drives and multi-speed transmission systems, the requirement of high torque at low speeds has been considerably reduced.

Further, as the engine is accelerated, the fuel supply to the engine is immediately increased, but the turbocharger takes time to speed up, as a result of which an instantaneous proportionate increase in the supply of compressed air to the engine is delayed. This results in incomplete combustion producing smoky exhaust. Also due to increased valve overlap, slots are provided in the piston which inevitably jeopardise the engine's breathing and com-

ustion officiency. With increased supercharge pressures, the valvve overlap can be reduced which results in the widening of the speed range for acceptable smoke levels. Bradbury (31) has suggested that the smoke can be eliminated by providing a torque stop on the fuel pump which is controlled by the turbocharger pressure. Some engine manufacturers in the United States have also reported about the elimination of smoke.

It may, therefore, be expected that in the near future the turbo-charged engines will occupy an important position in the automotive field as well.

For high altitude flights the turbocharger is already in an advantageous position. The mechanically supercharged engines are derated by 3 to 4 per cent per 1,000ft. altitude, whereas the turbocharged engine maintains its increased sea- level rating up to 1,500 ft. with the more increase in rotor speed by 3 per cent. At the same time, due to reduce intake pressure and temperature, the cylinder pressure, b.m.c.p, and the exhaust temperature remain unaltered.

In all other fields, the turbo-charged engine already dominates due to its superiority.

CHAPTER 5

ENGINE TURBO-CHARGER MATCHING

5.1 Need for Matching- A turbocharged engine consists of three auxiliaries - the aerodynamic compressor, the engine and the exhaust gas turbine. These individual components may be designed according to requirements, so that the complete unit will yield the performance required of it at the 'design point', that is when running at the particular speed and mass flow for which the components were designed. The unit will not always be operating at its design conditions, but will also be subject to fluctuations of load from time to time. Thus when the operation takes place at 'off-design point', there is great likelihood for either of the components to fall in a region of instability. This is detrimental to the component and may produce arduous effects on the unit as well. Thus matching of the individula components is done to avoid instability at operating conditions removed from the design point.

The power absorbed by the compressor and the power developed by the turbine can be readly predicated, provided the initial and final conditions are known. The performance characteristics of these components can also be found out by actual test without difficulty. But the prediction of the performance of a reciprocating engine is too complicated because of the multiplicity of the variables involved in the problem, and so this can only be found out experimentally. Now when all these components are linked together, the operating range of each of the components is reduced considerably. Hence in order to ensure proper matching for each equilibrium condition of the unit, the corresponding operating points are obtained on the characteristics of each of the components. These are

then used for the typical computation of the various quantities so as to determine the operating range of the combination.

5.2. Requirements of Matching. The matching requirements may be different in different cases depending upon the duties to which the engine is put. Thus in a power station the engine should operate at high efficiency only within a restricted range of the designed output. In a passenger or cargo vessel, the engine is required to operate with good economy at normal cruising power, which may be only a small fraction of the rated output of the engine. There may also be engines used in aircraft and rail-traction which require a fairly uniform efficiency at normal cruising outputs which is normally half or three-quarters of the maximum power. Thus in different cases different part-load performances are required and these are achieved in an actual case by proper selection of the components, arranged in a suitable order. Thus according to Hallinan (40), matching leads to the choice of the best arrangements of components, to satisfy the requirements of the different duties, to be made with some degree of certainty.

5.3. Effect of Mis-matching on the Performance of a Turbo-charged Engine and its Remedial Measures. If the components of a unit are mismatched, the turbo-charger will run at either too low a speed or at too high a speed. This will decrease or increase the manifold pressure respectively. Thus the engine performance and the specific fuel consumption will be affected, as is illustrated in Fig. 5.1. It may be seen that with incorrect matching the performance of the engine goes down considerably.

The mismatching can be corrected by employing different blade lengths and nozzle areas without any loss of efficiency on the turbine side. In the compressor, the diffuser and the impeller decre-

ve particular attention. One of the alternatives is the vaneless diffuser, which widens the range of stable operation but suffers from the loss in efficiency. The use of impellers of varying capacity in the same turbo-charger casing provides the compressor characteristics in different ranges. This is clear from Figs. 5.2 and 5.3. It may be observed that the larger rotor widens the compressor range, whereas the smaller one shortens it. The latter alternative is of great help in automotive applications where precise matching has to be achieved.

5.4. Application of Dimensional Analysis to Compressor and Turbine Performance- The characteristic performance of compressor and turbine can be represented in a simplified form by the use of dimensionless parameters containing the variables that govern the component's behaviour. For a compressor these variables are:

1. The pressure of the inlet air- - - - P_1
2. The temperature of the inlet air- - - - T_1. Now since $\frac{P_1}{\rho_1} = RT_1$, where R is the gas constant, instead of T_1, ρ_1 (the density of the gas at inlet) may be taken so that the extra dimension of temperature is not involved.
3. A characteristic linear dimension of the unit, say D.
4. The mass flow of gas, Q.
5. The rotational speed, N.
6. The outlet pressure of gas, P_2.

Thus we have

$$P_2 = f_1(P_1, \rho_1, D, Q, N) \qquad (5.1)$$

The Rayleigh's method consists in writing the function f_1 as the product of powers of the variables P_1, ρ_1, D, Q and N.

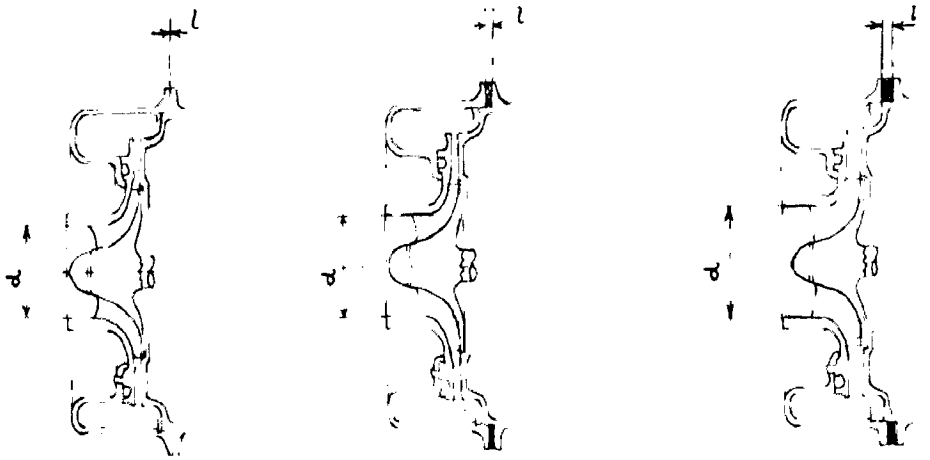

COMPRESSOR CASING ARRANGEMENT TO TAKE VARIOUS SIZES OF ROTORS

FIG. 5·2.

(a) COMPRESSOR ACCOMODATING SMALL ROTOR
(b) COMPRESSOR ACCOMODATING MEDIUM ROTOR
(c) COMPRESSOR ACCOMODATING LARGE ROTOR

REF. 32.

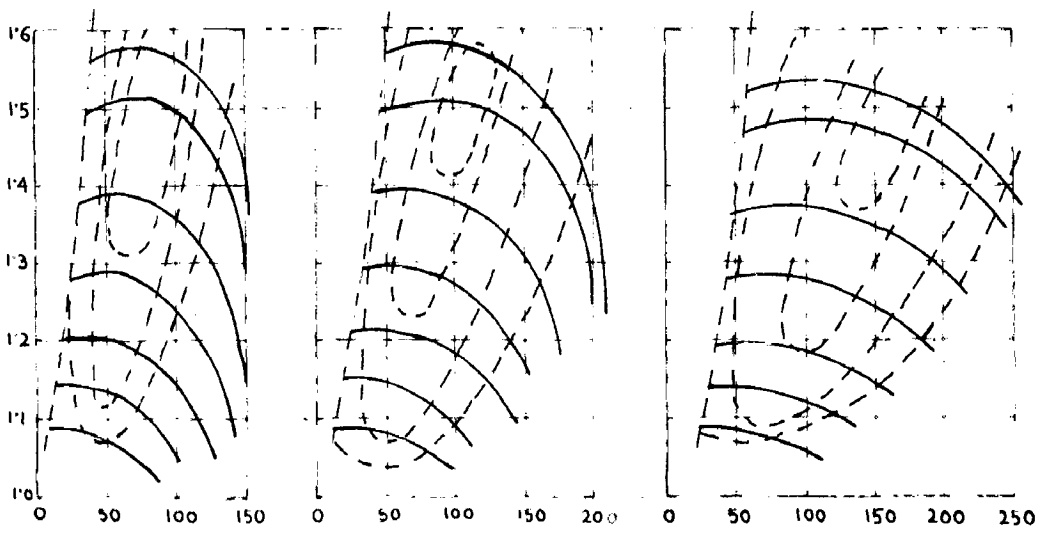

COMPARISON OF COMPRESSOR CHARACTERISTICS FROM ROTORS OF VARIOUS WIDTHS ACCOMADATED IN COMPRESSOR CASING AS SHOWN IN FIG. 5·2

FIG. 5·3.

REF 32

Thus eqn (4.1) may be written as

$$P_2 = C \cdot P_1^a \cdot \rho_1^b \cdot D^c \cdot Q^d \cdot N^e \qquad (5.2)$$

where C is a dimensionless constant and a,b,c,d,e are the numbers whose values are to be determined.

Taking the fundamental dimensions as mass M, length L, and time T, the above equation may be expressed, in terms of the fundamental dimensions, as below:

$$ML^{-1}T^{-2} = (ML^{-1}T^{-2})^a \cdot (ML^{-3})^b \cdot (L)^c \cdot (MT^{-1})^d \cdot (T^{-1})^e$$

Since the above equation must be dimensionally homogeneous, equating the indices of the dimensions gives

$$1 = a + b + d$$
$$-1 = -a - 3b + c$$
$$-2 = -2a - d - e$$

There are five unknowns and three equations, so let c, d and e be determined in terms of a and b.

Thus

$$d = 1-a-b$$
$$c = -1+a+3b$$
$$e = 1-a+b$$

Substituting in eqn (4.2),

$$P_2 = C \cdot P_1^a \cdot \rho_1^b \cdot (D)^{-1+a+3b} \cdot (Q)^{1-a-b} \cdot (N)^{1-a+b}$$

Dividing by P_1 to obtain a non-dimensional quantity on the left hand side.

$$\frac{P_2}{P_1} = C \cdot P_1^{a-1} \cdot \rho_1^b \cdot (D)^{-1+a+3b} \cdot (Q)^{1-a-b} \cdot (N)^{1-a+b} \qquad (5.3)$$

The Buckingham π theorem states that if n variables are connected by an unknown dimensionally homogeneous equation, the equation can be expressed in the form of a relationship between

(n-r)independent dimensionless products, where r is the number of fundamental dimensions. There being six variables involved in the problem with three fundamental dimensions, the number of dimensionless products in this case will,therefore, be three.

Thus equation (5.3) gives

$$\frac{P_2}{P_1} = C \cdot \left(\frac{ND \cdot \sqrt{\rho_1}}{\sqrt{P_1}}\right)^{1-a+b} \cdot \left(\frac{Q}{D^2\sqrt{P_1\rho_1}}\right)^{1-a-b}$$

Or, alternatively

$$\frac{P_2}{P_1} = f_2 \cdot \left(\frac{ND \cdot \sqrt{\rho_1}}{\sqrt{P_1}}\right) \cdot \left(\frac{Q}{D^2 \cdot \sqrt{P_1\rho_1}}\right)$$

But $P_1 = \rho_1 R T_1$

therefore, $\frac{ND\sqrt{\rho_1}}{\sqrt{P_1}} = \frac{ND}{\sqrt{RT_1}}$

and $\frac{Q}{D^2\sqrt{P_1\rho_1}} = \frac{Q\sqrt{RT_1}}{D^2 P_1}$ (5.4)

For a given compressor working with a given gas, R and D will be constant. Hence these may be deleted from the groups. Thus the eq^n (5.4) finally comes

$$\frac{P_2}{P_1} = f\left(\frac{N}{\sqrt{T_1}}, \frac{Q\sqrt{T_1}}{P_1}\right) \qquad (5.5)$$

Since $\frac{T_2}{T_1}$ (T_2 being the compressor outlet temperature)is a direct function of $\frac{P_2}{P_1}$ in a compressor, eq^n(5.5) may also be written as

$$\frac{T_2}{T_1} = f'\left(\frac{N}{\sqrt{T_1}}, \frac{Q\sqrt{T_1}}{P_1}\right) \qquad (5.6)$$

If the suffices 3 and 4 refer to the inlet and outlet conditions of the turbine, by performing a similar analysis, it will be found that the equations representing the performance characteristics of a turbine are

$$\frac{P_3}{P_4} = f\left(\frac{N}{\sqrt{T_3}}, \frac{Q\sqrt{T_3}}{P_3}\right) \qquad (5.7)$$

or in terms of the temperature ratio

$$\frac{T_3}{T_4} = f'\left(\frac{N}{\sqrt{T_3}}, \frac{Q\sqrt{T_3}}{P_3}\right) \qquad (5.8)$$

Since in compressor and turbine performance, the values of pressure and temperature used are the total head quantities, these will henceforth mean the total head pressure and the total head temperature, and, to be more specific, the letter 't' will be suffixed to the symbols.

The necessity of dimensional analysis in these cases may be realized from the fact that in terms of the non-dimensionless parameters the complete performance of either the compressor or the turbine may be represented by two sets of curves only. In terms of the actual variables, the performance would require a formidable number of tests and test curves.

5.5. Non-dimensional Representation of Compressor Performance :-

Figs. 5.4 and 5.5. represent the non-dimensional performance curves for a centrifugal compressor and an axial flow compressor respectively. Here pressure ratios are plotted on the ordinate against non-dimensional mass flows on the abscissa, such that each curve is for a fixed value of the non-dimensional rotational speed. Sometimes, instead of the pressure ratios, the temperature ratios are plotted on the ordinate. The figures show the efficiency contours as well. To the left of the surge line is the region in which the operation of the compressor is unstable. This is due to the phenomenon of "surging". Also with considerably increased mass flows the choking occurs in the diffuser throat. Here the air angles become different from the vane angles, resulting in the break away of air and in the deterioration of efficiency. Thus the compressor operation is limited by the surge line on the left and by the choking limit on the

right.

The comparison of Figs. 5.4. and 5.5 will show that, for fixed values of $\frac{N}{\sqrt{T_{1t}}}$, the axial compressor characteristics cover a much narrower range of mass flow than the centrifugal compressor. Also the surge limit is reached before the curves reach a maximum value of pressure ratio or efficiency. Thus the range of stable operation of axial compressors is too limited calling for greater need of matching to avoid instability at operating conditions away from the design point.

5.6. Non-dimensional Representation of Turbine Performance- Fig. 5.6 represents the non-dimensional performance of a turbine where the pressure ratios are plotted against the non-dimensional mass flows for different values of the non-dimensional rotational speeds. The temperature ratios being a simple function of the pressure ratios may also be plotted on the ordinate. From the figure it may be seen that the constant speed curves run into an single straight line. This means that at this particular value of $\frac{Q\sqrt{T_{3t}}}{P_{3t}}$ the choking occurs in the turbine, and so this is the maximum flow possible through it. Thus the turbine operation is also limited over a particular range.

5.7. Location of Engine Operating Line- In the engine and turbocharger matching, the compressor performance map is a suitable and convenient base upon which the engine operating points can be located. Thus the very problem of analysing the off-design operation may be deemed as that of mapping the desired engine parameters in the compressor performance field.

The engine always draws its supply of air from the compressor. Whatever may be the speed of the engine, the latter will suck in a fairly constant volume of air during every cycle of

operation depending upon its volumetric efficiency and engine dimensions. But the density and so the weight of air inducted will be different depending upon the load conditions on the engine. Assuming for the sake of simplicity the adiabatic compression of air through the compressor, the volume of air at compressor suction can easily be evaluated for a particular requirement of the engine which will merely be a function of the speed and the pressure ratio, the volume at delivery remaining constant. Thus for a particular engine speed, for different values of pressure ratios, $\frac{Q\sqrt{T_{1t}}}{P_{1t}}$ may be evaluated, and so the engine speed line is plotted on the compressor performance map. By considering a set of such speeds within a reasonable range of operation of the engine, several such engine- speed lines may be plotted. To illustrate the nature of these lines, a few such engine-speed lines have been shown arbitrarily in Fig. 5.4. It may be marked that the lines diverge at higher pressure ratios.

An engine-speed line is in effect a plot of the path which the engine would follow when running at a constant speed. Thus the actual point of operation of the engine may be anywhere on the line depending upon the load conditions. But since the turbo-charged engine is a composite unit comprising the compressor, the engine and the turbine, for optimum performance the engine operating point at that particular speed must be where the compressor is capable of delivering the air at high efficiency. This criterion leads to locate the engine operating line on the compressor performance map. Thus at every engine speed line, a point may be marked corresponding to the most efficient operation of the compressor, keeping in view that the points are not very near the surge line. Several such points may then be joined by a smooth and continuous

curve which is normally called the 'engine operating line'. The intersection of this line with engine speed lines will give the actual points of operation of the engine at the respective speeds under design conditions.

It may be seen that for these operating points the turbo-charger speed, the air consumption and the charging air pressure can be directly read from this combined compressor-engine performance map. The charging air temperature can be easily calculated, because the isentropic efficiency of the compressor at these points is known from the map.

6.8. Matching of Compressor and Turbine. In a turbo-charged unit there is no mechanical coupling of the engine with either the compressor or the turbine. Thus the compressor is driven directly from the turbine which accomplishes the first fundamental relationship for the compressor-turbine combination, i.e.

compressor r.p.m. = turbine r.p.m.,

which when expressed in terms of the dimensionless parameters is

$$\frac{N}{\sqrt{T_{1t}}} = \frac{N}{\sqrt{T_{3t}}} \cdot \sqrt{\frac{T_{3t}}{T_{1t}}} \qquad (6.9)$$

The second condition relates with the mass flow through the compressor and the turbine. The exact relationship is

compressor flow + fuel flow = turbine flow.

In an engine the mass of fuel burnt is too small in comparison with the larger air quantities required. The usual fuel air ratio varies from 0.45 - 1.0 x stoichiometric ratio which is about 0.0333 - 0.037:1 for gasoline and 0.0334 - 0.0370 for diesel oil. Thus the fuel flow can safely be neglected without any appreci-

able error. The modified equation now becomes

compressor flow = turbine flow,

which when expressed in terms of non-dimensional parameters is

$$\frac{Q\sqrt{T_{1t}}}{P_{1t}} = \frac{Q\sqrt{T_{3t}}}{P_{3t}} \cdot \sqrt{\frac{T_{1t}}{T_{3t}}} \cdot \frac{P_{3t}}{P_{1t}} \qquad (5.10)$$

The third condition concerns with the turbine output which must atleast equal the work requirement for the compressor. Thus

compressor input $\leq$ turbine output

i.e. $C_{p_{12}}(T_{2t} - T_{1t}) \leq \eta_m \cdot C_{p_{34}}(T_{3t} - T_{4t})$,

or expressed in the non-dimensional form

$$\frac{T_{2t} - T_{1t}}{T_{1t}} \leq \eta_m \cdot \frac{C_{p_{34}}}{C_{p_{12}}} \left(\frac{T_{3t} - T_{4t}}{T_{3t}}\right) \cdot \frac{T_{3t}}{T_{1t}} \qquad (5.11)$$

where η_m is the mechanical efficiency of the compressor and is about 98-99 per cent for a direct drive.

The non-dimensional plot of the compressor and turbine characteristics in terms of the mass flow and both the pressure ratio and the temperature ratio is of intensive use in satisfying the above relationships. For any operating point the non-dimensional quantities $\frac{N}{\sqrt{T_{1t}}}$ and $\frac{Q\sqrt{T_{1t}}}{P_{1t}}$ are known. P_{1t} and T_{1t} being the delivery conditions for the compressor can be calculated easily. Also P_{3t} and T_{3t} may be determined from the engine cycle analysis. Thus equation (5.9) gives the corresponding value of $\frac{N}{\sqrt{T_{3t}}}$ and equation (5.10) that of $\frac{Q\sqrt{T_{3t}}}{P_{3t}}$ for the turbine. With these two coordinates the corresponding point on the turbine characteristic map may be located, so that $\left(\frac{T_{3t} - T_{4t}}{T_{3t}}\right)$ is read out directly. $\left(\frac{T_{2t} - T_{1t}}{T_{1t}}\right)$ is read out from the compressor characteristic map.

Thus if the equation (5.11) is satisfied, the operation of the combination unit will be satisfactory.

The procedure for matching discussed in this chapter has been applied to an actual engine in the next chapter.

CHAPTER 6

LOW PRESSURE TURBO-CHARGING OF A NATURALLY ASPIRATED ENGINE AND ITS PERFORMANCE PREDICTION

6.1. Specifications of Naturally Aspirated Engine Selected for Conversion. The engine selected for conversion into a low pressure turbo-charged engine is the standard Meadows 6DJ970 six-cylinder naturally aspirated 4-stroke engine which has the data (41) as follows:

Rated b.h.p.	-	150 at 1500 r.p.m.
Cylinder bore	-	5.9 in.
Stroke length	-	6.0 in.
Piston speed	-	1,475 ft./ min.
Compression ratio	-	16:1
B.M.E.P.	-	82 psi

The engine has two detachable cast iron cylinder heads fitted with two inlet and two exhaust valves for each cylinder. A C.A.V. fuel pump supplies fuel, through duplex change-over filters, to long stem C.A.V. injectors placed centrally on the cylinder head between the four valves. The fuel pump and 24-v dynamo are driven through gearing at the drive end of the engine. The water pump, mounted on the cylinder block, is belt driven from a pulley on the free end of the crankshaft. The engine has two 24-V starter motors.

The performance curves obtained experimentally from the naturally aspirated Meadows engine are shown in Fig. 6.1.

6.2. Selection of Turbo-charger from Manufacturer's Catalogue.

Swept volume of one cylinder $= \frac{\pi}{4} (5.9)^2 . 6.0$

$= 161$ cu. in.

If N = number of engine revolutions per min., we have

$$\frac{2 \times 6.9 \times N}{12} = 1475.$$

$\therefore$ N = 1500 r.p.m.

Thus, the quantity of free air handled by the compressor = (swept volume of one cylinder) x (number of cylinders served by the turbo-charger) x (working strokes per min.)x

$$= \frac{161}{12 \times 12 \times 12} \times 6 \times \frac{1500}{2} \times 1.4 \quad \text{approx.}$$

$$= 420 \times 1.4 = \underline{588 \text{ cu. f. per min.}}$$

As the engine is to be low pressure turbo-charged, let us assume a pressure ratio of 1.6 in order to obtain the maximum possible output from the engine.

Thus referring to Table 6.1 of Appendix II for the representative series of turbo-chargers manufactured by . Napier & Sons Ltd., we get the basic size of turbocharger as 90 for a pressure ratio of 1.6:1 and the free air capacity of 588 cu. ft. per min.

The <u>specifications of H.S. 90 turbocharger</u> from (table 6.3 (Appendix II) are -

<u>For maximum continuous rating:</u>

Speed - 24,000 r.p.m.

Boost - 7.35 lb. per sq. in.

Permissible temperature at turbine inlet = 600°C or 1112°F

<u>For maximum overload (one hour limit)</u>

Speed - 27,000 r.p.m.

Boost - 10.3 lb. per sq. in.

Permissible temperature at turbine inlet = 650°C or 1202° F

As the performance characteristics of H.S. 90 turbocharger were not available, the prediction of engine performance with this

turbo-charger combination could not be done. However, to illustrate the procedure, the compressor and turbine characteristics suited for low pressure operation have arbitrarily been adopted and the typical set of calculations performed.

63. Choice of Compressor Characteristics- As the engine is to be low pressure turbo-charged (pressure ratio 1.5:1), the centrifugal compressor will be the correct choice. The performance characteristics of a compressor plotted in terms of non-dimensional parameters are given in Fig. 6.2. The design-point of the compressor is located at A. The pressure ratio corresponding to the design point is 1.485 and its speed is 24,000 r.p.m. The design mass flow of the compressor is 550 cu.ft./min. under atmospheric conditions.

Now for the engine.,

rated speed = 1500 r.p.m.

swept volume of all the 6 cylinders = $\frac{161 \times 6}{144 \times 12} = 0.56$ cu.ft.

Thus assuming 100% volumetric efficiency of 100%, the volume of air required by the engine when operating at 1500 r.p.m. = $\frac{0.56 \times 1500}{2} = 420$ cu.ft. / min. In an ideal case, all the units should operate at their design points simultaneously. Thus under rated conditions 420 cu. ft. per min. of air will be required by the engine at a pressure of 14.7 x 1.485 = 21.8 psia where the standard value of the atmospheric pressure assumed is 14.7 psia.

With isentropic compression, the temperature of air at compressor exit,

$$T_{2i} = T_1 \left(\frac{p_2}{p_1}\right)^{\frac{\gamma-1}{\gamma}}$$

$$= (460+60)\ (1.485)^{\frac{1.4-1.0}{1.4}}$$

$$= 582.5^{\circ}F \text{ abs.,}$$

where the temperature of suction air taken is $60^{\circ}F$.

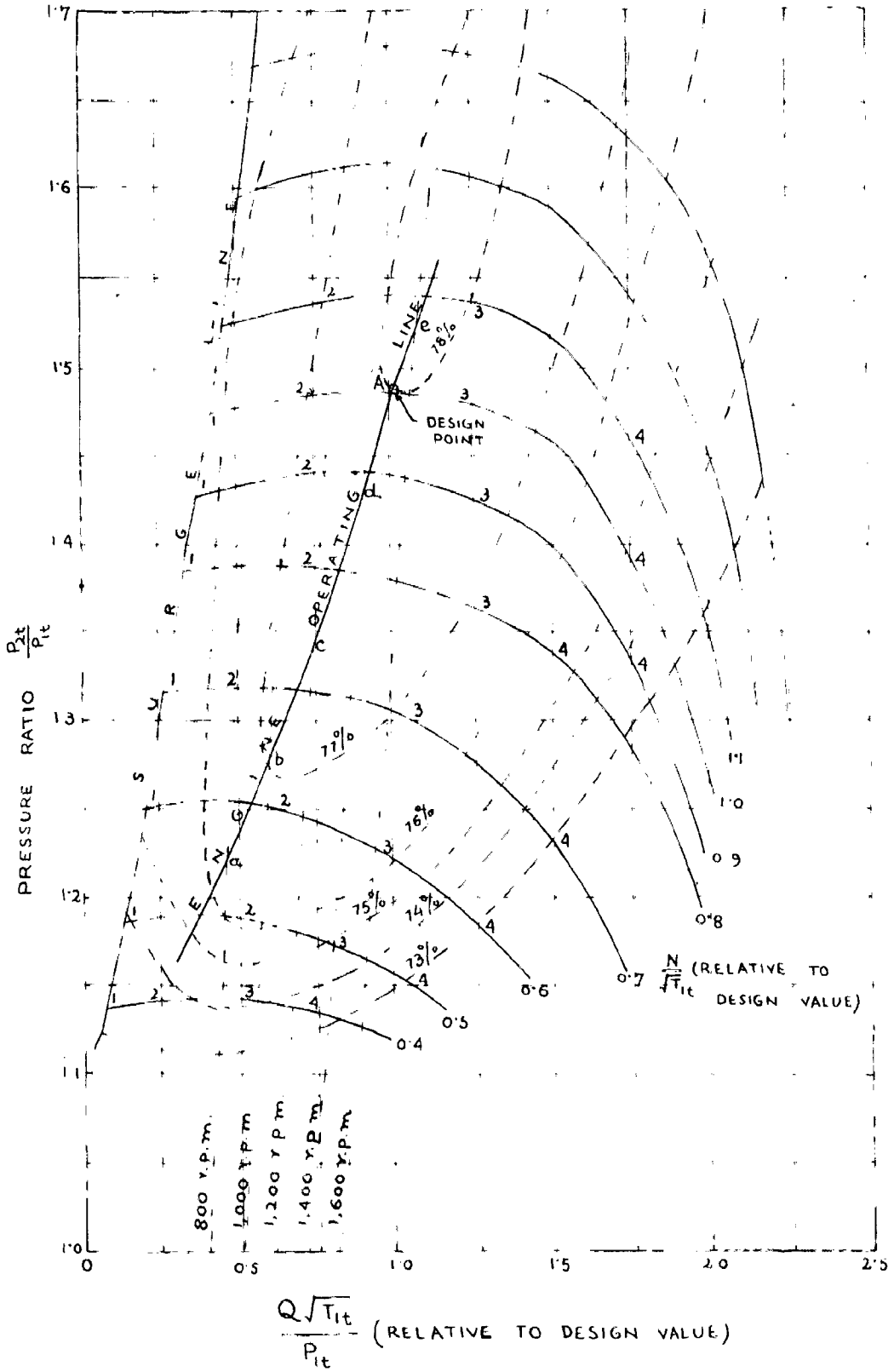

CENTRIFUGAL COMPRESSOR PERFORMANCE

FIG. 6·2.

Taking a compressor isentropic efficiency of 78% at the design point (Fig. 6.2), we have

$$\frac{T_{2i} - T_1}{T_{2a} - T_1} = 0.78$$ (where the subscript 'i' refers to ideal case and 'a' to actual one).

$$\text{or} \quad T_{2a} = T_1 + \frac{T_{21} - T_1}{0.78}$$

$$= 520 + \frac{582.5 - 520}{0.78}$$

$$= 600^{\circ}R.$$

Thus if the subscript 1 refers to the compressor inlet and 2 the compressor exit conditions, we have

$$\frac{p_1 V_1}{T_1} = \frac{p_2 V_2}{T_2}$$

$$\text{or} \quad V_1 = \frac{p_2}{p_1} \cdot \frac{T_1}{T_2} \cdot V_2$$

$$= \frac{21.8}{14.7} \cdot \frac{520}{600} \cdot 420$$

$$= 640 \text{ cu.ft.}$$ (Explain why this is different from 660 cu.ft.)

As the compressor is designed for a mass flow of 660 cu.ft. per min. under atmospheric conditions, it will suit the requirements of the engine fully.

6.4. Engine Speed Lines - These lines may be plotted by determining the suction volume of the compressor for different pressure ratios and engine operating speeds.

We have the swept volume of the engine

= 0.56 cu.ft. (for all the six cylinders).

This will obviously be the volume of air required by the engine every two revolutions. Hence the air required by the engine while

operating at N r.p.m.,

$$V = 0.50 \times \frac{\Pi}{2} = 0.23\ N \text{ cu.ft./ min.}$$

Assuming isentropic compression, the volume of air at compressor suction may be calculated. Thus if R = pressure ratio, the compressor suction volume, $V_1 = V(R)^{\frac{1}{\gamma}} = V(R)^{1.4}$

That is $n = \left(\frac{Q\sqrt{T_{1t}}}{P_{1t}}\right) \Big/ \left(\frac{Q\sqrt{T_{1t}}}{P_{1t}}\right)_{Design} = \frac{V(R)^{1.4}}{550} = \frac{0.23N(R)^{1.4}}{550}$

The calculation of these values has been shown in Table 3.5.

The engine speed lines have been plotted on the compressor performance map in Fig. 6.2. A point giving the maximum isentropic efficiency for the compressor is located on each of these lines, taking account that the point is far removed from the surge line. A smooth curve has been drawn joining these points, and is marked as the <u>engine operating line</u>. Thus the points a, b, c, d and e refer to the optimum operating conditions of the engine when the latter is running at 800, 1000, 12 00 , 1400 and 1600 r.p.m. respectively.

6.5. <u>Compressor Cycle Analysis-</u> After the points a, b, c, d and e have been located, the values of pressure and temperature at the compressor delivery and the speed of the compressor can be calculated as shown in Table 6.6. The delivery temperature will be determined by the relationship

$$\eta_c = \frac{\left[\left(P_{2t}/P_{1t}\right)^{\frac{\gamma-1}{\gamma}} - 1\right]}{\left(T_{2t} - T_{1t}\right)/T_{1t}}$$

or $$\frac{T_{2t}}{T_{1t}} = 1 + \frac{1}{\eta_c}\left[\left(\frac{P_{2t}}{P_{1t}}\right)^{\frac{\gamma-1}{\gamma}} - 1\right]$$

$$= 1 + \frac{1}{\eta_c}\left[(R)^{\frac{1}{3.5}} - 1\right]$$

where η_c is the isentropic efficiency of the compressor.

Also the suction volume of compressor

$$V_1 = 60 \times 550 \left[\left(\frac{Q\sqrt{T_{1t}}}{P_{1t}} \right) \Big/ \left(\frac{Q\sqrt{T_{1t}}}{P_{1t}} \right)_{Des.} \right] \quad \text{cu.ft./hr.}$$

6.6. Remapping of Compressor Characteristics in Terms of Temperature Ratio- Here the compressor characteristic curves given in Fig. 6.2. have been re-plotted in terms of $\left(\frac{T_{2t} - T_{1t}}{T_{1t}} \right)$ on the ordinate and relative mass flow on the abscissa. It has been done by taking a few points on the relative constant efficiency curve and calculating the values of $\left(\frac{T_{2t} - T_{1t}}{T_{1t}} \right)$ at these points. The calculations for the re-mapping are given in Table 6.7 and the modified performance curves shown in Fig. 6.3.

6.7. Turbine Characteristics and their re-mapping in Terms of Temperature Ratio - Figs. 6.4 and 6.5 give the non-dimensional performance characteristics of a turbine selected arbitrarily suitable for the pressure range in this case. In order to re-map the turbine performance, the temperature ratios have been calculated by the relationship

$$\frac{\Delta T}{T_{3t}} = \frac{T_{3t} - T_{4t}}{T_{3t}} = \eta_t \cdot \frac{\left[\left(\frac{P_{3t}}{P_{4t}} \right)^{\frac{\gamma'-1}{\gamma'}} - 1 \right]}{\left(\frac{P_{3t}}{P_{4t}} \right)^{\frac{\gamma'-1}{\gamma'}}}$$

$$= \eta_t \cdot \frac{\left[\chi^{\frac{1.33-1.0}{1.33}} - 1 \right]}{(\chi)^{\frac{1.33-1.0}{1.33}}} = \eta_t \cdot \frac{\chi - 1}{\chi}$$

The calculations have been shown in Table 6.8 and the modified performance curves in Fig. 6.6.

6.8. Analysis of Engine Cycle- The engine cycle has been analysed for an ideal case, as shown in Fig. 6.7. Here at point 4" blow down takes place, so that the conditions at the turbine inlet may be assumed to assumed be given by 4'. For determining the values at 4', the blow down maybe assumed to take place adiabatically. Furthermore it may be assumed that the fuel-air ratio for the supercharged operation is the same as for the naturally aspirated case when the

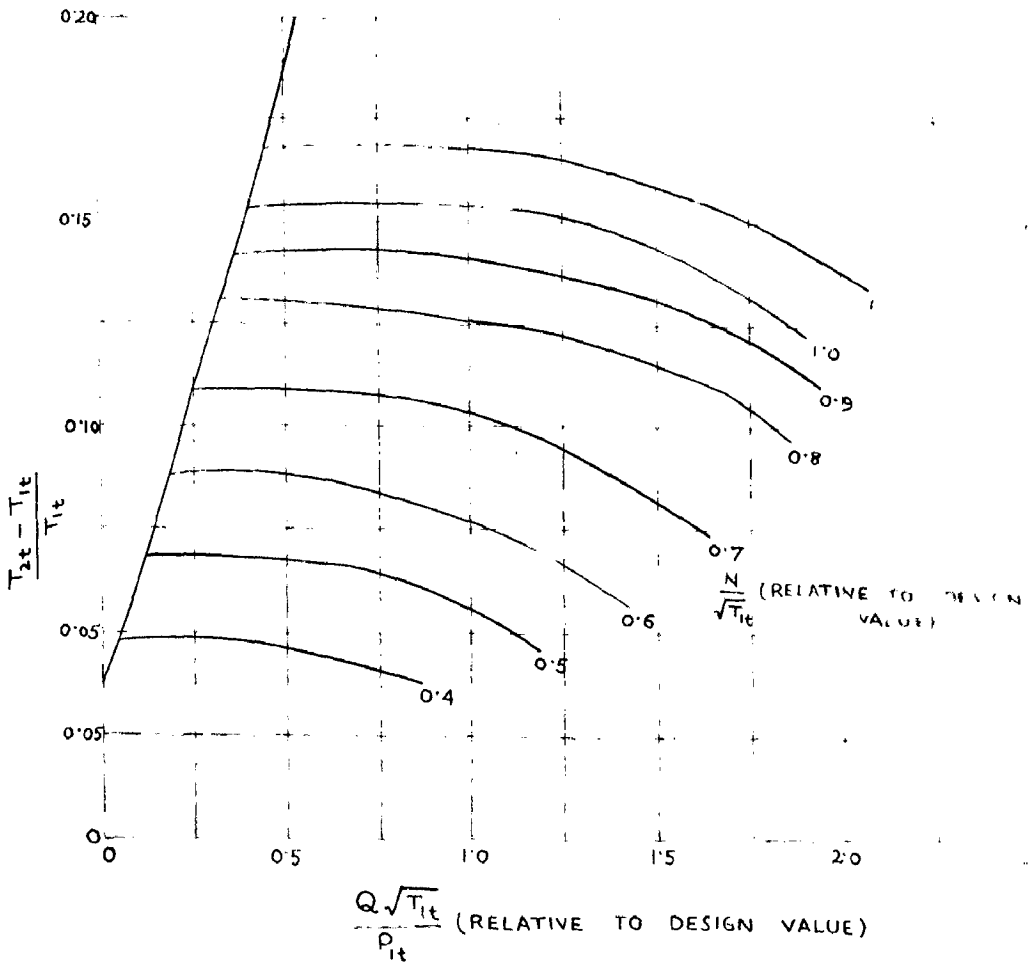

CENTRIFUGAL COMPRESSOR PERFORMANCE.
FIG. 6·3.

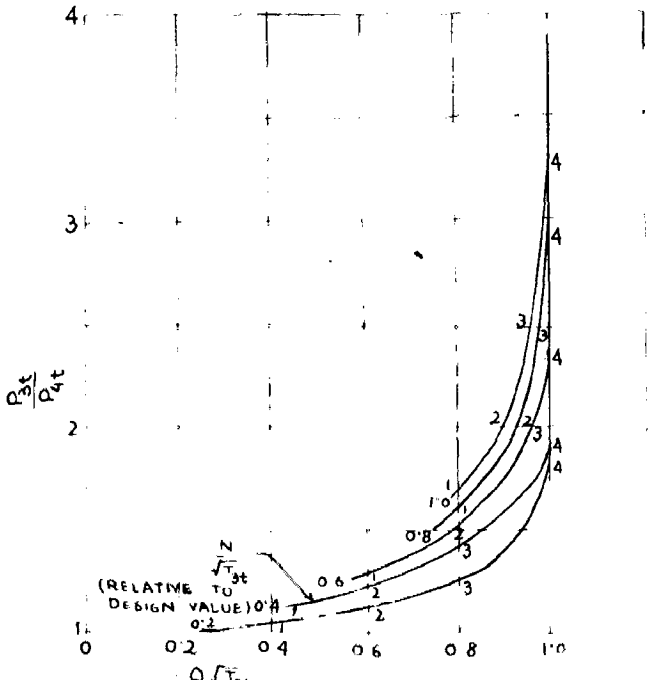

TURBINE PERFORMANCE
FIG. 6·4

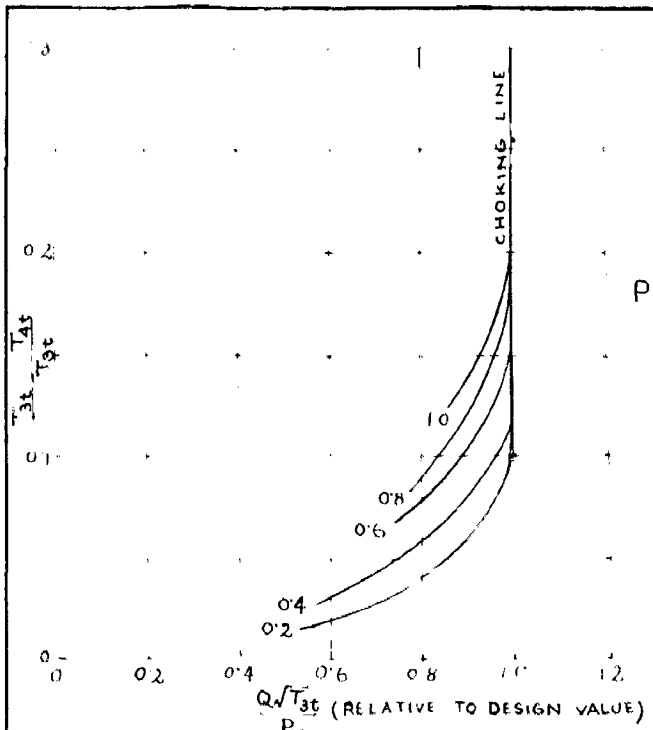

FIG. 6·6.

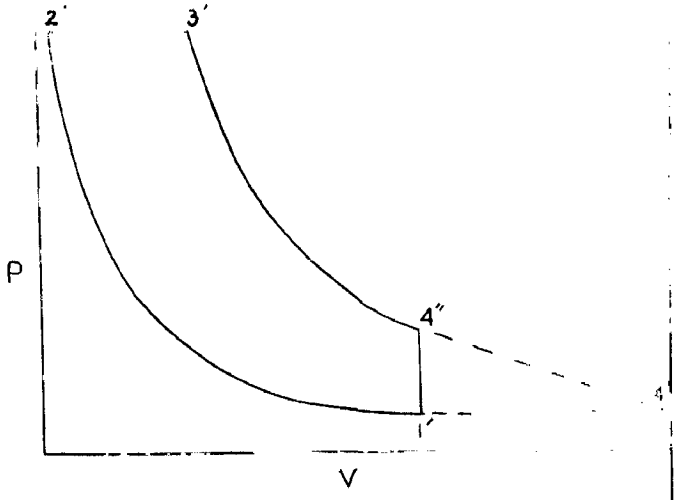

FIG. 6·7.

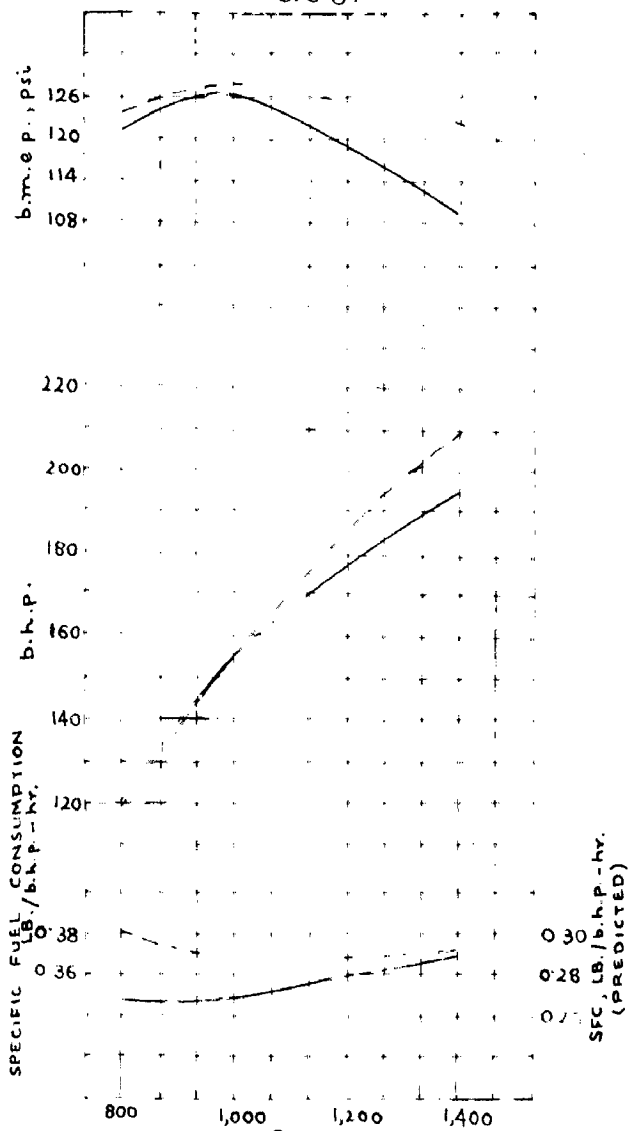

PREDICTED PERFORMANCE CURVES OF TURBO-CHARGED ENGINE

FIG 6·8

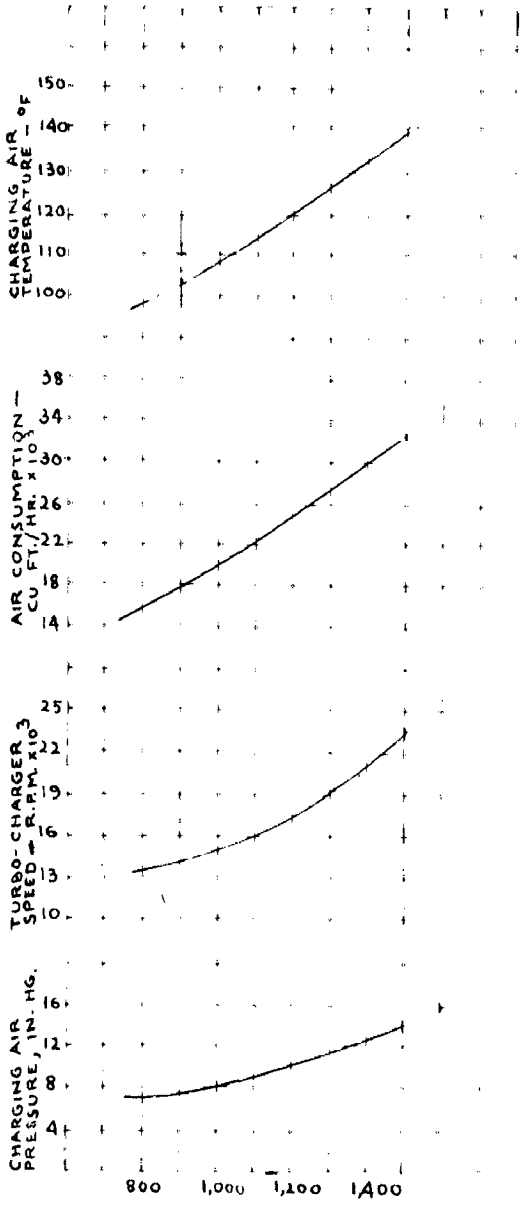

PREDICTED PERFORMANCE CURVES OF TURBO-CHARGED ENGINE

FIG 6·9

– – – PREDICTED . . . . EXPERIMENTAL

engine is running at the same speed. This assumption is not valid in practice, but it approximates to the actual operating conditions to quite a fair extent. The fuel for the engine may be taken to be medium diesel oil, the heating value of which is 18,000 B.T.U./Lb. The compression ratio of the engine is assumed to remain unaltered. The values of constant pressure specific heat and the ratio of specific heat may be taken as follows:

For compression $C_p = 0.24$; $\gamma = 1.4$

For heating and expansion $C_p' = 0.276$; $\gamma = 1.33$

Since for low pressure turbo-charged engine, aftercooling is not economic, the pressure and temperature at the engine suction may be reasonably assumed to be the same as at the compressor outlet. This means that

$$T_{2t} = T_1' \quad \text{and} \quad P_{2t} = P_1'$$

The calculations giving the values of pressure and temperature for the various cardinal points of the engine cycle are shown in table 6.10, in which the values of fuel-air ratio have been taken from Table 6.9.

6.9 <u>Compressor- Turbine Combination-</u> As already discussed in the previous chapter, the conditions for the compressor and turbine combination are-

$$\frac{N}{\sqrt{T_{1t}}} = \frac{N}{\sqrt{T_{3t}}} \cdot \sqrt{t} \qquad \text{where} \quad t = \frac{T_{3t}}{T_{1t}} \qquad (6.1)$$

$$\frac{Q\sqrt{T_{1t}}}{P_{1t}} = \frac{Q\sqrt{T_{3t}}}{P_{3t}} \cdot \frac{1}{\sqrt{t}} \cdot \frac{P_{3t}}{P_{1t}} \qquad (6.2)$$

and $C_{p_{12}}(T_{2t} - T_{1t}) \leq \eta_m C_{p_{34}}(T_{3t} - T_{4t})$ where $C_{p_{12}} = C_p = 0.24$

and $C_{p_{34}} = C_p' = 0.273$

or $$\frac{T_{2t} - T_{1t}}{T_{1t}} \leq \eta_m \cdot \frac{C_{p34}}{C_{p12}} \left(\frac{T_{3t} - T_{4t}}{T_{3t}} \right) \cdot \frac{T_{3t}}{T_{1t}} \leq P \qquad (6.3)$$

Since the conditions at the turbine entry are given by 4', we have $P_{3t} = P_4'$ and $T_{3t} = T_4'$. The mechanical efficiency of compressor for direct drive may be taken as 98%. The calculations for this case are shown in Table 6.11.

It may be seen that for all operating conditions $\left(\frac{T_{2t} - T_{1t}}{T_{1t}}\right)$ is always less than P. Hence the combination of compressor and turbine will work satisfactorily.

6.10 Mean Effective Pressure of turbo-charged Engine. For the cycle diagram shown in Fig. 6.7, the work done per cycle,

$$W = P_3'(V_3' - V_2') + \frac{P_3'V_3' - P_4''V_4''}{\gamma' - 1} - \frac{P_2'V_2' - P_1'V_1'}{\gamma - 1}$$

$$= P_3'V_2'\left(\frac{V_3'}{V_2'} - 1\right) + V_2' \cdot \frac{P_3'\frac{V_3'}{V_2'} - P_4''\frac{V_4''}{V_2'}}{\gamma' - 1} - V_2' \cdot \frac{P_2' - P_1'\frac{V_1'}{V_2'}}{0.4}$$

$$= P_3'V_2'(x-1) + V_2' \frac{P_3'x - 16P_4''}{0.33} - \frac{P_2' - 16P_1'}{0.4}$$

where $x = \frac{V_3'}{V_2'}$

Hence mean effective pressure,

$$\text{m.e.p.} = \frac{W}{15V_2'} = \frac{1}{15}\left[P_3'(x-1) + \frac{P_3'x - 16P_4''}{0.33} - \frac{P_2' - 16P_1'}{0.4}\right]$$

$$= \frac{Q}{15} \text{ , say.}$$

The brake mean effective pressure may be found out from the above expression by assuming a mechanical efficiency of 80 per cent for the engine. The values of brake mean effective pressure have been calculated in Table 6.12.

6.11. Specific Fuel Consumption of Turbo-charged Engine. From the brake mean effective pressure, the brake horse-power has been calculated by the relationship.

$$\text{B.H.P.} = \frac{(\text{B.M.E.P.})\ LANK}{33{,}000}$$

$$= \frac{(\text{B.M.E.P.})\ 161 \times N \times G}{33{,}000 \times 12 \times 2}$$ where B.M.E.P. is in lb./in.^{2} and N is the engine r.p.m.

$$\text{Turbo B.H.P.} = \frac{1.22\ N}{1,000}\ (\text{N.A.L.P.})$$

The volume of air handled by the compressor for different operating speeds of the engine can be read out from Table 6.6. The density of air at compressor suction is known, so the rate of air consumption will be determined. Now the fuel-air ratio and the brake horse-power of the engine being known, the specific fuel consumption can be calculated as shown in Table 6.13.

6.11. Performance of Turbo-charged Engine- The curves for mean effective pressure, brake horse-power and the specific fuel consumption have been plotted in Fig. 6.3 from tables 6.12 and 6.13. These curves predict the performance of the engine in the low pressure turbocharged version. The actual performance of the engine which can be found experimentally would be much different from the predicted performance. This has been shown diagrammatically in Fig. 6.3 where along with the predicted curves the experimental curves (41) have also been plotted side by side.

It may be observed that the predicted b.m.p. curve and so also the b.h.p. curve is more drooping than the experimental curves. However, the maximum value of the b.m.e.p. is nearly the same in both the cases. Further the specific fuel consumption as predicted is rather less than the actual consumption. All these deviations are due to the following reasons:

(1) For calculating the performance of the engine in the turbocharged version, the fuel-air ratio is assumed to have the same value as in the unsupercharged form. This assumption is not at all valid in practice, and is greatly responsible for yielding a lower value of the b.m.e.p. as well as the b.h.p. at higher speeds.

(2) how does the fuel air ratios vary in actual supercharged engines? The cardinal points of the engine cycle have been alter-

lated by assuming an ideal constant pressure cycle. An actual cycle always differs materially from the ideal cycle and gives a lower value of the power output. The reason for the lower values of the predicted specific fuel consumption may be greatly attributed to this assumption of ideal cycle and also to some extent to the assumption of constant fuel-air ratio in both the supercharged and unsupercharged cases.

(3) The fuel used by the engine under test may have a different heating value.

(4) The volumetric efficiency of the turbocharged engine may be different from the assumed value of 100 per cent.

(5) The conditions at the engine suction are not exactly known.

(6) The loss of air pressure in passing through the connecting ducts has not been taken into consideration.

(7) The effect of residual gases upon the cylinder charge has been ignored, because perfect scavenging of the burnt gases has been assumed.

There are several other factors also like the throttling at the valves, combustion efficiency, pneumatic vortices etc. which have not been considered while estimating the performance of the engine.

On comparison of the curves for the turbocharged engine given in Fig. 6.8 with the curves for naturally aspirated engine shown in Fig. 3.1, it may be seen that turbocharging has resulted in the increase of b.m.ep. by about 45 per cent. Also there is an improvement in the specific fuel consumption.

The variation of the charging air pressure and temperature, turbocharger speed and the air consumption has also been exhibited in Fig. 6.9 plotted from the values calculated in Table 6.3.

CHAPTER 7

CONCLUSION AND SUGGESTIONS

7.1. Present Position of Supercharged Engines- With the advent of the two stroke engines, the inherent disadvantages of the four stroke engines in respect of low power output and non-uniform torque characteristics etc. were put to light, and supercharging was the sole alternative to make it a sound competitor in the field. Mechanical supercharging by reciprocating compressor and Roots blower was initially applied, but the discontent stillprevailed due to their unwieldy size, low efficiency and noisy operation. Growing interest in the field later resulted in the development of vane and screw blowers, Ricardo and Bicera Compressors. The possibility to conserve the heat of exhaust could not long escape the attention of the engineers and gave birth to turbo-charging. At every stage there has been a neck to neck competition between mechanical supercharging and exhaust gas turbocharging, but the latter undoubtedly dominates in all applications except in the automotive field.

From the existing statistical data, an economic minimum has been struck where the gains from turbocharging are offset by the use of a slightly larger naturally aspirated engine. Here the increase in engine cost works out to be less than the first cost of the turbocharger. This size, though not assessed accurately, is probably below 80 b.h.p. But the use of engines of smaller sizes is so extensive as compared to their counterpart in larger sizes, that the lackof adaptability of turbo-charging to these engines is a terrible handicap. A more comprehensive and sound knowledge of aerodynamic principles leading to the economic design of small size centrifugal and axial flow compressors may lead to their economic use in smaller size engines. Another serious handicap is the low effic-

iency of axial turbines with blade heights less than 0.75 in., which may possibly be overcome by the use of small radial flow turbo-chargers.

High pressure turbocharging is becoming increasingly popular, and commercial engines employing a pressure ratio of 2.2 developing b.m.e.ps. of 220 - 225 lb. per sq. in. are in the market. Boost pressures of the order of 80 psig. are being tried which will increase the b.m.e.p. by 100 to 120 per cent. The delivery temperature being as high as 170 to 200°F, alternative cooling systems are being tried. The Miller, the Bono and the Buchi Duplex systems have already been put forward. A step towards the efficient design of charge coolers may also make a vital contribution in the field. The engine exhaust, extra rich in energy, has assisted to dispense with the impulse turbines of the conventional Buchi turbocharging by rendering possible the use of more efficient reaction turbines. Also to decrease the loading on the fuel equipment, the common rail system, the accumulator injection system, and the servo-operated injection pump have already been introduced.

7.2. Future Prospects of Supercharging. On the basis of the progress made to date, it may be anticipated that the development of high pressure supercharging may probably take place on the lines indicated in Fig. 7.1. Part of the graph is based upon the existing data up to pressure ratios about 3:1. But with the anticipated value of the maximum pressure attainable, the system would probably resemble more to the gas turbine cycle, with the difference that the cylinder would work largely as a gas generator still crankshaft controlled and the power would be taken on a common shaft from both the cylinder and the turbine geared together. With high supercharge the valve overlap may probably be reduced, which will, to some extent, reduce

the smoke hazard. Due to high temperatures produced there may possibly be a danger of siezing of the rings which may also call for some modification. Adequate cooling will be extremely essential.

It is expected that with further success in economic and improved design of small radial flow turbo-chargers, turbocharging may possibly be extended up to engines of 50 h.p. There cannot be any doubt that turbocharging will soon occupy a unique position in the automotive field as well.

7.3 Suggestions for Research- The following are the probable fields for further work-

(1) High pressure supercharging- Economic design of turbo-charged engines employing pressure ratios greater than 2.2, so that these may also be commercially introduced. The difficulties encountered in this respect have been the heavy improportionate control gear for the fuel injection equipment, siezure of piston rings due to very high temperatures produced and a limitation upon the temperature of the exhaust gases entering the turbine.

(2) Design of efficient systems of cooling of air charge. The use of coolant in the form of volatile liquids with high latent heat might possibly offer a better solution.

(3) Development of the design criteria for small radial flow turbo-chargers. Unfortunately, the aerodynamic chargers when scaled down to minute sizes required for engines rated under 100 h.p., have not shown good efficiency. The development of radial flow turbines is still immature and requires a thorough investigation, both theoretical and experimental, regarding the flow phenomena.

This will help to make turbocharging suitable for small size engines and automotive applications.

(4) Development of high heat-resistant material for the turbine

blades, so that the limit on high pressure supercharging imposed by the high exhaust temperatures is waived off.

(6) From the results of Taylor (42) on the basis of the experiments performed by him on a Lycoming liquid-cooled air-craft type cylinder, it is evident that at high altitudes the turbine m.e.p. is much in excess of the compressor m.e.p. requirements. This means a sacrifice in the output in current turbo-supercharger installations. By suitably gearing the engine and the turbine shafts, possibly greater output could be obtained. This requires further experimental verification.

APPENDIX

APPENDIX I

SUPERPOSITION OF FINITE AMPLITUDE WAVES

Let us consider a pipe containing air at a pressure p_0 and density ρ_0. Then the propagation and particle velocities for a plain wave of finite amplitude at a wave point where the pressure and density are p and ρ respectively, will be (Ref. Earnshaw 1860),

$$C = a_0\left[6\left(\frac{p}{p_0}\right)^{\frac{1}{7}} - 5\right] \qquad (1)$$

and $$w = 5a_0\left[\left(\frac{p}{p_0}\right)^{\frac{1}{7}} - 1\right] \qquad (2)$$

where a_0 is the undisturbed sonic velocity in the pipe, and C and w are the propagation and particle velocities respectively.

The particle velocity of a gas column AH (in Fig.1) moving right) is from eq^n (2)

$$w_1 = 5a_0\left[\left(\frac{p_1}{p_0}\right)^{\frac{1}{7}} - 1\right]$$

and of CF moving to the left

$$w_2 = -5a_0\left[\left(\frac{p_2}{p_0}\right)^{\frac{1}{7}} - 1\right]$$

For points between E and B (Fig. 2), the particle velocity relative to column AH is

$$w = -5a_1\left[\left(\frac{p_t}{p_1}\right)^{\frac{1}{7}} - 1\right]$$

Now $$a_1 = \sqrt{\frac{\gamma p_1}{\rho_1}} \quad ; \quad a_0 = \sqrt{\frac{\gamma p_0}{\rho_0}}$$

$$\therefore \quad a_1 = a_0\left[\frac{p_1}{p_0}\cdot\frac{\rho_0}{\rho_1}\right]^{\frac{1}{2}}$$

, but since the conditions are isentropic in nature, we have

$$\frac{p_1}{\rho_1^{\gamma}} = \frac{p_0}{\rho_0^{\gamma}} \quad \text{or} \quad \frac{\rho_0}{\rho_1} = \left(\frac{p_0}{p_1}\right)^{\frac{1}{\gamma}}$$

$$\therefore \quad a_1 = a_0\left(\frac{p_1}{p_0}\right)^{\frac{\gamma-1}{2\gamma}}$$

$$\therefore \quad w = -5a_0\left(\frac{p_1}{p_0}\right)^{\frac{1}{7}}\left[\left(\frac{p_t}{p_1}\right)^{\frac{1}{7}}-1\right] \qquad \text{where } \gamma = 1.4$$

According to Bannister and Hicklow (43), the summation of waves of finite amplitude gives the absolute velocity,

$$\begin{aligned} w_t &= w_1 + w \\ &= 5a_0\left[\left(\frac{p_1}{p_0}\right)^{\frac{1}{7}}-1-\left(\frac{p_t}{p_1}\right)^{\frac{1}{7}}\left(\frac{p_1}{p_0}\right)^{\frac{1}{7}}+\left(\frac{p_1}{p_0}\right)^{\frac{1}{7}}\right] \\ &= 5a_0\left[2\left(\frac{p_1}{p_0}\right)^{\frac{1}{7}}-\left(\frac{p_t}{p_0}\right)^{\frac{1}{7}}-1\right] \end{aligned} \qquad (3)$$

Again, considering the regions EB, and CB, we get

$$w_t = 5a_0\left[-2\left(\frac{p_2}{p_0}\right)^{\frac{1}{7}}+\left(\frac{p_t}{p_0}\right)^{\frac{1}{7}}+1\right] \qquad (4)$$

Equating (3) and (4), we get I

$$\left(\frac{p_t}{p_0}\right)^{\frac{1}{7}} = \left(\frac{p_1}{p_0}\right)^{\frac{1}{7}}+\left(\frac{p_2}{p_0}\right)^{\frac{1}{7}}-1$$

substituting the value of $\left(\frac{p_t}{p_0}\right)^{\frac{1}{7}}$ in eqn (4), we get

$$\begin{aligned} w_t &= 5a_0\left[2\left(\frac{p_1}{p_0}\right)^{\frac{1}{7}}-\left(\frac{p_1}{p_0}\right)^{\frac{1}{7}}-\left(\frac{p_2}{p_0}\right)^{\frac{1}{7}}\right] \\ &= 5a_0\left[\left(\frac{p_1}{p_0}\right)^{\frac{1}{7}}-\left(\frac{p_2}{p_0}\right)^{\frac{1}{7}}\right] \end{aligned} \qquad \text{II}$$

Equations (5) and (6) may be extended to cover the summation of any number of finite amplitude waves.

Thus if the values of the pressure and particle velocity for an incident wave be p_1 and w_1, and for its reflected wave from an open or close pipe end be p_r and w_r, the net values of absolute pressure, p_t and particle velocity, w_t at any point will be (from eqns I and II)

$$\left(\frac{p_t}{p_0}\right)^{\frac{1}{7}} = \left(\frac{p_1}{p_0}\right)^{\frac{1}{7}}+\left(\frac{p_r}{p_0}\right)^{\frac{1}{7}}-1$$

and $$w_t = 5a_0\left[\left(\frac{p_1}{p_0}\right)^{\frac{1}{7}}-\left(\frac{p_r}{p_0}\right)^{\frac{1}{7}}\right]$$

APPENDIX II

PERFORMANCE DATA FOR DIFFERENTIAL SERIES OF TURBO-CHARGERS MANUFACTURED BY D. BROWN & SONS LTD.

TABLE G.1

Approximate Free Air Capacities for Maximum Continuous Rating

Basic rating	Free Air Capacities for various pressure Ratios - Cu. ft./min.		
	1.35 : 1	1.60 : 1	2.00 : 1
00	-	720 - 1,155	875 - 1,400
100	1,015 - 1,645	1,155 - 1,870	1400 - 2,270
200	1,645 - 2,620	1,870 - 2,975	2270 - 3,600
300	2,620 - 4,100	2,975 - 4,725	-
400	4,100 - 6,320	4,725 - 7,185	-
500	-	7,185 -11,100	-
600	-	11,100 -17,250	-

TABLE G.2
T.S. Series : 1.35 : 1 Pressure Ratio

Rating	Turbo-charger			
	TS.100	TS.200	TS.300	TS.400
Maximum Continuous				
Speed - R.P.M.	17,000	13,500	11,000	9,000
Boost - lb./sq. in.	5.0	5.0	5.0	5.0
Permissible t.i.t., °C	600	600	600	600
Maximum (one-hour limit)				
Speed - R.P.M.	21,600	17,000	14,000	11,000
Boost - lb./sq. in.	8.5	8.5	8.5	8.5
Permissible t.i.t. °C	650	650	650	650

TABLE 6.3
H.S. Series; 1.5:1 Pressure Ratio

Rating	Turbo-Charger						
	H.S.90	H.S.100	H.S.200	H.S.300	H.S.400	H.S.500	H.S.60
Maximum Continuous Speed-r.p.m.	24,000	20,000	15,750	13,000	10,500	8,240	6,440
Boost-lb./sq.in.	7.35	7.35	7.35	7.35	7.35	7.35	7.35
Permissible t.i.t.,°C	600	600	600	600	600	600	600
Maximum (one hour limit)							
Speed -r.p.m.	27,000	22,500	18,000	15,000	12,000	9,400	7,330
Boost-lb./sq.in.	10.3	10.3	10.3	10.3	10.3	10.3	10.3
Permissible t.i.t.,°C	650	650	650	650	650	650	650

TABLE 6.4
H.P. Series; 2.0:1 Pressure Ratio

Rating	Turbo-charger		
	H.P.90	H.P.100	H.P. 200
Maximum Continuous			
Speed- r. p.m.	32,500	23,500	21,500
Boost - lb./Sq.in.	14.7	14.7	14.7
Permissible t.i.t.,°C	600	600	600
Maximum (one hour limit)			
Speed - r.p.m.	34,800	28,000	23,000
Boost - lb./Sq.in.	17.6	17.6	17.6
Permissible t.i.t.,°C	650	650	650

Note: t.i.t. = turbine inlet temperature .

TABLE G.5

Engine speed R.P.M.	V=0.283 cu.ft./min.	R = 1.0		R=1.1		R = 1.2		R = 1.3		R = 1.4		R = 1.5		R=1.6	
		$(R)^{1.4}$	□	$(R)^{1.4}$	□	$(R)^{1.4}$	□	$(R)^{1.4}$	□	$(R)^{1.4}$	□	$(R)^{1.4}$	□	$(R)^{1.4}$	□
800	224	1.0	0.407	1.07	0.433	1.139	0.463	1.23	0.500	1.272	0.517	1.333	0.544	1.4	-
1000	280	1.0	0.510	1.07	0.543	1.139	0.581	1.23	0.627	1.272	0.649	1.333	0.681	1.4	-
1200	336	1.0	0.611	1.07	0.655	1.139	0.699	1.23	0.752	1.272	0.779	1.333	0.817	1.4	-
1400	392	1.0	0.712	1.07	0.733	1.139	0.811	1.23	0.876	1.272	0.908	1.333	0.951	1.4	-
1600	448	1.0	0.813	1.07	0.870	1.139	0.925	1.23	1.000	1.272	1.035	1.333	1.087	1.4	1.131

° R = Pressure Ratio

TABLE G.6

Engine speed R.P.M.	$\left(\frac{Q\sqrt{T_{1t}}}{P_{1t}}\right)\Big/\left(\frac{Q\sqrt{T_{1t}}}{P_{1t}}\right)$ (Fig. G.2)	Suction volume of compressor cu.ft./hr.	Pressure Ratio, $R = P_{2t}/P_{1t}$ (Fig. G.2)	P_{2t} lb./in.^{2}	P_{2t} in. Hg. (Gauge)	$\left(\frac{P_{2t}}{P_{1t}}\right)^{\frac{1.4-1.0}{1.4}}$	η_c (Fig. G.2)	$\frac{T_{2t}}{T_{1t}}$	T_{2t} °R	t_{2t} °F	$\left(\frac{N}{\sqrt{T_{1t}}}\right)\Big/\left(\frac{N}{\sqrt{T_{1t}}}\right)$ (Fig. G.2)	Turbocharger speed, N, r.p.m.
800	0.465	15,250	1.220	17.90	6.60	1.056	0.732	1.0735	595	99	0.55	13,200
1000	0.600	19,800	1.230	18.80	8.40	1.071	0.770	1.0822	569	109	0.65	15,600
1200	0.748	24,600	1.29	19.70	10.20	1.089	0.773	1.1150	580	120	0.73	17,500
1400	0.900	29,700	1.415	20.80	12.45	1.102	0.777	1.1410	593	133	0.83	21,100
1600	1.075	35,800	1.530	22.45	15.90	1.129	0.730	1.1652	606	145	1.03	25,000

TABLE G.7

Constant Speed Ratio (Fig. G.3)	POINT X: Relative Mass Flow (Fig. G.2)	Pressure Ratio (Fig. G.2)	$\left(\frac{P_{2t}}{P_{1t}}\right)^{\frac{\gamma-1}{\gamma}} = x$	$x-1$	η_c (Fig. G.2)	$\frac{T_{2t}-T_{1t}}{T_{1t}} = \frac{x-1}{\eta_c}$	POINT Z: Relative Mass Flow	Pressure Ratio	x	$x-1$	η_c	$\frac{T_{2t}-T_{1t}}{T_{1t}}$
0.4	0.075	1.133	1.035	0.035	0.732	0.0473	0.25	1.14	1.020	0.033	0.737	0. 0439
0.5	0.125	1.185	1.050	0.050	0.739	0.0377	0.50	1.10	1.052	0.032	0.730	0. 0334
0.6	0.200	1.260	1.037	0.037	0.733	0.0390	0.60	1.23	1.033	0.033	0.734	0. 0390
0.7	0.260	1.315	1.033	0.033	0.756	0.1035	0.80	1.32	1.033	0.033	0.735	0. 2085
0.8	0.320	1.335	1.100	0.100	0.737	0.1320	0.75	1.30	1.100	0.100	0.772	0. 1295
0.9	0.375	1.425	1.103	0.103	0.753	0.1420	0.75	1.44	1.110	0.110	0.770	0. 1430
1.0	0.425	1.470	1.116	0.116	0.750	0.1533	0.75	1.43	1.110	0.119	0.770	0. 1540
1.1	0.460	1.520	1.127	0.127	0.750	0.1076	0.75	1.44	1.130	0.130	0.730	0. 1690

	POINT 3: Relative Mass Flow	Pressure Ratio	x	$x-1$	η_c	$\frac{T_{2t}-T_{1t}}{T_{1t}}$	POINT 4: Relative Mass Flow	Pressure Ratio	x	$x-1$	η_c	$\frac{T_{2t}-T_{1t}}{T_{1t}}$
0.4	0.50	1.140	1.035	0.035	0.741	0.0472	0.75	1.13	1.030	0.030	0.730	0. 0410
0.5	0.75	1.104	1.050	0.050	0.750	0.0330	1.00	1.16	1.042	0.042	0.733	0. 0573
0.6	1.00	1.225	1.030	0.030	0.730	0.0700	1.25	1.18	1.050	0.050	0.730	0. 0355
0.7	1.00	1.210	1.032	0.033	0.770	0.1035	1.50	1.23	1.031	0.031	0.730	0. 0335
0.8	1.25	1.335	1.034	0.034	0.733	0.1240	1.50	1.24	1.030	0.030	0.735	0. 1175
0.9	1.25	1.425	1.107	0.107	0.777	0.1370	1.75	1.33	1.030	0.030	0.753	0. 1220
1.0	1.25	1.490	1.119	0.110	0.773	0.1520	1.75	1.30	1.100	0.100	0.763	0. 1320
1.1	1.25	1.540	1.131	0.131	0.730	0.1030	1.75	1.44	1.114	0.114	0.735	0. 1510

TABLE G.8

Relative $N/\sqrt{T_{3t}}$ (Fig. G.4)	POINT X: Relative Mass Flow	Pressure Ratio (Fig. G.4)	$\left(\frac{P_{3t}}{P_{4t}}\right)^{\frac{\gamma'-1}{\gamma'}}=\gamma$	$\gamma-1$	η_t	$\frac{T_{3t}-T_{4t}}{T_{3t}}$	POINT 2: Relative Mass Flow	Pressure Ratio	γ	$\gamma-1$	η_t	$\frac{T_{3t}-T_{4t}}{T_{3t}}$
0.2	0.40	1.025	1.005	0.005	Not available	-	0.60	1.12	1.023	0.023	0.60	0.0163
0.4	0.42	1.120	1.027	0.027	"	-	0.60	1.20	1.045	0.045	0.60	0.0268
0.6	0.60	1.300	1.033	0.036	"	-	0.80	1.60	1.103	0.103	0.78	0.0747
0.8	0.80	1.600	1.127	0.127	"	-	0.92	2.00	1.187	0.187	0.80	0.1260
1.0	0.80	1.700	1.141	0.141	"	-	0.90	2.00	1.187	0.187	0.72	0.1310

Relative $\frac{N}{\sqrt{T_{3t}}}$	POINT 3: Relative Mass Flow	Pressure Ratio	γ	$\gamma-1$	η_t	$\frac{T_{3t}-T_{4t}}{T_{3t}}$	POINT 4: Relative Mass Flow	Pressure Ratio	γ	$\gamma-1$	η_t	$\frac{T_{3t}-T_{4t}}{T_{3t}}$
0.2	0.80	1.25	1.055	0.055	0.70	0.0365	1.0	1.85	1.162	0.162	0.74	0.103
0.4	0.80	1.40	1.038	0.038	0.78	0.0309	1.0	2.00	1.187	0.187	0.70	0.111
0.6	0.93	2.00	1.187	0.187	0.80	0.1230	1.0	2.50	1.255	0.255	0.80	0.162
0.8	0.93	2.50	1.255	0.255	0.81	0.1645	1.0	2.85	1.297	0.297	0.82	0.188
1.0	0.94	2.50	1.255	0.255	0.73	0.1545	1.0	3.25	1.340	0.340	0.81	0.203

TABLE G.9

Engine Speed r.p.m.	Suction volume of compressor cu.ft./hr. (Table G.6)	Density of air at ambient conditions.	Wt. of air consumed lb./hr.	Specific fuel consumption lb./bhp. hr. (Fig. G.1)	B.H.P. (Fig. G.1)	Fuel consumed lb./hr.	Fuel/Air Ratio
800	16,250	0.0733	1,100	0.375	83.0	32.2	0.0273
1,000	19,000	0.0733	1,445	0.375	103.0	40.9	0.0283
1,200	24,600	0.0733	1,090	0.332	123.5	48.0	0.0260
1,400	29,700	0.0733	2,230	0.333	143.0	53.2	0.0247
1,60							

TABLE G.10

Engine speed r.p.m.	$P_1' = P_{2t}$ (Table G.6)	$T_1' = T_{2t}$ °R (Table G.6)	$(R)^{0.4}$	$T_2' = T_1'(R)^{0.4}$	$(R)^{1.4}$	$P_2' = P_3' = P_1'(R)^{1.4}$	Fuel/Air Ratio $= Q_s$ (Table G.9)	$\frac{Q}{18000}$ $\frac{Q_s}{0.276}$	$T_3' = T_2' + \frac{Q_{F.18,000}}{0.276}$	$\frac{P_3'}{P_4'} = \frac{P_3'}{P_1'}$	$\left(\frac{P_3'}{P_4'}\right)^{\frac{0.33}{1.33}}$	$T_4' = T_3' \cdot \left(\frac{P_4'}{P_3'}\right)^{\frac{0.33}{1.33}} = \frac{T_3'}{T_2'}$	$\frac{V_3'}{V_2'}$	$\frac{V_4''}{V_3'} = \frac{16}{\frac{V_3'}{V_2'}}$	$\left(\frac{V_4''}{V_3'}\right)^{0.33}$	$T_4'' = T_3' \cdot \left(\frac{V_3'}{V_4''}\right)^{0.33}$
800	17.90	550	3.035	1005	43.5	863	0.0273	1770	2463	43.5	3.62	1321	2.045	7.83	1.971	1759
1000	18.80	559	3.035	1725	43.5	911	0.0283	1845	3570	43.5	2.62	1331	2.070	7.73	1.935	1816
1200	19.70	530	3.035	1730	43.5	957	0.0260	1606	3466	43.5	3.62	1317	1.032	8.15	2.000	1727
1400	28.80	593	3.035	1800	43.5	1000	0.0247	1510	3410	43.5	3.62	1300	1.005	8.44	2.020	1703

TABLE 6.11

Engine Speed r.p.m.	$T_{3t} = T_4'$ °R (Table 6.6)	T_{1t} °R	$t = \frac{T_{3t}}{T_{1t}}$	$\sqrt{t}$	Relative $N/\sqrt{T_{1t}}$ (Table 6.6)	Relative $N/\sqrt{T_{3t}}$ from eqn (6.1)	Relative $Q\sqrt{T_{1t}}/P_{1t}$ (Table 6.6)	$P_{3t} = P_{3t}$ (Table 6.6)	$\frac{P_{1t}}{P_{3t}}$	Relative $e\sqrt{T_{3t}}/P_{3t}$ from (6.2)	$\frac{T_{3t} - T_{1t}}{T_{1t}}$ (Fig. 6.3)	$\eta_m \cdot \frac{c_{p34}}{c_{p12}}$	$\frac{T_{3t} - T_{4t}}{T_{3t}} \cdot P$ (Fig. 6.6)
800	1,321	520	2.54	1.592	0.55	0.345	0.465	17.90	0.822	0.609	0.079	1.126	.028 .080
1000	1,361	520	2.62	1.620	0.65	0.402	0.600	18.80	0.783	0.761	0.098	1.126	.052 .154
1200	1,317	520	2.53	1.590	0.73	0.461	0.750	19.70	0.746	0.890	0.115	1.126	.082 .232
1400	1,300	520	2.50	1.582	0.88	0.556	0.900	20.80	0.706	1.000	0.140	1.126	.140 .394

TABLE 6.12)

Engine speed r.p.m.	P_1' (Table 6.10)	$P_2' = P_3'$ (Table 6.10)	T_4'' °R (Table 6.10)	P_4'', $= P_1'$ $(\frac{T_4''}{T_1'})$ (Table 6.10)	$x = \frac{V_3'}{V_2'}$	$x-1$	$P_3'(x-1)$	$P_3'x$	$16P_4''$	$\frac{P_3'x - 16P_4''}{0.33}$	$\frac{P_3'x - 16P_4''}{16P_1'}$	$P_2' - \frac{P_2' - 16P_1'}{0.4}$	Q	m.e.p.	b.m.e.p. ($\eta_m = 95\%$)
800	17.90	868	1759	60.9	2.045	1.045	908	1779	974	805	2440	286	582	1455	1893	126.2	120.5
1000	18.80	911	1816	65.6	2.070	1.070	975	1890	1050	840	2550	301	610	1525	2000	130.5	126.6
1200	19.70	957	1727	65.4	1.962	0.962	922	1881	1045	836	2540	315	640	1600	1862	124.2	118.0
1400	20.80	1009	1695	67.8	1.895	0.895	904	1911	1083	828	2550	333	676	1691	1763	117.5	111.5

TABLE 6.13

Engine Speed R.P.M.	B.H.P. (Table 6.12)	I.H.P. = 1.221 × (B.H.P. × R.P.M.) / 1,000	Air consumption lb./hr. (Table 6.8)	Fuel-Air Ratio (Table 6.9)	Fuel consumption lb./hr.	Specific Fuel Consumption lb./B.H.P.hr.
800	120.6	117.0	1,180	0.0273	32.2	0.233
1,000	126.6	154.3	1,445	0.0233	40.9	0.235
1,200	118.0	174.0	1,800	0.0260	48.9	0.230
1,400	111.6	193.2	2,200	0.0247	56.2	0.237

APPENDIX III

BIBLIOGRAPHY

1. Davidson, C.St.C., 'Internal Combustion Engines (Some early stages in its development)', Engineering, Vol. 182, p.253, 1956.

2. Judge, A.W., 'High Speed Diesel Engines', Chapman and Hall Limited, London, p.1, 1957.

3. Fedden, A.H.R., 'Aircraft Engines', Proceed. I. Mech.E., Vol. 129, p.197, 1935.

4. 'The Charging of Four Stroke Marine Diesel Engines', Brown Boveri Review, p.300, 1942.

5. Buckley, G.F., 'Experiments with a supercharged Single Cylinder High Speed Petrol Engine', Proceed. I Mech.E., Vol. 123, p. 373, 1932.

6. Judge, A.W., 'Aircraft Engines', Vol. I, D. Van Nostrand Co. Inc., New York, p. 199, 1940.

7. Lichty, L.C., 'Internal Combustion Engines,' Mc Graw Hill Book Co., p. 103, 1951.

8. Beerlage and Broeze, 'The Ignition Quantity of Fuels in Compression Ignition Engines,' Engg., p. 687, Dec.4, 1931.

9. Pye, D.R., 'The Internal Combustion Engine', Vol. II, Oxford University Press, London, p. 57, 1953.

10. Barber, 'Knock Limited Performance of Several Automobile Engines,' Trans. S.A.E., p. 401, 1948.

11. Teyhorn, W.D., 'An Approach to the Problem of Pressure Charging The Compression Ignition Engine,' I. Mech. E., Automobile Divn. Proceed., p. 217, 1956-57.

12. Millington, D.W., 'The Supercharging of High Speed Diesel Engines by Mechanically Driven Compressors,' I.Mech.E.,

Automobile Divn. Proced, p. 229,1956-57.

13. Lichty, L.C., 'Internal Combustion Engines', Mc Graw Hill Book Co., p. 470, 1951.

14. N.A.C.A. Technical Note No. 423.

15. Schmitzer, P.M., 'Scavenging of Two Stroke Cycle Diesel Engines', The Macmillan Company, New York, p. 113, 1949.

16. Rowbee Cox, Harold, 'Gas Turbine Principles and Practice', George Newnes Limited, London, p. 7-9, 1955.

17. Pounder, C.C., 'Diesel Engine Principles and Practice', George Newnes Limited, London, p. G-25, 1960.

18. Vincent, L.Z., 'The Theory and Design of Gas Turbines and Jet Engines', Mc Graw Hill Book Co., Inc., New York, p. 290, 1953.

19. Campbell. K, and Talbert, J.L., 'Some Advantages and Limitations of Centrifugal and Axial Aircraft Compressors', S.A.E. Journal, Vol. 53, p. 607, 1945.

20. Honger, H., 'Problems of Turbocharger Design and Manufacture', Brown Boveri Review, Vol. 37, p. 420, 1950.

21. Buchi, A.J., 'Supercharging of Internal Combustion Engines with Blowers Driven by Exhaust Gas Turbines,' Trans. A.S.M.E., Vol. 59, p. 85, 1937.

22. Buchi, A.J., 'Supercharging of Internal Combustion Engines,' The Engineer, Vol. 140, p. 171, 1925.

23. Noodig W.J., 'Pressure-charging Velox Boiler and Gas Turbine,' Brown Boveri Review, p. 183, 1941.

24. Jenny, E., 'The Utilisation of Exhaust Gas Energy in the Supercharging of the Four-Stroke Diesel Engine,' The Brown Boveri Review, Vol. 37, p. 433, Nov. 1950.

25. Buchi, A.J., 'Turbocharging and Gas Turbines,' Journal of

Am. Soc. Nav. Engrs., Vol. 60, p. 261, 1948.

26. Harmin, Troels, 'Polar Diagram for Tuning of Exhaust Pipes,' Trans. A.S.M.E., Vol. 68, p. 31, 1946.

27. Pullman, W.A., 'Exhaust Pulse Energy,' Engineering, Vol. 183, p. 14, Jan.4, 1957.

28. Bannister, F.K. and Mucklow, G.F., 'Wave Action following Sudden Release of Compressed Gas from a Cylinder', Proc. I Mech.E., Vol. 159, p. 260, 1948.

28. Wallace, F.J. and Hassif, N., 'The Effect of Friction on Compression and Rarefaction Waves of Finite Amplitude,' Engineering, Vol. 175, p. 674, May 29, 1953.

30. Stahel, R., 'Power Increase of Four Stroke and Two Stroke Diesel Engines by Brown Boveri Exhaust Turbochargers', Brown Boveri Review, Vol. 33, p. 153, 1946.

31. Bradbury, C.N., 'The Turbocharging of High Speed Diesel Engines, Present Position and Future Prospects', I.Mech.E. Automobile Division Proceedings, 240, 1956-57.

32. Judson, C.A., and Kellett, E., 'The Design and Development of Small Radial - Flow Turbo-chargers,' I. Mech. E. Automobile Divn. Proceed., p. 249, 1956-57.

33. Balje, O.E., 'A Contribution to the Problem of Designing Radial Turbomachines,' Trans. A.S.M.E., Vol. 74, p. 451, 1952.

34. Van Den Nuell, W.T., 'Single Stage Radial Turbines for Gaseous Substances with High Rotative and Low Specific Speed.,' Trans. A.S.M.E., Vol. 74, p. 499, 1952.

35. Shepherd, D.G., 'Principles of Turbomachinery', The Macmillan Co. New York, p. 387, 1956.

36. Kelly, P.L., 'High Speed Diesel Engines,' Chilton Co.,

Philadelphia, p. 377, 1953.

37. Taylor, C.F., 'The Internal Combustion Engine in Theory and Practice,' The Technology Press of the M.I.T., p. 463, 1960.

38. Maleev, V.L., 'Internal Combustion Engines,' Mc Graw Hill Book Co., Inc. New York, p. 367, 1945.

39. Judge, A.W., 'Aircraft Engines,' Vol. I, D. Van Nostrand Co., Inc., New York, p. 237, 1940.

40. Hallinson, P.M., and Lewis, W.G.E., 'The Part Load Performance of Various Gas Turbine Engine Schemes,' Proceed. I Mech. E., Vol. 159, p. 183, 1948.

41. Pounder, C.C., 'Diesel Engine Principles and [illegible] George Newnes Limited, London , p. 29-10.

42. Taylor, C.F., 'Effect of Engine Exhaust Pressure on Performance of Compressor- Engine- Turbine Units,' S.A.E., Trans., Vol. 54, p. 64, 1946.

43. Bannister, F.K., and Mucklow, G.F., 'Wave Action Following Sudden Release of Compressed Gas from a Cylinder,' Proc.I Mech. E., Vol. 159, p. 269, 1948.